EOCENE SEQUENCE STRATIGRAPHY

OF THE NORTH SEA BASIN

Approved by

Dissertation Committee:

[redacted]

William E. Galloway, Co-Supervisor

[redacted]

Martin B. Lagoe, Co-Supervisor

[redacted]

John M. Armentrout

[redacted]

Peter R. Thompson

[redacted]

Michelle A. Kominz

[redacted]

Richard T. Buffler

EOCENE SEQUENCE STRATIGRAPHY OF THE NORTH SEA BASIN

by

BENJAMIN JOHN SLOAN, B.A.

DISSERTATION

Presented to the Faculty of the Graduate School of

The University of Texas at Austin

in Partial Fulfillment

of the Requirements

for the Degree of

DOCTOR OF PHILOSOPHY

THE UNIVERSITY OF TEXAS AT AUSTIN

May, 1995

dedicated to
Arthur Milam Gruenler

Acknowledgements

There are many who deserve credit for their assistance in various stages of this project. John Armentrout gave a talk in 1987 that provided the inital impetus to undertake a study combining seismic and micropaleontological data. Supervising professors Galloway and Lagoe were indescribably generous, supportive, patient, and understanding from beginning to end. Outside committee members Armentrout and Thompson lent timely and patient assistance to my efforts. Several committee members, particularly Galloway, provided thorough reviews of the initial draft which led to substantial revision and strengthening of the dissertation.

Norwegian Exploration Consultants (NOPEC a.s.), Amoco, Marathon, BP, and Statoil provided critical geophysical data and financial support. Felix Gradstein of the Canadian Geological Survey in Halifax, Nova Scotia provided micropaleontological data, scientific support, and a cod-cheek dinner. The University of Texas Department of Geological Sciences and Geology Foundation provided money (including travel to Nova Scotia, Italy, England, Scotland, France, San Francisco, Dallas, Houston, New Orleans, West Texas, New Mexico, Colorado, and Smithville) and equipment critical to this work. Larry Lawver and the Institute for Geophysics provided equipment, support, and money for this and other projects which enabled me to finish this one. I learned stratigraphy from Amos Salvador, sequence stratigraphy from Frank Brown, genetic sequence stratigraphy and depositional systems from Bill Galloway and quantitative stratigraphy from Martin Lagoe, Sally Zellers, and Andy Czebeniak. György Marton helped me appreciate bulk reduction, baboonal environments, Spanish and Hungarian telephone etiquette.

Of course, I never would have made it this far without the support of my friends in the ice cream club: Sally, John, and Colleen. Most of all I thank my constant, gnawing source of inspiration, Mr. Chuck Stone.

EOCENE SEQUENCE STRATIGRAPHY
OF THE NORTH SEA BASIN

Publication No.____________

Benjamin John Sloan, Ph.D.
The University of Texas at Austin, 1995

Supervisors: William E. Galloway, Martin B. Lagoe

Eocene clastic sediments of the central and northern North Sea comprise five stratigraphic sequences. Oldest is the sand-dominated, basin-centered Frigg sequence, which includes submarine fan and apron deposits on the Beryl Terrace and in the Central and Viking Grabens. Middle Eocene Lower and Upper Hordaland sequences are mixed mud and sand units which prograded from the East Shetland Platform and Moray Firth and include discrete slope aprons and basin-center fans. The thin, regressive sand-prone Belton sequence marks the top of the Eocene in most of the basin, except on the eastern margin of the Shetland Platform, where the foreshelf prograding prism of Thet sequence sandstones and siltstones was deposited.

Foraminiferal biofacies analysis of a well on the Beryl Terrace indicates that four of the five sequence boundaries coincide with significant changes in the benthic and planktic foraminiferal assemblages. Cluster analysis confirms the distinct biofacies characterizing each sequence, an impoverished coarsely agglutinated fauna with radiolaria in the Frigg sequence, normal abundances of coarsely agglutinated forms in the Hordaland units, and "Velasco"-type deep-water calcareous benthics in the Upper Eocene, including planktic foraminifera in the Belton. Paleoenvironmental analysis of these biofacies shows an overall Eocene shallowing from lower slope to outer shelf. Subsidence analysis using the derived water depths indicates that the Eocene was part of a major phase of subsidence which began in the Late Paleocene and abated by Oligocene time.

Overall, the Eocene constitutes a tectonosequence, or stratigraphic sequence attributable to tectonic influences. Eocene circum-North Sea tectonics include Atlantic domain seafloor-spreading to the north and west and the encroaching Alpine compression from the south. The base Eocene, top Frigg, and top Eocene all correlate with changes in seafloor spreading thought to have contributed, through intraplate stresses, to the stress regime and differential topography of the source area and basin. Latest Eocene eustatic lowering, climatic cooling, and Arctic water circulation are thought to have influenced the Thet sequence.

TABLE OF CONTENTS

LIST OF TABLES AND FIGURES

TABLES

Chapter One

INTRODUCTION

Eocene clastic sediments of the northern North Sea have been the subject of numerous studies to describe and interpret the deepwater sand deposits which are producing reservoirs at several petroleum fields, including two giant fields. However, questions remain as to the larger regional picture of sand and mud distribution in the basin, sediment dispersal pathways, and factors influencing these patterns and their evolution through the Eocene. The purpose of this study is to provide that regional framework of understanding. Sequence stratigraphic concepts and methods are applied to reflection seismic and wireline log data. The three-dimensional lithostratigraphic character of each sequence is described and interpreted. The relationship between foraminiferal biofacies and the sequences is closely examined in one well in which the subsidence history and sediment accumulation rates are also calculated Finally, the observed regional stratigraphy is related to local, regional, and global factors, including sealevel, subsidence history, sediment supply, and climate.

Sequence stratigraphy, a significant innovation in sedimentary basin analysis, is not universally accepted, particularly the interpretations of eustatic control of third-order sequence development espoused by the proponents of the method (Vail and others, 1977; Vail and others, 1984; Haq and others, 1988). Although consensus is building for climate as a cause of fourth order (<100 ky) variations (Goldhammer and others, 1987; Koerschner and Read, 1989; Mitchum and Van Wagoner, 1990) and tectonics, including regional and globally linked tectonics, producing second order (10 my) cycles (Pitman and Talwani, 1978; Kominz, 1984), the origin of third order (1 my) cycles is hotly debated (Miall, 1986; Kendall and Lerche, 1988; Cloetingh, 1988; Sloss, 1991). Mechanisms for eustatic change are part of the problem. Polar, particularly Antarctic, ice accumulation on a scale large enough to affect sea level is generally considered to have begun in the early Oligocene or latest Eocene (Shackleton and Kennett, 1975; Matthews and Poore, 1980; Miller and others, 1987; Barron and others, 1991).

The Eocene of the North Sea is a good section for sequence stratigraphic study for several reasons. Regional seismic data span the Cenozoic basin from the Shetland Platform on the west to the Horda Platform on the Norwegian side (Figure 1.1). In the event that significant volumes of sediment were derived from both shelves simultaneously, interfingering in the basin center, it ought to be possible to distinguish mechanisms responsible for their genesis. Eustatically-induced downward shifts in coastal onlap ought to be synchronous in both areas. Tectonic or sediment supply-driven shifts may not occur at the same time on opposing sides of the basin. Secondly, North Sea seismic data and circum-North Sea outcrops have been used in construction of the Haq and others (1988) sea level curve, which may bias the curve toward regional tectonic influences, as suggested for the Jurassic (Hallam, 1988; Underhill and Partington, 1993). This is an opportunity to check the stratal geometries, biostratigraphic resolution, and possible influence of non-eustatic factors on the Haq and others (1988) coastal onlap chart.

1.1 Geologic Setting

North Sea geologic history has been greatly influenced by a series of external tectonic influences, both long- and short-term, which have compressed, extended, or

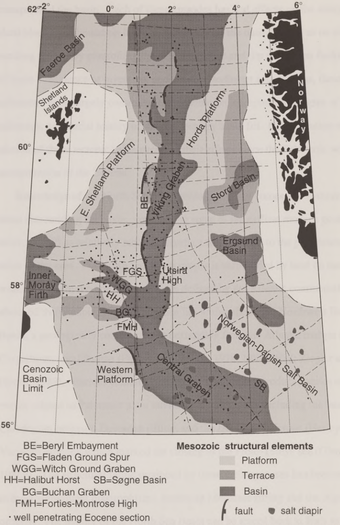

Figure 1.1. Regional seismic and well locations superimposed on major tectonic elements of the North Sea Basin (modified after Sears and others, 1993). Most of the labelled structural elements are referred to in the text at least in geographic terms since only subtle relief of these Mesozoic features persisted into the Eocene.

transpressed the basin. Each of these episodes has had effects on the many individual blocks and bounding faults which comprise the basin as well as on the surrounding areas. By controlling the extent of strike and dip motion on faults, amount of basin subsidence or inversion, and uplift of sediment source areas, these tectonic influences have largely controlled the distribution, composition, degree of marine influence, and burial history of the sedimentary basin fill. Consideration of the evolution of these tectonic influences and their effects since the Paleozoic will assist interpretation of the Eocene.

Knowledge of the North Sea basin geologic history comes via onshore studies in areas surrounding the basin, constituting some of the earliest modern geologic work, as well as relatively recent subsurface work related to the petroleum exploration of the area. The North Sea Basin proper is surrounded by land on the east, west, and south; the northern margin is defined by the Atlantic continental margin at about 62°N (Glennie, 1987). The basin lies within the larger Northwest European Basin, a geologically complex region extending from the Atlantic margin to the Carpathians and Ukraine (Figure 1.2; Ziegler, 1978, 1982; 1988; Ziegler and van Hoorn, 1989). Various crustal blocks in the area are the product a series of tectonic events related to Paleozoic plate interactions, principally including the late Silurian Caledonian orogeny, Devonian rifting, and the late Carboniferous (Her-cynian) Variscan orogeny which marked the closing of the Proto-Tethys sea (Glennie, 1986b). The structural fabric produced by these taphrogeneses has been reactivated in most subsequent diastrophisms, including Mesozoic rifting and the Alpine orogeny. The history of the North Sea Basin can be traced back at least as far as early Permian time, when it was divided into southern and northern sub-basins by

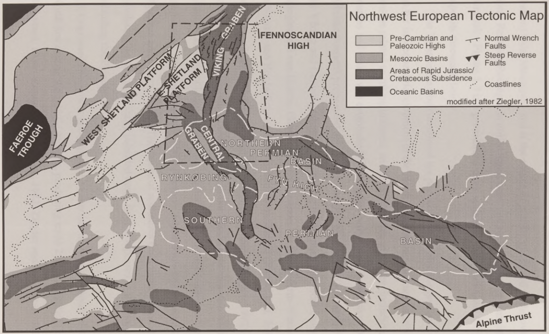

Figure 1.2 Tectonic map of Northwest Europe (after Ziegler, 1982) including structural elements of the area spanning the Phanerozoic. The study area is enclosed by the dashed box.

the Mid-North Sea Ringkøbing-Fyn High. The southern Permian basin, extending into Germany and the Netherlands, is underlain by the thick Carboniferous (Westphalian) Coal Measures, and is the source of prolific gas stored in the overlying lower Permian Rotliegende eolian sandstones and sealed by upper Permian Zechstein salt. Figure 1.3 is a generalized cross section of these rocks and the younger deposits discussed below.

The Triassic may be considered the period during which the geologic stage was set for subsequent development of the North Sea. During this time east-west extension related to rifting initiated, and the basic basin geometry, including sediment sources and sinks, was established. During the early Triassic, an arm of the North Atlantic megarift propagated southward from the Norwegian-Greenland Sea to open the Viking and Central grabens, cross-cutting the Permian and older basement trends (Ziegler and van Hoorn, 1989). At the same time, the Moray Firth-Witch Ground sub-basin and Horda-Ergsund half-grabens were formed (Figure 1.1). In these areas, which continued to subside as parts of the Permian Basin (Ziegler, 1992), Triassic sediment accumulations exceed 3,000 m in the Viking Graben and 2,000 m in the Central Graben, including coarse clastics derived from the Fenno-scandian Shield, the Scottish Highlands, and Shetland Platform, which form im-portant oil reservoirs (Spencer and others, 1987). The theme of sediments from these source areas accumulating on the tectonically subsided basin floor is repeated in the basin evolution, including the Paleogene.

Continued rifting was accompanied by thermal doming and uplift of the central North Sea during the middle Jurassic, producing up to 2500 m of relief (Hallam and Sellwood, 1976; Enyon, 1981; Ziegler, 1982; Ziegler and van Hoorn, 1989; Ziegler,

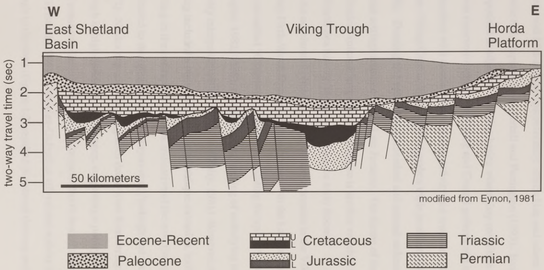

Figure 1.3 Generalized structural cross section of the northern North Sea Basin emphasizing pre-Eocene strata. Block faulting reflects Jurassic rifting and extension. Note thicker Chalk and Paleocene to west, erosion of Mesozoic units on the Horda Platform, and bathymetric low corresponding to glacially-scoured Norwegian trough. (Modified after Eynon, 1981.)

1992). Lower Jurassic, Triassic and Permian sediments were eroded, forming the widespread Mid-Jurassic unconformity, which Haq and others (1988) interpret as a eustatic fall, disputed by Underhill and Partington (1993). Eroded sediments were redeposited in adjacent subsiding basins where they constitute important hydrocarbon reservoir rocks in the Viking and Central grabens and in northern Germany. Coincident with doming was volcanic activity and eruptions of ash from the vicinity of the Viking/Central/Witch Ground graben triple junction (Ziegler and van Hoorn, 1989). Doming and volcanism diminished and normal sedimentation patterns and marine settings returned by the Late Jurassic. The theme of thermal uplift, erosion of clastics, volcanic eruption, and collapse is another which is recapitulated later in the North Sea history, including during the early Eocene.

An accelerated phase of rifting-related extension in the Viking, Central, and Moray Firth-Witch Ground grabens occurred in the Late Jurassic-Early Cretaceous (the so-called "Cimmerian" event), accounting for up to 19 km of crustal stretching (Ziegler, 1982, 1988), and probably upwelling of underlying mantle (based upon gravity interpretations of Donato and Tully, 1981) However, this second phase of rifting included a component of dextral oblique extension, indicated by wrench faulting in the southern North Sea, indicative of the new European stress regime attributed to the opening of the Tethyan sea (Cloetingh and Kooi, 1992; Ziegler, 1992). Shales deposited in the graben deeps from Kimmeridgian to Berriasian time are rich in high-yield, oil-rich kerogen, suggesting a poorly-circulated, anoxic basin, and constitute the principle source for most North Sea oil (Barnard and Cooper, 1981; Baird, 1986). Callovian-Oxfordian rift-related activity in the Faeroe-Rockall trough to the west (Figure 1.2) resulted in thermal doming and relative uplift of the

Shetland Platform from which clastics were shed eastward into the Viking and Moray Firth-Witch Ground grabens as submarine fan deposits, similar to Paleogene sedimentation and tectonics, (Ziegler and van Hoorn, 1989). Early Cretaceous basin foundering, due both to subsidence and gradual eustatic sea level rise (Tyson and Funnell, 1987; Christie-Blick, 1990), led to deposition of fine-grained sediments during this time.

The Late Cretaceous and Paleocene comprise the "late stage" during which rifting activity abated and was replaced by simple thermal and load-induced subsidence in the North Sea while stretching continued to the west of the basin in the Norwegian-Greenland Sea. The Upper Cretaceous is represented by the Chalk series throughout the North Sea and well onto the basin margins. The unit represents further basin quiescence, save reactivation along some bounding faults which led to chalk resedimentation, particularly during the Danian (Hancock, 1984). This tectonism may be partly attributable to the growing intraplate compressional stress regime which affected much of northwest Europe as the Tethys ocean closed and Africa collided to the south in the Alpine orogeny, inverting sub-basins in the southern North Sea (Ziegler, 1978, 1987).

Alpine stresses to the south were accompanied during the Paleocene by progressive thermal doming related to Faeroe-Rockall rifting, uplifting the Shetland Platform and Scottish Highlands, which then shed coarse clastics into the basin during apparently low eustatic sea level. Thick, sand-rich Paleocene fans and fan-aprons accumulated in the basin during possibly accentuated basin margin-basin center differential topography given the compressive stress regime (Cloetingh and others, 1987; Kooi and Cloetingh, 1989; Galloway and others, 1993).

Volcanic activity in the Hebrides was associated with the build-up of rifting stresses in the North Atlantic; both phenomena increasing during the Paleocene and culminating with the early Eocene Balder (Thulean) volcanic outpouring, associated with plateau basalt extrusion and dike emplacement in Northern Ireland and Western Scotland, all of which was coincident with the final crustal separation of Eurasia and North America via spreading in the Norwegian-Greenland Sea (Pitman and Talwani, 1972; Glennie, 1986b). Collapse of the Shetland Platform and relatively high sea level in a quiescent, foundered basin set the stage in the early Eocene (Ziegler, 1990). The now post-rift stage basin subsided thermally and under sediment loading with only minor load-induced fault reactivation.

1.2 Previous Work

The Eocene is an appropriate unit for study as the logical extension (stratigraphically upward) of previous work in the Paleocene and lower Eocene sections, and because it appears to constitute a distinct major regional depositional supercycle (Galloway and others, 1993). Geographically, the scope of the study was chosen based on coverage by seismic and well data and the limits of Cenozoic basin deposition (Figure 1.1). The southern limit of the study area is so defined as to avoid the halokinetically disturbed Cenozoic section in the southern North Sea, where the Eocene is relatively thin and argillaceous. The term "Eocene" as the subject of this dissertation is used informally because, just as some workers have informally lumped the lower Eocene with the Paleocene depositional episode (*e.g.* Rochow, 1981), the post-Balder to Oligocene age sediments form a coherent package of genetically related sediments.

Publications on the Eocene North Sea Basin, the generalized seismic stratigraphy, lithostratigraphy, biostratigraphy, and subsidence history, are a useful basis from which to build. Considerable work on the Paleogene of the North Sea has been published since this dissertation study commenced, including works in a volume on British petroleum and tectonics (Hardman and Brooks, 1990), the proceedings of the Symposium on Sequence Stratigraphy of Cenozoic and Mesozoic Basins of Europe (Vail and Jacquin, 1992), and the Fourth Conference on Petroleum Geology of Northwest Europe (Parker, 1993).

The greater northwest European basin has been the focus of sequence stratigraphic work for over 200 years, dating back at least to the work on transgressive and regressive units in the Paris basin by Antoine Laurent de Lavoisier in 1792. The high quality and quantity of seismic data acquired for modern exploration of the North Sea basin, coupled with the wealth of age-equivalent sections described onshore, has prompted substantial modern sequence stratigraphic investigation of the area, including many reference sections for the Mesozoic and Cenozoic global eustatic curve proposed by Haq and others (1987; reference sections listed in Haq and others, 1988).

Lower Tertiary deposits include some of the earliest and largest oil and gas fields discovered in the North Sea basin, including Paleocene Montrose (Fowler, 1975) and Forties (Thomas and others, 1974) fields and the Eocene Frigg field (Heritier and others, 1979; McGovney and Radovich, 1985; Conort, 1986; Enjolras and others, 1986; Mure, 1987). Early stratigraphic and sedimentologic work was centered on understanding these Paleogene reservoir rocks. Parker (1975) described a Paleocene coastal deltaic complex which prograded from the Moray Firth area and fed coarse sediments over the shelf edge onto the slope and into the basin. The first major lithostratigraphic scheme for the North Sea basin was published by Deegan and Scull (1977). They subdivided the Paleocene into submarine fan sandstones of the Montrose Group (Maureen, Andrews and Forties Formations), proximal shelfal and deltaic deposits of the Moray Group (Dornoch and Beauly Formations), and distal shalier deposits of the Rogaland Group (Sele and Balder Formations) (Figure 1.4). Further differentiation of the Tertiary section was minimal. The Nordland and Hordaland groups were named in the Norwegian sector and include formations for the most significant sand accumulations, Frigg and Utsira. The gross simplification of the post-Balder stratigraphy is attributable to the fact that very little was known about the section in 1977 and most of it was considered argillaceous and therefore indivisible or uninteresting. Mudge and Copestake (1992) present a revision of the scheme for the Outer Moray Firth Paleogene which includes a biozonation of foraminiferal, diatom, and palynomorph markers allowing a refined chronostratigraphy. They proposed no substantial changes for the lower Eocene, but the Paleocene is further divided into formations and members and the time-transgressive Rogaland Group is abandoned.

A proposal for major subdivision of Eocene lithostratigraphy, including many new names, was made by Knox and Holloway (1992). This was adopted by Mudge and Bujak (1994) in their chronostratigraphic subdivision of the section. Based upon gamma log patterns and correlations calibrated to a detailed dinoflagellate biozonation (documented by Bujak and Mudge, in press), they divided the Eocene basin into five genetic stratigraphic sequences: Dornoch, Balder, Frigg, Alba, and Grid (Figure 1.5). The shelfal Eocene is named "Mousa", Alba sequence sands are

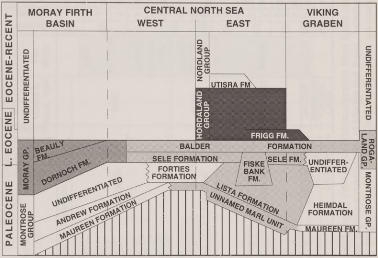

after Deegan and Scull, 1977

Figure 1.4 The first formal Tertiary lithostratigraphic scheme for the North Sea Paleogene (Deegan and Scull, 1977). The post-Balder is not differentiated except for the Frigg and Utsira sands. The Rogaland Group (later revised) lumps distal shales in an oddly time-transgressive manner.

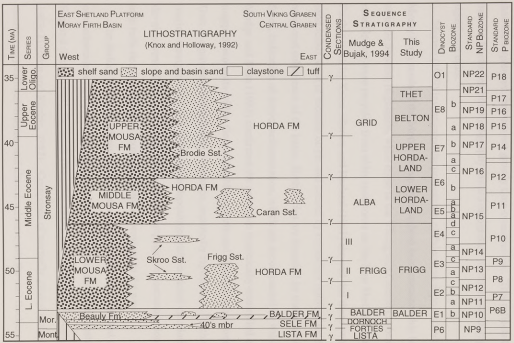

Figure 1.5 Eocene stratigraphy (after Mudge and Bujak, 1994, with lithostratigraphy from Knox and Holloway, 1992). Note the correlation between sequence stratigraphy of Mudge and Bujak, locations of condensed sections, and sequence stratigraphy proposed in this study. Condensed sections are marked by radioactive (high-gamma) mudstones.

referred to as "Caran", and upper Eocene sands are "Brodie". Note that although the lithostratigraphic units are of less spatial extent and, in some cases, temporal extent than the sequences, they are not grossly time-transgressive. This reflects the general trend in North Sea lithostratigraphy toward recognition of chronostratigraphically significant units.

Morton (1979) investigated the provenance of Paleocene deposits and found that Moray Firth sands of the Moray Group were derived from metamorphic basement near the Scottish Highlands, while those in the Viking and Central Graben (Montrose Group) were recycled from older sandstones on the East Shetland Platform. Further work by Knox, Morton and Harland (1981) showed that these two cycles of sand influx were of tectonic origin and caused by coincident uplift of the source areas and subsidence of the basin. Both cycles are bounded by transgressive surfaces, indicative of slower sedimentation, which are accompanied by volcanism. Mudge and Bliss (1983) confirmed the same two tectonically-controlled cycles and mapped four units within them in the Moray Firth and Viking Graben areas. Their Unit 4, equivalent to the Balder Formation, reportedly represents a "basinwide marine transgression" and "quiet-water deposition with restricted circulation and the development of anoxic bottom conditions" accompanied by accumulation of volcanic tuffs derived from the Scottish Hebridean province to the west.

The Balder Tuff is the main unit of a series of pyroclastics deposited over much of northwestern Europe during the Paleocene and Eocene, including onshore England (King, 1981), Denmark (Bøggild, 1918), and the Faeroe Trough (Ridd, 1983; Hitchen and Ritchie, 1987). Composed of normally graded microcrystalline quartz, recrystallized diatoms, and altered volcanic ash, the unit thickens to the northwest, the inferred source area (Jacqué and Thouvenin, 1975). The main outpouring is dated as 53.5 Ma (Knox and Morton, 1983). Recent work (Morton and Knox, 1990) suggests the source volcanism was along the proto-Greenland-Scotland Ridge along which the Norwegian-Greenland Sea opened. Although it is an anomalously large tephra outpouring for basaltic pyroclastic volcanism, the associated basalts are of correspondingly high volume, rivaling the Cretaceous/Tertiary boundary Deccan Trap deposits (Elliott and others, 1992).

Seismic Stratigraphy

Papers on regional seismic and sequence stratigraphy applied to the Tertiary section appeared in the 1980's, beginning with work by Rochow (1981) in which he documented the previously described Montrose Group submarine fan deposits and overlying Moray Group deltaics with reflection seismic and well log data. Stewart (1987) presented a rigorous treatment of the Paleogene, which he divided into ten sequences from Danian to Ypresian age, using seismic and well data (both of unstated quantity or distribution), including biostratigraphic information (Figure 1.6). Eight Paleocene depositional sequences were mapped, including reworked Danian Chalk and the submarine fan deposits of the Maureen, Andrew, and Forties, each composed of a regressive, basin-centered sandy lowstand component followed by a thin, transgressive argillaceous highstand onlapping the margin. These sequences are reconciled with the lithostratigraphy of Deegan and Scull (1977) and resolve some stratigraphic problems. For example, the coals of the upper Beauly Platform (Sequence 8) are shown to be equivalent to basinward deposits underlying the Ypresian Balder Tuff. Stewart (1987) identified two early Eocene age sequences

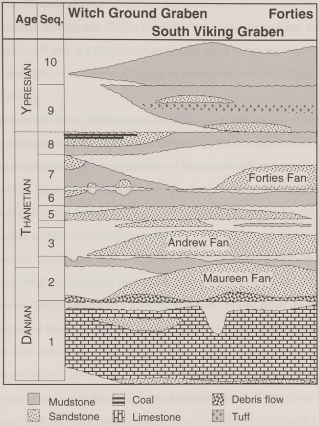

Figure 1.6 Chronostratigraphic representation of the widely cited ten stratigraphic sequences described and mapped by Stewart (1987). With regard to the Eocene, Sequence 9 includes Balder deposits and Sequence 10 encompasses the Frigg, although Stewart's study area did not include Frigg Field.

The lower (Sequence 9) is a transgressive shale unit containing minor basin floor submarine fan sands in the southern Viking Graben. This sequence passes upward into the tuffaceous shales of the Balder Formation, including a second incidence of localized fan development (Balder Field), and culminates with a hiatal surface. Stewart's tenth unit is a thin transgressive shale which onlaps the basin margin and is characterized in its basinward reaches by reddish clays and red-stained planktic foraminifera.

Milton and others (1990) applied the methodology of Galloway (1989a) to the same area and concluded that most of Stewart's (1987) sequence boundaries correspond to radioactive beds representative of hiatal surfaces between pulses in sedimentation. They further elucidated the relationship between the stratigraphies of Stewart (1987) and Deegan and Scull (1977), equating Sequence 9 to the Beauly Formation updip and Balder Formation in the basin, and Sequence 10 to the Frigg Formation. Based upon erosion of the units in the Inner Moray Firth, Milton and others (1990) interpreted the large coarse-grained submarine fan deposits of the Montrose Group as products of basin margin uplift (relative fall of sea level) and the finer-grained Moray Group units as products of reduced uplift and landward migration of an axis of tilting the Shetland Platform (relative sea level rise in the basin). Jones and Milton (1994) showed that the "third-order" sequences of Stewart (1987) show enchancement of Montrose Group lowstand deposits during the second-order tectonic uplift and thickening of Moray Group transgressive systems as a result of combined second- and third-order relative sea level rise.

Armentrout and others (1993) identified six Paleocene and four Eocene sequences in the outer Moray Firth area (Figure 1.7) and mapped them using seismic

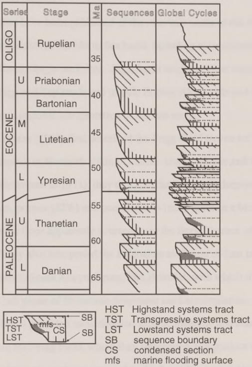

Figure 1.7. Cycle chart for the North Sea Paleogene by Armentrout and others (1993) includes six Paleocene and four Eocene depositional sequences versus 22 events on the "global" curve of Haq and others (1988). They found transgressive systems tracts to be very thin or nonexistent in the North Sea basin.

and well log data. They concluded that tectonic activity modified sequence geometries on the third-order (million year) scale, including an early Eocene subsidence event.

Petroleum Field Studies

Detailed studies have been published of the reservoir sands of the Paleocene and Eocene oil and gas fields of the North Sea basin, including their seismic, biostratigraphic, and sedimentologic attributes. Significant work has been completed on the lower Eocene Frigg and Tay sands and middle Eocene Alba sands and must be accommodated by any regional interpretation of Eocene rocks.

Heritier and others (1979) first described the Frigg Field (seven tcf of gas), a submarine fan deposit in the north Viking Graben. Using seismic and well log data over the field (discovered in 1971), they describe the Frigg as a deep-sea fan deposit of massive, clean, porous (22%) and permeable (>1mD) sands in a birdfoot-shaped mound on the basin floor apparently sourced from the Beryl Terrace of the east Shetland Platform. They also interpreted the Paleogene evolution of fans in the area, including the Ninian, South Alwyn, Bruce, and Heimdal, with which they lumped the Frigg as the last phase of Paleocene deepwater sand accumulation. McGovney and Radovich (1985) provided more detailed seismic mapping and detailed log correlation within the Frigg Field, which they interpreted as a product of the late Ypresian (49.5 Ma) sealevel drop proposed by Vail and Hardenbol (1981), although the palynological dating of the sand by Heritier and others (1979) is not more precise than "Ypresian". They also identified and mapped five discrete lobes of sand and divided them into channel and sheet sands. Brewster and Jeangeot (1987) presented evidence of a Paleocene topographic high under the field, syndepositional faulting (documented using 3D seismic data by De Clarens and others, 1992), and the possibility of eastern sourcing of some of the sand, much of which they interpreted as grain flows and debris flows based on core analysis. Enjolras and others (1987) and Conort (1986) confirmed the lack of grading in the Frigg sands, which the former believed to have been substantially reworked by bottom currents.

Lower Eocene basin and slope sandstones, equivalent to the Frigg Formation, are found in the north Central Graben and are named the "Tay" sands. Armstrong and others (1987) described and interpreted lower, middle and upper Tay sandstones from an investigation including 3D seismic data at Gannet Field (800 mmbbl of oil), which produces from the Jurassic Fulmar, Paleocene Forties, and Tay Formations. Brewster and Jeangeot (1992) differentiated sand-dominated, mounded fans of Tay age from underlying Balder-equivalent mud-dominated fans with "shoestring" channels. Both were thought to have been sourced from the Western Platform and thin over a nearby salt dome.

Harding and others (1990) described a sand-prone middle Eocene shelf which prograded southeasterly across the Fladen Ground Spur and shed sands onto the slope and basin (Witch Ground Graben). The latter of these include sinuous, leveed channel deposits of the greater Alba Fan which are productive at the Alba Field (1100 mmbbl of oil) (Mattingly and Bretthauer, 1992). Harding and others (1990) and Mattingly and Bretthauer (1992) considered sea level to be a major control on development of the Alba fan, but gave no explanation as to why. Newton and Flanagan (1993) reinterpreted the Alba sands as the product of high-density turbidity flows which deposited sands in a pre-existing unleveed erosional channel based on the fact that they are massive and clean (up to 35% porosity and 5 D permeability) and the proposed levee facies is, in fact, autocthonous hemipelagic shale rather than submarine overbank fines.

Biostratigraphy

Biostratigraphically signficant micropaleontologic study of the North Sea basin has focused on two major microfossil groups: foraminifera and palynomorphs. Diagnostic diatoms and radiolarians are present only in a few parts of the section. Foraminifera are of limited chronostratigraphic utility but are good indicators of benthic and planktic paleoenvironments. Dinoflagellates, spores, and pollen have been established as excellent age indicators. However, insofar as they are generally distributed over large areas or terrestrially derived, they are not representative of the paleoenvironments of the marine rocks in which they are found. They may be used to infer regional paleoclimates. Some dinoflagellates are thought to be sensitive to water temperatures (Bujak and Mudge, in press).

The Paleogene of the North Sea is characterized by an enigmatic assemblage of agglutinated foraminifera, first documented in onshore German wells by Staeshe and Hiltermann (1940). Gradstein and Berggren (1981) provided a detailed account, including taxonomy, of the agglutinated fauna found in central North Sea wells between the top of the Danian and base of the Oligocene. Similar assemblages occur simultaneously in alpine flysch basins, such as the Carpathian flysch of Poland (Grzybowski, 1898), the Newfoundland continental margin (Labrador Basin), and North Sea. Inferred common paleoecological conditions of these areas include rapid deposition of organic-rich, carbonate-poor clastics under somewhat restricted bottom water circulation conditions leading to low pH and Eh in at least 200 meters of water(Gradstein and Berggren, 1981).

Calcareous foraminifera are found in wells penetrating shelf sections in the Paleogene of the North Sea basin and throughout the basin in the Neogene, apparently as a result of an overall shallower basin by this time. King (1983) identified two calcareous Paleogene biofacies: an "inner sublittoral" assemblage and an "outer sublittoral - epibathyal" group. He also recognized agglutinating foraminifera, the so-called *Rhabdammina* biofacies, in the basin center .

King (1983; minor revisions in 1989) proposed Cenozoic biozonations composed of interval zones for the benthic (17 zones) and planktic (16 zones) foraminifera. Within this scheme, the Eocene was divided into four parts based upon ranges of 36 species of benthic foraminifera and six species of planktic foraminifera. Each interval is defined by the highest occurrence of a single particularly widespread or diagnostic species and is further characterized by other species which typically occur within the zone. The biozonation included only a few agglutinated species, very much reducing its utility in the center of the basin where agglutinants dominate the biofacies. Age control on the biostratigraphy was provided by correlation to nearby northwest European sections containing the planktic foraminifera and nannoplankton found in standard biozonations (*e.g.* Blow, 1969; Martini, 1971) as well as a few planktic index fossils which occur in the North Sea Basin, such as *Globigerinatheka index.*

Dinoflagellates are common in the North Sea Cenozoic and are the basis of a number of biostratigraphic zonations considered to be of stratigraphic resolution superior to foraminiferal zonations. Ioakim (1979) divided the Tertiary section in the Norway 16/1-1 well into nine biozones. More comprehensive regional studies by Costa and Manum (1988) and Powell (1988) further divided the Tertiary section and related the zones to surrounding outcrops and to nannoplankton zones. Bujak and Mudge (in press) erected the most robust and highest resolution biozonation in the area. They identified eight dinocyst zones and 32 subzones in the Eocene (Figure 1.8) which they related to genetic stratigraphic sequences (Mudge and Bujak, 1994), and tied closely to onshore nannofossil zones thus providing accurate correlation to global chronostratigraphy. Each zone and subzone correponds to the highest occurrence or highest abundant occurrence of one or more species among a succession which is consistent throughout the study area.

Gradstein and others (1992, 1994) produced the first combined foraminiferal and dinoflagellate cyst zonation for the Cenozoic, and the only scheme constructed using relatively objective quantitative techniques (Figure 1.8). They apply methods of Ranking and Scaling (RASC) and graphic correlation (STRATCOR) to determine the most probable sequence (or average) occurrence of faunal events in 33 wells (Figure 1.9; first presented in Gradstein and others, 1988). A product of the RASC method is the "interfossil distance", which represents the degree of interchange-ability of adjacent events, which actually include last occurrences of fossils and other events considered synchronous basinwide, such as log markers, ash beds, radiolarian blooms, etc. Events tend to cluster into groups having high intragroup interchangeability (all occurring about the same time basinwide) and are separated from other groups by low intergroup interchangeability (high interfossil distance). Groups are assigned ages based on contained index (wide-ranging) fossils and/or correlation to age-calibrated sections. Using these methods, they divide the

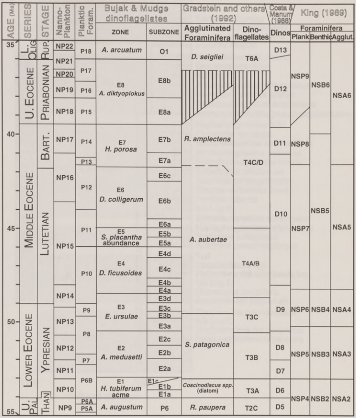

Figure 1.8 Composite North Sea biostratigraphic chart. All biozonations are plotted relative to the global "NP" nannofossil zones of Martini (1971) and "P" planktic foraminiferal zones of Blow (1969). The recent dinoflagellate zonation by Bujak and Mudge (in press) shows the highest resolution, particularly in the lower Eocene section (E1a-E6a), where each subzone corresponds to the highest occurrence of one or more species. Gradstein and others (1992, 1994) interpret a Priabonian hiatus not recognized by the other workers. King (1989) recognizes slightly different zonations based on planktic, benthic, and agglutinated foraminifera.

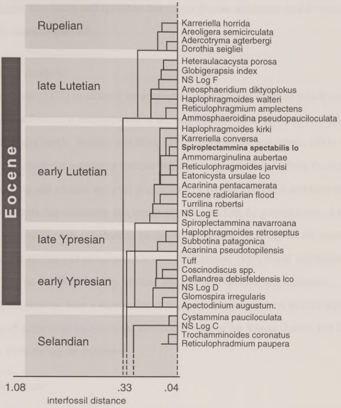

Figure 1.9 A portion of the Scaled Optimum Sequence of Gradstein and others (1988). The dendogram plots optimally ranked events (microfossil tops, floods, and log markers) on the y-axis versus their rank or interfossil distance (interchangeability between nearby events) on the x-axis. The Eocene is divisible into four major units and the late Eocene (Priabonian) is missing.

Eocene into four zones, and speculate that Upper Eocene sediments may be missing from the basin (Figure 1.8).

Subsidence Analysis

Van Hinte (1978) introduced the concept of geohistory analysis, in which burial history of sediments is reconstructed by decompaction of sediments and correction for paleowater depth. Steckler and Watts (1978; and Guidish and others, 1985) developed methods for evaluating tectonic subsidence by removal of effects from sediment loading and eustatic sea level fluctuations. Calculations of this sort have been made on North Sea sediments as a means of understanding the geodynamics of the basin, particularly with reference to the amount of stretching during the rift phase versus post-rift thermal subsidence (Sclater and Christie, 1980; Wood and Barton, 1983; Thorne and Watts, 1989). Nielsen and others (1986) mapped Cenozoic subsidence patterns from a distribution of wells which allowed them to infer depocenters of differential load-induced subsidence, such as the Viking Graben and Outer Moray Firth during the Paleogene.

1.3 Objectives

The published work described above includes many studies which are subregional in scope or, if regional, focus upon one particular aspect of the geology, such as the biostratigraphy. The purpose of this study is to produce an integrated regional stratigraphic framework for the North Sea Eocene, within which to conduct local biofacies and subsidence analyses, and to attempt to understand controls on sequence development. This is summarized as four main objectives:

(1) To describe the geometry, bounding surfaces, distribution, thickness, and lithofacies of Eocene sequences using seismic and well data, and interpret their component depositional systems and sediment sources.

(2) To describe and evaluate the foraminiferal biofacies in a representative well, both qualitatively and quantitatively, interpret paleoenvironmental conditions they represent and compare the results with the seismic and log lithofacies sequences in the well.

(3) Using the most accurate lithologic information available and paleobathymetry derived from the benthic foraminiferal biofacies, perform subsidence analysis on Eocene and younger sediments for a well in order to understand the history of tectonic subsidence and rates of sediment accumulation.

(4) By synthesizing results from the first three objectives with previous work, attempt to interpret the factors most likely to have contributed to sequence development, particularly differentiating between tectonics, eustasy, sediment supply, and climate.

1.4 Database

Primary data for the study include reflection seismic, well log, and paleontologic data (summarized in Table 1.1). Seismic information includes about 7,500 kilometers of 1980's vintage regional data acquired by GECO for NOPEC (Norwegian Exploration Consultants) and donated for use in a study of the Cenozoic basin by Professor William Galloway's depositional systems study group at the University of Texas at Austin (Galloway and others, 1993; Reinsborough, 1993; Garber, in prep., Liu, in prep.). The lines span the Cenozoic basin with most oriented close to reg-

TYPE	DESCRIPTION		SOURCE
Seismic	approx. 7,500 kilometers GECO regional multichannel reflection seismic data: -1981 vintage CGT81 grid, Central Graben area -1982 vintage CNST82 grid; Moray Firth area -lines 6, 17, 19 reprocessed in 1988 -1984 vintage NNST84 grid; Viking Graben area		NOPEC
Wireline Logs	13 Danish sector composite logs	Gr, sonic	donation*, purchase
	157 Norwegian sector logs	typically only Gr, sonic	donation*, purchase
	204 U.K. sector composite logs	Gr, sonic, lith, velocity	donation*, purchase
Paleonto-logic Control	31 wells: Gradstein foraminiferal biostratigraphy		Published, shared
	30 wells: interpreted foraminiferal/palynological tops		donation*
	1 well: (U.K. Union 9/12-2) 10 meter ditch cuttings		Unocal U.K. Ltd

* log donors: Amoco, Marathon, BP, Statoil

Table 1.1 Summary of data used in this study.

ional strike or dip (Figure 1.10). Line spacing averages about 40 kilometers which is enough to identify patterns from line to line which are significant over large areas (note that the basin is about 400 kilometers wide by 1100 kilometers long). The data are divided into three major surveys, the northern NNST84 series, central CNST82 lines, and southern CGT81 grid. Because these correspond to geologically meaningful divisions (NNST covers the Viking Graben, CNST the Moray Firth, CGT the Central Graben), correlation is generally straightforward within each grid, but not so simple from one survey to the next, a problem exacerbated by minimal overlap of tie lines between surveys (particularly the NNST and CNST grids).

Because the seismic data were regional in scope when acquired and processed, the paper copies provided for this study were displayed at relatively small scales (50 traces per inch horizontal and two inches per second vertical). By petroleum industry standards, this is a compressed scale. As a result, only relatively large features are expected to be resolvable. It is possible that localized geologic features, such as narrow incised canyons, slump scars, low-relief mounds, leveed channels, and others are beyond resolution in these data.

Well logs were available from over 500 petroleum exploration and development wells drilled in the UK, Norwegian, and Danish sectors acquired through purchase from log vendors and donation from project sponsors. Of these, about 350 are full scale log suites, including at least gamma-ray and sonic logs. Spontaneous potential, or "sp", logs are not normally acquired in the basin due to the use of saline drilling mud and the difficulty of grounding the tool on offshore platforms. Many logs from the UK sector are "composite" logs, filed by the operator in accordance with

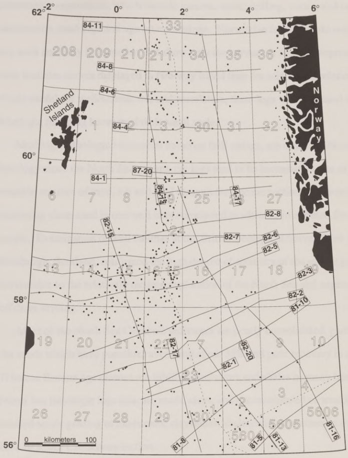

Figure 1.10 Index map showing locations of reflection seismic lines and wells used in this study as well as exploration quadrant numbers (outline) used to identify well locations and international sector boundaries for Norway, United Kingdom, Netherlands, and Germany (dashed lines).

government regulations, which include gamma, sonic, drilling, coring and casing information, mud logs and age interpretations. Norwegian logs often do not include any such ancillary information, but show only the curves. A further proprietary log suite includes curves displayed in two-way travel time for seismic correlation. While useful for well/seismic ties and correlation, these logs were not used in lithologic mapping because of their small scale.

Mud logs, lithologic summaries based on drill uttings, are crucial indicators of lithology since the North Sea gamma-ray logs tend to be inconsistent due to the variable mixture of sand, silt and mud through the Eocene section. Gamma readings indicating clean sand in one well may correspond to siltstone in another, for example. Examination of well cuttings at the British Geological Survey Core Store in Edinburgh, Scotland, confirmed the high degree of accuracy of the mud logs, in part attributable to the relatively modern exploration of the North Sea and expense of offshore drilling.

Most of the North Sea Cenozoic sediments are poorly consolidated, particularly the sands which have porosities averaging about 35% and poor recovery in cores. Whereas Eocene age clastics are lithified sandstones and shales in many basins, North Sea lithologic logs indicate muds, clays, and unconsolidated or weakly cemented sands grading to mudstones, claystones, shales, and sandstones in the Paleocene or lower Cretaceous section.

Paleontologic data were available in varying degrees of detail and usefulness and only for select wells, ranging from unsubstantiated age interpretations to faunal lists. Established North Sea Cenozoic biostratigraphy relies on both foraminiferal and palynological microfossils as age-indicators, with the latter being considered more reliable for purposes of correlation (*e.g.* consistent age indicators). Commercial interests, such as Robertson Research and BP, have subjectively erected operational biostratigraphic zonations for these organisms, including the first occurrence, last occurrence, and acme (maximum development) of key taxa (those which are the most widespread). These generalized zonations are widely used in industry. However, the unique nature of the faunal assemblages which lived at each well location, convolved with the set of variables including reworking, preservation, and borehole contamination affecting their ultimate appearance under the microscope, make each site a special case. With this in mind, the age interpretations, for example, which appear on composite logs are gratifying to the extent they agree with interpretations based on other information. However, without knowledge of the particular criteria used to assign the ages, it would be foolish to place such emphasis on them as to force correlations inconsistent with other available data.

Gradstein and others (1988, 1992, 1994) published a probabilistic biostratigraphy of 33 wells in the North Sea based on the most likely order of first occurrence of foraminifera and other events in those wells (described above). The tops of their four Eocene biozones for each of 29 North Sea wells were made available by Felix Gradstein (Canadian Geological Survey, Halifax) (Figure 1.8). These objective, quantitative interpretations were given considerable weight in correlating the well logs and nearby seismic data, particularly the base Eocene, top Ypresian, and top Eocene markers.

Ditch cuttings were acquired for two wells located directly on seismic lines on the outer part of the Shetland Platform, intersecting all five sequences, with the intention of studying both of them. Samples from ten meter intervals were acquired for UK 9/8-4 and UK 9/12-2. Cuttings from the former were acquired at the British Geological Survey Core Store facility in Edinburgh, Scotland. Unfortunately, the sample sizes were quite small (as were most samples at the repository) and did not prove useful. As a result, efforts were made to acquire larger sample sizes through industry. Unocal UK Ltd provided adequately large samples from UK 9/12-2 and the study proceeded. The very sparse occurrence of foraminifera in these samples confirmed that processing and picking of the much smaller samples from the UK 9/8-4 well would be fruitless.

Chapter Two

METHODOLOGY

The purpose of this chapter is to briefly discuss issues related to the methods applied to the data before describing the results in successive chapters. Some of the methods are straightforward (mapping, log correlation, foraminiferal analysis) whereas others may be considered unorthodox (quantitative analysis) or even controversial (genetic sequence stratigraphy), the latter requiring explanation.

2.1 Methods of Sequence Stratigraphic Analysis

The methods employed are a modification of the type of integrated sequence stratigraphic analysis widely practiced in academia and industry, combining seismic, wireline log, and biostratigraphic information. Identification of sequences was initially made from seismic data on which the stratal geometries, including surfaces of onlap, downlap, and toplap constituting conventional sequence boundaries, are visible and mappable (Figure 2.1; Vail and others, 1977). These geometries define the basic stratigraphic units and their relationship to one another in terms of relative position, thickness, and distribution, while also allowing interpretation of relative sea level changes, sediment sources, and tectonic influences.

A variation of sequence stratigraphy proposed by Galloway (1989a) is a useful means of understanding basin evolution and a logical approach to basin analysis. Based on concepts set forth by Frazier (1974), Galloway's "genetic sequence stratigraphy" recognizes the same surfaces and stratal geometries as those described by the Exxon group, but places more emphasis on regional flooding surfaces as prac-

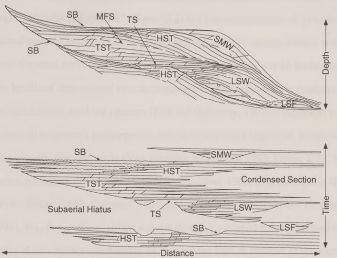

LEGEND

HST	**Highstand Systems Tract**
TST	**Transgressive Systems Tract**
LSW	**Lowstand Wedge Systems Tract**
LSF	**Lowstand Fan Systems Tract**
SMW	**Shelf Margin Wedge Systems Tract**
SB	**Sequence Boundary**
MFS	**Maximum Flooding Surface**
TS	**Transgressive Surface**

Figure 2.1 Exxon-type depositional sequence stratigraphic model depiciting depositional systems tracts and their bounding surfaces (after Haq and others, 1988). Geometry shown in top figure is in depth (as on a cross section), on bottom is in geologic time (as on a Wheeler or chronostratigraphic diagram).

tical sequence boundaries. The basis of the paradigm is that during periods of basin margin transgression, paleogeographies are redefined and drainage systems reorganized. Thus, the array of depositional systems represented by the rocks within a single "depositional episode" (Figure 2.2) is a logical succession of *genetically related* systems sharing common basin paleogeography, source area(s), and sediment dispersal pathways. Regional depositional episodes may be further subdivided into localized depositional events, composed of progradational, aggradational, and retrogradational stacking patterns (Xue and Galloway, 1993) comparable to the depositional sequence's parasequence sets and component highstand, lowstand, and transgressive systems tracts (Van Wagoner and others, 1988; Figure 2.3). In many basins, including the Gulf of Mexico (Armentrout, 1991; Schaffer, 1990; Galloway, 1989b; Miller, 1989; Coleman, 1990) and North Sea (Underhill and Partington, 1993), flooding surfaces (often seismic downlap surfaces) are represented by radioactive shales widely correlatable on gamma-ray logs, in contrast to the localized "unconformity" and difficult to identify "correlative conformity" of Mitchum and others (1977). If fact, the high degree of correlatability of high gamma markers in the North Sea has been demonstrated for Jurassic sediments by Underhill and Partington (1993) and Partington and others (1993), and for Paleogene deposits by Knox and others (1981) and Mudge and Copestake (1992). Galloway (1989a) also stressed the importance of regional tectonics as an influence on sediment source areas and the quantity and texture of clastic sediments preserved in a sequence, and the role of slope and basin floor deposition during the transgressive phase via retrogradational slumping.

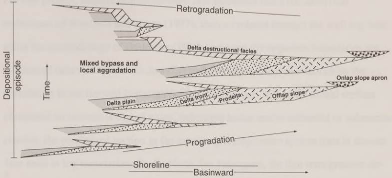

Figure 2.2. Chronostratigraphic representation of a depositional episode (Frazier, 1974) illustrating lateral and vertical depositional environment associations in a single basin margin pulse of sediment (after Galloway, 1989a).

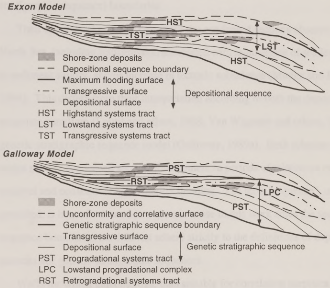

Figure 2.3. Comparison of Vail/Exxon depositional sequence model with Galloway genetic stratigraphic sequence model. Surfaces recognized are the same but packaging and naming of components is different (after Xue and Galloway, 1993).

For this project, seismic sequences were first identified using the analytical techniques of Mitchum and others (1977), then correlated through the well log data using the methodology of Galloway (1989a) wherein the sequence boundaries are condensed intervals. Seismic downlap surfaces are condensed intervals so the correlation to the tie-well is straightforward. However, where the stratal surface correlated on seismic is one of onlap, indicating hiatus and/or subaerial or submarine erosion, the condensed section in the overlying transgressive system tract is the surface used in log correlation. In the North Sea Paleogene, the thin transgressive deposits relative to lowstand deposits (Neal, 1992) typically results in a small stratigraphic distance between the seismic (depositional sequence) and well log (genetic stratigraphic sequence) boundaries.

Their are several possible causes for the condensed sections observed in the North Sea, including transgression associated with relative rise of sea level, decrease in sediment supply, and/or increase in tectonic subsidence (Mudge and Bujak, 1994). This differs from their interpretation according to both the depositional sequence paradigm (Loutit and others, 1988; Van Wagoner and others, 1990) and genetic stratigraphic sequence model (Galloway, 1989a). Both schemes restrict major marine condensed section development to periods of relative or eustatic rise of sealevel and consequent basin margin flooding. The term "sequence", unless further specified, is henceforth used in a generic sense in this work since the sequences and sequence boundaries used do not adhere strictly to the definitions of depositional sequences nor genetic stratigraphic sequences.

Wells for which paleontologic data suitable for correlation purposes were available were used to date sequences and important unit boundaries. These were chiefly the 33 wells studied by Gradstein and others (1992, 1994) and about ten others with proprietary information. Where the combination of seismic and well log data did not provide a unique interpretation of the correlation, paleontologic age information was especially useful. Cross sections derived from both seismic interpretations and reduced-scale digital well logs were useful for both correlation purposes and in visualization of the larger patterns and trends in basin filling.

2.2 Methods of Lithostratigraphic Analysis and Mapping

Once the sequences comprising the Eocene section were identified and correlated on seismic data and well logs, lithostratigraphic maps of the distribution of sediment thickness and framework sands were drawn. Framework or bed-load sand distribution reveals the skeletal architecture of a clastic sediment dispersal system and provides an indication of sediment sources and component depositional systems (Galloway and Hobday, 1983). Although it is often desirable to have a structure map for each unit under consideration, in order to assess the influence of structure on sediment dispersal and accumulation patterns, North Sea Eocene structure is so simple that maps of successive structural datums basically reflect the infill of sediment from one sequence to the next, an evolution better studied with isopach maps. A structure map at the base of the Eocene sets the scene for subsequent Eocene deposition. In addition, for each sequence, isopach, net sandstone, percent sandstone, log facies and paleogeographic maps were compiled.

Isopach maps of each sequence were created by subtracting the depth at the top of each sequence from that of the underlying sequence boundary. As with the base Eocene structure, seismic data were incorporated to accurately map the updip limits of each unit and inter-well variations in sequence thickness. Time-to-depth conversion was made using the nearest or otherwise most applicable velocity information, either a velocity log (preferred) or seismic stacking velocities. Maps of the unit thickness are useful for understanding its distribution, sediment sources, and depocenters.

For purposes of sandstone identification, it was necessary to establish a gamma-ray reading which was considered to reflect the presence of reasonably clean sand within each well. A common practice is to establish a shale baseline, a gamma-ray or spontaneous-potential reading which characterizes the shale units, then assign a particular distance, such as halfway from the baseline to the maximum sand deflection, as the sandstone cutoff. As discussed above, there is not a gamma-ray cutoff which is useful basinwide or even regionally in the North Sea basin to differentiate sand from silt. In the Paleocene and Eocene section, this is partly attributable to the varying fraction of clay-rich pyroclastics of low natural radioactivity in the sediments (Berstand and Dypvik, 1982). Wells with composite logs, most of which include reliable lithologic information, were straightfoward. For wells without other information, gamma-ray cutoff values were estimated from interpretations of sandiness based on known sandstone intervals (such as the Frigg sandstone, where present) or extrapolated from nearby wells. Once a cutoff value is determined for a well, its application to the Eocene section allows calculation of the net sand thickness and sand percentage (Figure 2.4).

Net sand maps show the total thickness of sand for each sequence. While net sand maps indicate the absolute amount of sand within a unit, percent sand maps indicate the *relative* sandiness, regardless of the total thickness. The maps are often

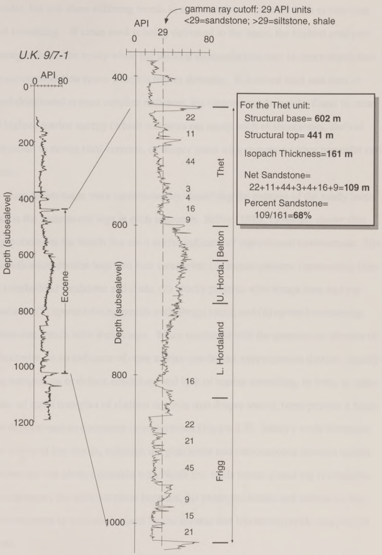

Figure 2.4. Method of unit thickness, net sand and percent sand calculation.

similar, but can show differing trends in sand distribution related both to sourcing and reworking. If clean sand is being delivered to the basin, the highest sand percentages should be updip while the thickest accumulations may be more dependent on accommodation space which is higher downdip. If a mixed sand and mud or mud-dominated system supplies sediment, the cleanest sands *may* be found in areas of highest marine energy (which winnows out mud), such as shorezones, shelves subjected to strong tidal currents, or deeper areas with contour or other powerful currents.

Log facies maps were constructed by classifying the patterns of the sandy interval on the gamma-ray logs in each sequence. Selley (1976, 1979) has shown that log patterns in the North Sea are a useful indicator of depositional environment. His classification divides logs into four categories: (1) serrate patterns representing thinly interbedded sandstone and shale, (2) blocky patterns with abrupt base and top contacts, (3) upward-fining motifs with abrupt bases, and (4) upward-coarsening grain-size trends with abrupt tops. When combined with the presence or absence of glauconite, as an indicator of open marine conditions, carbonaceous detritus, signifying terrigenous or deltaic conditions and lack of marine reworking, or both, an indicator of rapid transport of shallow deposits into deeper water), these provide a basis for depositional environment interpretations (Figure 2.5). Selley's work illustrates the utility of log motifs, although the glauconite and carbonaceous material qualifications are not always possible with North Sea wells unless a mud log is available. Furthermore, the differentiation between, for example, deltaic and submarine fan environments is well-constrained by the seismic and lithostratigraphic mapping of units.

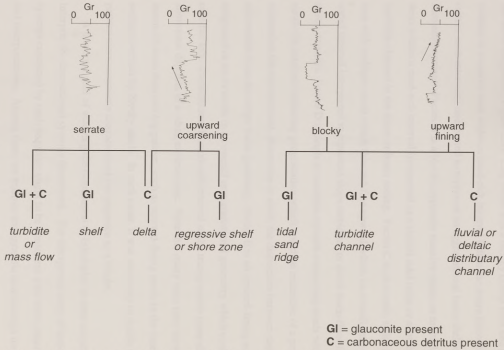

Figure 2.5 Flow chart for deducing possible depositional environments from log character combined with presence/absence of glauconite and plant debris (After Selley, 1976.)

Their map distribution indicated that of the ten initially defined log motifs, five were the most diagnostic (Figure 2.6). Log facies A is a blocky (sharp base and top) bedded or massive sand within a sand-rich interval (often the entire Eocene is sand-rich in such intervals) interpreted to represent an aggradational inner shelf or shoreface environment. Facies B is a blocky, typically massive single or multiple sand units within a mud-rich interval interpreted as a shelfal tidal ridge or submarine turbidite channel in the slope or basin setting. Facies C is an erratic, spiky log pattern with multiple sands which thin and fine upward within an overall mud-dominated interval interpreted to represent slope turbidites or distal basin-floor fan and apron deposits. Facies D is single or multiple upward-coarsening sands within a sand-rich interval indicating progradation which could be indicative of a proximal submarine fan environment, shorezone or shelf, the distinction between should be discernible from the larger basin geometry. Facies E is an upward-fining and thinning sand or set of sands in an overall retrogradational geometry which could indicate fan lobe abandonment in mud-rich interval or the transgressive inner shelf and shorezone deposits of a shelf environment. Note that many units may show elements of more than one log pattern, such as upward-fining sands in the base of the section overlain by blocky sands. In such cases, it was necessary to decide which pattern more accurately characterized the sequence as a whole.

A principal goal of studying the distribution of lithofacies in each sequence is to interpret the depositional systems framework. The interpreted array of depositional systems contained by each sequence ought to be consistent with other observations and interpretations. Among these are seismic stratigraphic relationships including stratal geometries and seismic facies (reflection amplitude and continuity), litho

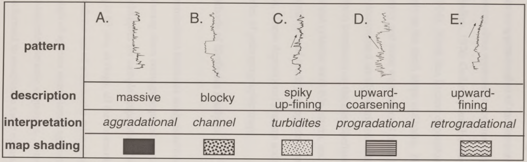

Figure 2.6 Eocene log patterns. The five motifs shown were those used in Chapter Four log motif maps, shaded using the patterns indicated. The example logs shown are actual gamma-ray logs from North Sea wells, with increasing gamma values from left to right.

logic information from well logs, and three-dimensional lithofacies distributions defined by net sand, percent sand, and log motif maps. Log motif mapping commonly provides an approximation of the depositional systems distribution in that common log patterns often represent a common depositional setting (Galloway, 1968; Fisher, 1969; Selley, 1976; Galloway and Hobday, 1983; Armentrout and others, 1993; Xue, 1994). North Sea Eocene depositional systems include marine clastic environments on the shelf, slope and basin. No major delta systems were observed seismically and none were inferred from mapping, although Condon and others (1992) documented areally restricted middle Eocene tidally-influenced deltaic deposits from boreholes on the East Shetland Platform. The basic range of important depostional systems were tide, storm, and wave-reworked shelf systems, sandy progradational and muddy retrogradational slope aprons, and basinal submarine fan systems. These depositional systems and other pertinent information were compiled on a series of paleogeographic maps.

2.3 Methods of Biofacies Analysis

Foraminiferal biofacies analysis of the Eocene section on the outer shelf was performed using ditch cuttings acquired for Unocal well UK 9/12-2. Following standard techniques for sample preparation (boiling in sulfinated amine to disaggregate, sieving at 63 μm, drying), all the foraminifera in each sample were picked and identified with the aid of a binocular microscope. Relative abundances of key species and groups of species were plotted against depth to determine their variation relative to the interpreted seismic sequences. Quantitative analyses, chiefly cluster analysis, were performed to establish a more robust, objective grouping of the biofacies represented by each sample. A model was applied which allowed interpretation of their paleoenvironmental and paleobathymetric significance which was compared to the interpretations from the stratal geometries and log lithofacies.

2.4 Methods of Subsidence Analysis

Geohistory, or subsidence analysis, is a method of sequentially decompacting and removing sedimentary layers ("backstripping") in order to deduce their original thickness, crustal subsidence due to loading by water and sediment, and subsidence, including negative subsidence (uplift), attributable to tectonics. By stripping off the layers of post-Eocene sediment for wells in the basin, one can estimate the amount of tectonic subsidence in the Eocene and compare it to that predicted by geodynamical models or to regional tectonic history. Furthermore, by decompacting the sediments, we can determine the relative rates of sediment accumulation in the basin.

An equation relating the pertinent factors which combine to produce subsidence in sedimentary basins was developed by Steckler and Watts (1978). The equation equates tectonic subsidence to the combined effects of sediment and water loading given a particular basement response to loading:

$$Y = \Phi\left[S^*\left(\frac{\rho_a-\rho_s^*}{\rho_a-\rho_w}\right)-\Delta SL\left(\frac{\rho_w}{\rho_a-\rho_w}\right)\right]+(WD-\Delta SL)$$

where

Y	=	loaded basement depth
Φ	=	lithospheric response to loading
S^*	=	uncompacted sediment thickness
ρ_a	=	mean density of the aesthenosphere (3.40 g/cm^3)

ρ_s^* = mean density of uncompacted sediments

ρ_w = mean density of sea water (1.0 g/cm^3)

WD = interpreted water depth at time of burial

ΔSL = height of sea level relative to today

Bond and Kominz (1984) developed a computer program to solve the subsidence equation given a sedimentary section of known thickness, lithology (including density and porosity), diagenetic cementation (including externally derived cement), geologic age, and paleowater depth. The least well-constrained variables in the Eocene of the North Sea are, in order of decreasing uncertainty, paleowater depth, original porosity, degree of cementation, and absolute age.

Chapter Three

SEQUENCE STRATIGRAPHY

3.1 Introduction

In this chapter, North Sea Eocene sequences are defined and documented, including their stratal architecture and bounding surfaces on seismic and well log data. The hierarchy of features, from the surfaces bounding the Eocene section, to the sequence boundaries, to intrasequence geometries and lithologies, are presented and discussed. Following definition of each sequence, it is illustrated on seismic lines and well log cross sections which demonstrate its attributes throughout the basin.

Initial well and seismic correlation defined the top and base of the Eocene within the Cenozoic basin fill. The base Eocene, top of the lower Eocene and top of Eocene are boundaries which are commonly marked in composite well logs and are within the resolution of the paleontologic information provided by F. Gradstein (Canadian Geological Survey). Using these data, rigorous correlations of the base and top of the Eocene were made and reconciled with the work on the Paleocene (Liu, in prep.) and Oligo-Miocene (Garber, in prep.). Once these bounding surfaces were established, finer subdivisions of the Eocene were made.

Five sequences are defined within the Eocene and have been informally named based on lithostratigraphic nomenclature in use when they were first defined. It is important to re-emphasize that these sequences are defined, chiefly, by bounding condensed intervals of chronostratigraphic significance. The lithostratigraphic units after which they are named are , naturally, defined based on their lithology and may be time-transgressive. By adopting the names of significant lithostratigraphic units which are contained within the sequence, the intention is to impart recognition of their approximate stratigraphic position to those familiar with North Sea stratigraphy (as practiced by Mudge and Bujak, 1994).

The sequences are, from base to top, Frigg, Lower Hordaland, Upper Hordaland, Belton and Thet. The relationship between these sequences and published lithostratigraphy is shown in Figure 1.5. The sequences record the evolution from the deep-water, sand-dominated Paleocene to the shoal-water, mud-dominated Oligocene. The Frigg sequence shares attributes of the Forties Formation while the Belton is more similar to the lower Oligocene. Figure 3.1 is a digitized interpretive section digitized from seismic line CNST 82-6, a line extending down the axis of the Moray Firth. The line is a key illustration of Paleogene sequences as it follows the axis of sediment input, and includes the most representative geometry of the sequences. Thick sand-prone sequences displaying continuous reflections on the Shetland Platform become thin, muddy, and show poor reflection continuity in the basin and onlap the Norwegian platform. Stratigraphically, the Frigg is basin-centered and onlapping, while the Hordaland sequences are preserved marginward, downlapping the Frigg and building across the basin. The Belton sequence is a thin unit with a Norwegian component of sediment input. The Thet is a prograded wedge of sediment perched along the margin of the Shetland shelf.

Figure 3.2 is a digital rendering of line 84-4 which crosses the Shetland Platform and Viking Graben about 150 kilometers north of line 82-6. At this position the Viking Graben is considerably wider and shallower. The contrast between the thick accumulation of Eocene sediments (about one second two-way travel time) on the British margin versus the thinner section (about 200 milliseconds) on the eastern

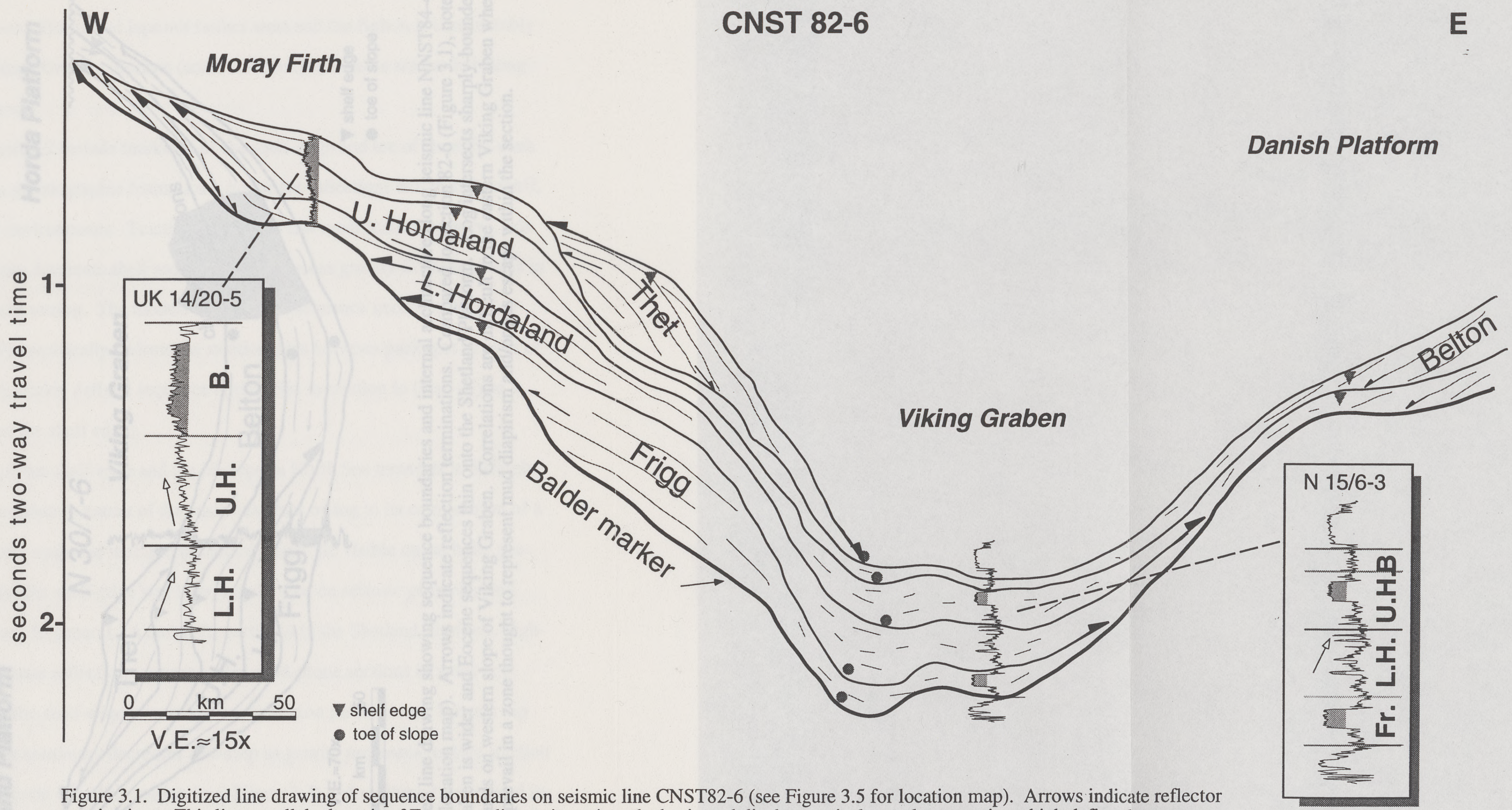

Figure 3.1. Digitized line drawing of sequence boundaries on seismic line CNST82-6 (see Figure 3.5 for location map). Arrows indicate reflector terminations. This line parallels the axis of Eocene sediment input into the basin and displays typical stratal geometries which define the sequences. Gamma ray log from a well on the shelf displays an upward-coarsening sandy Eocene section while another in the Viking Graben shows sand bodies with blocky log motifs encased in mudstone.

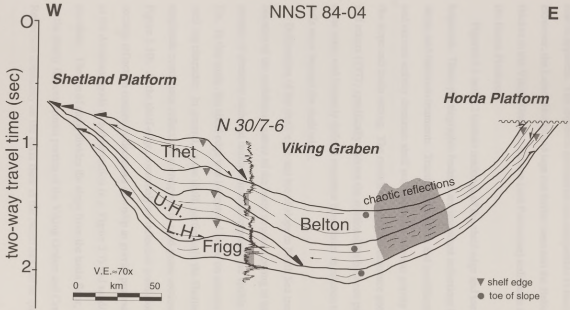

Figure 3.2. Digitized line drawing showing sequence boundaries and internal architecture along seismic line NNST84-4 (see Figure 3.5 for location map). Arrows indicate reflection terminations. Compared to section 82-6 (Figure 3.1), note how the Viking Graben is wider and Eocene sequences thin onto the Shetland Platform. Log intersects sharply-bounded Belton and Frigg sands on western slope of Viking Graben. Correlations are difficult in the eastern Viking Graben where chaotic reflections prevail in a zone thought to represent mud diapirism and/or gas escape within the section.

side is apparent. The sequence geometries are comparable to those in line 82-6. However, the Lower Hordaland laps out farther west and the Belton is considerably thicker in the Viking Graben. Eocene (and Paleocene) sediments are eroded along the Horda Platform.

Figures 3.1 and 3.2 include markings of the shelf-edge and toe of slope for each sequence. These physiographic features are important inflections between the shelf, slope, and basin environments. Traction deposition and modification by wave, tide and current activity dominate shelf sedimentation whereas gravity flow dominates in the slope and basin setting. The models of predicted sequence geometry by Vail and others (1977) specifically address the relationships between packages in each of these areas and formerly defined sequence boundaries in relation to them (Type 1 falls were beyond the shelf edge).

Delineation of the shelf-edge and toe of slope in North Sea transects is difficult because of the undulatory nature of the basin structure owing to its composition of a mosaic of elements such that multiple inflection points are visible on each dip profile. In this study, the shelf-edge was interpreted based on seismic geometry and well log character. In general, on the shelf, particularly the Shetland Platform, high-amplitude continuous reflections correspond to sand-prone sections in wells (*e.g.* Figure 3.10). At the shelf-edge, commonly an inflection point along a seismic dip section, reflection continuity decreases downdip as gravity processes replace traction as the dominant mode of sedimentation (*e.g.* Figure 3.7) and sand/mud ratios tend to decrease. The toe of slope divides the slope from the basin floor, which is taken to be the nearly flat centermost portion of the Viking Graben and Central Graben areas. Reflection continuity on the basin floor in the North Sea can be quite low to chaotic (e.g Figure 3.16) since basinal sediments are chiefly heterolithic, gravity-resedimented deposits. Basin floor fans with blocky log motifs, such as the Frigg Fan in the basinal Viking Graben, are differentiated from line-source fed slope aprons such as the Bruce accumulation on the Beryl Terrace.

With this brief overview of the Eocene sequences and their broad geometric relationships in mind, let us consider each of the units in detail beginning with a description of the base of the section: the Balder Formation.

3.2 Balder Tuff: base of the Eocene

As discussed in the section on published work, the Balder[1] Formation, a well-known airfall tuff deposited over much of northwest Europe and dated at about 53.5 Ma, is the logical division between Paleocene and Eocene strata, although it falls above the chronological Eocene boundary (Mudge and Bujak, 1994). The Balder Formation (Deegan and Scull, 1977; Knox and Holloway, 1992) is essentially equivalent to the Balder Tuff (Jacqué and Thouvenin, 1975; Malm and others, 1984) and to the Balder sequence of Mudge and Bujak (1994). It is a conspicuous seismic and gamma-ray marker due to its petrophysical properties (decreasing velocity, upward increasing gamma-ray response) which can be readily identified and traced across the seismic grid.

The Balder Tuff is the latest and largest in a hierarchy of Paleogene tephras deposited in the North Sea. It is the apparent culmination of the hot-spot activity which uplifted the Paleocene Shetland Platform, and is itself composed of a series of ash beds, up to 28 cm thick each (Malm and others, 1984; White, 1988). The for-

[1] In Norse mythology, *Balder* was the god of light and beauty.

mation averages about 50 m thick (Deegan and Scull, 1977), generally thickens northwestward (Knox and Morton, 1988), and shows a consistent "bell-shaped" log pattern reflecting increasing gamma-ray and decreasing sonic velocities (Figure 3.3) attributed to the gradual diminution of tephra deposition and decreasing thickness of individual beds. That the the Balder Tuff (with its characteristic diatom component, *Coscinodiscus* sp. 1) is preserved well onto the margins of the basin which indicates relative sea level was high during its deposition. The fact that the log and seismic character and ash thickness are uniform over such a large area suggests that little diluting clastic sediment was being deposited in the basin over the one to two million years of tuff accumulation (Jacqué and Thouvenin, 1975). The tuff, then, represents a period of reduced clastic sediment input and is capped by a condensed interval of both clastic and pyroclastic sediment starvation marked by a gamma-ray peak.

Having established the widespread distribution of the Balder, it is worth noting that there are localized exceptions to the generally low clastic input. Slope and basin sand deposits interfinger with the tuff, implying their contemporaneous deposition. The Balder Field (Norwegian Block 25/10 in the east Viking Graben) is an example and is described as a complex of southerly-prograded and channelized suprafan lobes (Sarg and Skjold, 1982). The reservoir sands at Balder Field are well-sorted, clean, and massive, as if derived from a source of clean, pre-sorted sand and transported cohesively in dense turbidity currents (Hanslien, 1987; Timbrell, 1993; Jenssen and others, 1993). Similar deposits occur on the Beryl Terrace in the Gryphon Field, which Newman and others (1993) interpreted as lowstand fans composed of amalgamations of "liquified flows". Timbrell (1993) invoked relatively low sea level for lower Balder sands on the Beryl Terrace and linked them to shelf

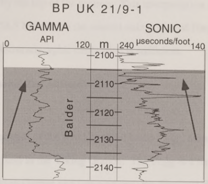

Figure 3.3 An example of the characteristic log signature of the Balder Formation. Gamma ray increases while sonic interval velocities decrease to form a "bell-shaped" pattern.

canyons and deltaic sediments on the outer Shetland Platform, and inferred a rapid rise and flooding by the top of the section. This interpretation is consistent with the 54.2 Ma fall and 53.5 Ma rise on the coastal onlap chart of Haq and others (1988), assuming Balder biostratigraphic calibration is sufficient.

3.3 Eocene Sequence Definitions

Frigg Sequence

The oldest sequence of the five identified is the Frigg, named for the Frigg[1] Field, a giant gas field in the Viking Graben. The Frigg is a basin-centered unit, thickest in the Viking Graben and thinning onto the Shetland Platform where it onlaps the Balder (Figure 3.1). Like most Paleogene units, it exhibits medium to variable amplitude continuous reflections on the outer shelf which pass gradually into variable amplitude, discontinuous reflections basinward. The top of the Frigg exhibits a high amplitude continuous reflection in areas where it marks the top of a thick (100-300 millisecond) sand accumulation. Heritier and others (1979) had sufficient control to map these reflections and the large submarine fans they represent (Figure 3.4). Elsewhere in the basinal setting, between sand lobes, a condensed section accumulated which can be traced over the top of the older sands as a gamma-ray peak. In its muddier lithofacies, the Frigg can be subdivided on the wireline logs into two units with a distinctive reddish colored clay marking the condensed section between the two. This log marker was correlated where possible as a "form line" (*e.g.* Viking Graben logs in Figure 3.17), but the subdivision is not identifiable or seismically mappable.

---

[1] *Frigg* was a mythological Scandinavian goddess, the wife of Odin (a satellite of the Frigg fan and a gas reservoir), mother of Balder. In teutonic mythology she was fused with Freya, for whom Friday is so named.

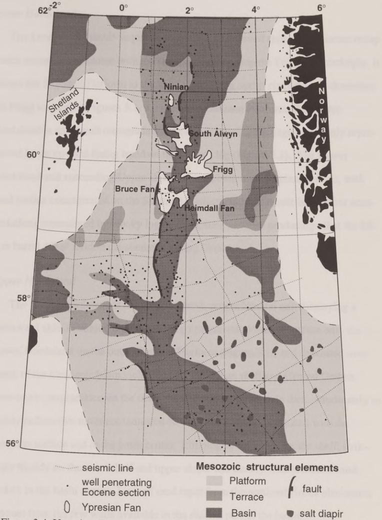

Figure 3.4 Ypresian (Frigg) sand distribution in the Viking Graben area (after Heritier and others, 1979). It is apparent that a closer grid of seismic and wells than that used in this study was necessary to map Frigg sand distributions. Note the Bruce Fan location on the Beryl Terrace.

Lower Hordaland

The Lower Hordaland[1] sequence represents a landward shift in submarine onlap which occurred coincident with the flooding surface atop the Frigg. Accordingly, it onlaps the Shetland Platform to the west of the Frigg updip pinchout and downlaps the Frigg sequence (Figures 3.1, 3.2). On the Shetland Platform, the Lower Hordaland is an overall retrogradational or backstepping package commonly represented by an upward-fining trend on the gamma log (Figure 3.1). The Lower Hordaland and succeeding Upper Hordaland are both mud-dominated units, with sand bodies concentrated on the Shetland Platform and in discrete basin floor accumulations represented by blocky log patterns, such as those producing oil at the billion barrel Alba[2] field in the southern Viking Graben.

Upper Hordaland

The Upper Hordaland is a mud-dominated, progradational unit displaying a basinward shift in coastal onlap, featuring a prominent downlap surface onto the Lower Hordaland on the outer Shetland Platform (Figure 3.1), and deposited over much of the Cenozoic basin including the Norwegian shelf and Central Graben. Low-angle progradation on the outer shelf is evident on seismic data. Moderately to highly radioactive muds are indicated on logs, particularly associated with the downlap surface and in the basin center. Lithologies are sandy on the shelf, strikingly muddy on the outer shelf and upper slope, and muddy with localized sand bodies in the basin center. Limited sand input from the northern Horda platform is evident from the few wells available in the eastern part of the basin.

---

[1] *Hordaland* is a Norwegian county on the coast; Bergen is the county seat and third largest city in that country.
[2] *Alba* was the Scottish kingdom formed in the ninth century by the unity of the Scots and the Picts.

Belton

A further basinward shift is represented by the Belton sequence, which is thin overall (less than about 100 msec), particularly on the shelf. Like the underlying Upper Hordaland, the Belton is widespread and includes a secondary component of sediment derived from Norwegian sources. Stratal geometries and lapouts are non-diagnostic for the sequence, thin as it is on the shelf, but a distinct medium to high amplitude seismic facies in the basin distinguishes it from the underlying Hordaland and overlying, typically low-amplitude Oligocene sequences. The Belton is a distinct genetic stratigraphic sequence in logs as it is bounded by thin, hemipelagic radioactive beds, particularly at the top which is a basinwide hiatal surface marked by a strong gamma-ray peak. Lithologically, the Belton is a mixed sand and mud system with thin, turbidite sands indicated on basin-center logs.

Thet

A major basinward shift in coastal onlap is apparent from the outer shelf position occupied by the upper Eocene Thet sequence, a progradational prism of sediments visible on seismic along the length of the outer Shetland Platform (Figure 3.1). The Thet onlaps the Belton near the Belton shelf edge and downlaps it near the base of slope. It is displays internally continuous reflections in an offlap geometry indicating progradation and at least one further basinward shift. Mixed sand and mud lithologies characterize this shelf-margin wedge of sediment. These are typically massive or upward-coarsening sand bodies updip grading laterally to thinner sand units downdip.

3.4 Seismic and Well Log Sequence Characterizations

The purpose of this section is to document the Eocene sequences as they are manifested in seismic and well log data. Because of the great quantity of analog and digital data used in subdividing and correlating the sequences, it is not possible to present all of it. However, nine representative portions of seismic sections are reproduced and nearly 100 digitized gamma-ray logs are shown in reduced-scale cross sections (Figure 3.5).

Representative seismic examples are reproduced to illustrate the stratal geometries displayed by the sequences on seismic sections and on selected digitized, time-converted, gamma-ray log segments. Seismic lapouts, termination of a reflection against another in a way thought stratigraphically meaningful (Mitchum and others, 1977), are marked with arrows. Most of the reproductions are at the same scale as that at which the seismic which was interpreted. The vertical exaggeration, based on the average thickness of the Eocene section in nearby wells, is given but should be regarded only as an approximation since the vertical axis is two-way travel time and not depth.

A series of cross sections depicting the sequence expression on gamma-ray logs is a useful means of examining the lithostratigraphic relationships within and between sequences. The sections illustrated are but a fraction of those produced for correlation purposes. The sections are displayed in depth (meters), as measured from mean sea level (by subtracting the kelly bushing height from the log depth). Sea level is the datum, as opposed to the top Eocene, in order to preserve the true structure of the section. This produces a compressed Eocene section since although it is generally about one kilometer thick, it spans a depth of about 2,500 meters. For

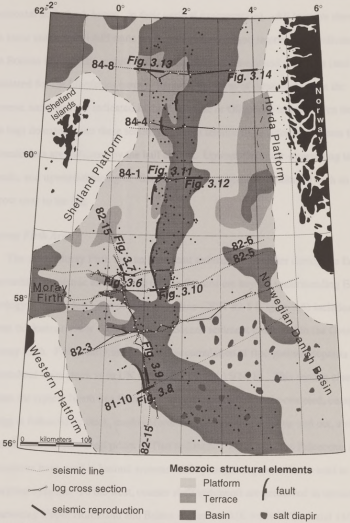

Figure 3.5 Location map indicating portions of seismic lines reproduced and wells in log cross sections presented in succeeding figures. Shading refers to Mesozoic structural elements presented in Figure 1.1.

comparison between sections, all are at the same vertical scale, but vary in their horizontal scale (and, hence, in their vertical exaggeration). All logs are shown at the same scale, 0-100 API units on the gamma-ray. Sand intervals are indicated for the Eocene in the wells as determined from the gamma-ray and mud logs (and as tabulated for the lithofacies maps). Because the focus of these sections is the Eocene, sand was *not* indicated in the Paleocene or Oligocene interval even though the logs do extend into these sections. Lapout relationships determined from the seismic data are indicated by the half arrows. Upward-fining or -coarsening textural trends, and upward-thinning or -thickening of sand beds, are indicated with an open arrow next to the log.

Moray Firth Area

The outer Moray Firth was an important sediment depocenter during the Eocene. Accordingly, seismic and well log data in the area are keys to understanding Eocene geology. A well log cross section along line CNST 82-5 (Figure 3.6) includes a great thickness (nearly 1000 meters) of Eocene sediment preserved in the Outer Moray Firth. Particularly notable is the accumulation of fine-grained deposits in the Hordaland units (such as in UK wells 15/23-3 and 15/24-1). This section also illustrates the typical North Sea Eocene sequence geometry: a basin-centered, onlapping Frigg is followed by thick, muddy Hordaland units which build up and out, a thin Belton, and the fore-shelf prism of Thet sediments. Also, as in the Paleocene, older sequences have sand in basinal systems while younger sequences have sand in marginal systems. To the west, coarser shelf sediments are preserved in upward-coarsening Upper Hordaland and Belton sequences (UK wells 14/29-2 and 14/29-1). Progradation is also evidenced in the Thet by upward-decreasing gamma response

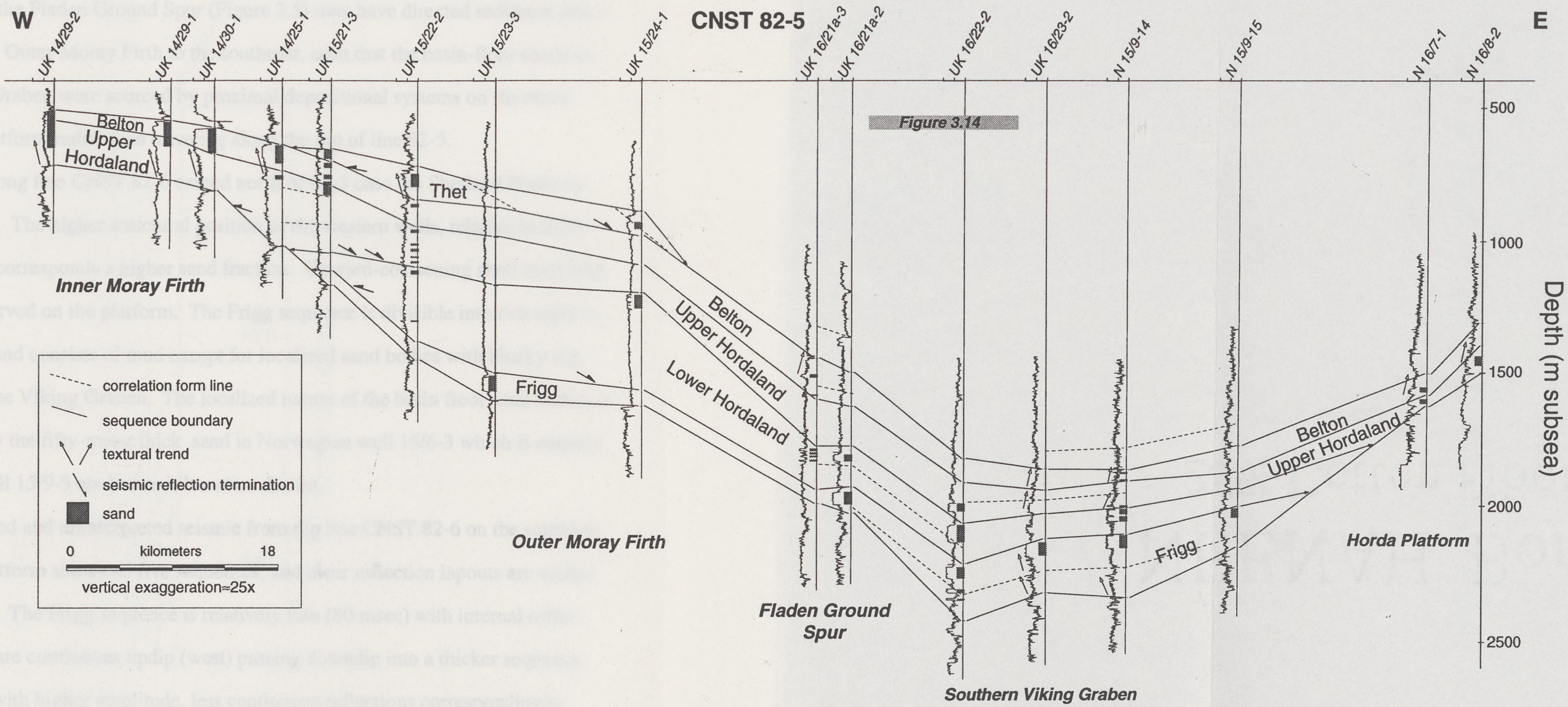

Figure 3.6 Log cross section along seismic line CNST82-5. See Figure 3.5 for location. Shaded rectangle indicates position of seismic example shown in Figure 3.14. Sandy updip section near south Shetland Platform sources to west is distinctly argillaceous at mid-dip position in the Outer Moray Firth. Sharply-bounded basin floor sand bodies found on basin floor in Viking Graben. Note the thick Lower Hordaland accumulation of mud in the Outer Moray Firth.

(such as well UK 15/22-2). In the southern Viking Graben, sand bodies with blocky gamma signatures diagnostic of basin floor fans are present. Note, however, that the presence of the Fladen Ground Spur (Figure 3.5) may have directed sediment delivery from the Outer Moray Firth to the southeast, such that the basin-floor sands in the Viking Graben were sourced by proximal depositional systems on the outer Shetland Platform rather than traveling along the dip of line 82-5.

Wells along line CNST 82-6 extend north of 82-5 onto the Shetland Platform (Figure 3.7). The higher structural position of the western wells, relative to those along 82-5, corresponds a higher sand fraction. Upward-coarsening shelf sand bodies are preserved on the platform. The Frigg sequence is divisible into two units in some wells and consists of mud except for localized sand bodies with blocky log patterns in the Viking Graben. The localized nature of the basin floor sand bodies is illustrated by the fifty-meter thick sand in Norwegian well 15/6-3 which is entirely absent in well 15/9-3 about two kilometers distant.

Interpreted and uninterpreted seismic from dip line CNST 82-6 on the southern Shetland Platform shows all five sequences, and clear reflection lapouts are visible (Figure 3.8). The Frigg sequence is relatively thin (80 msec) with internal reflections which are continuous updip (west) passing downdip into a thicker sequence (300 msec) with higher amplitude, less continuous reflections corresponding to mudstone in well 15/18-2. The Lower and Upper Hordaland have more continuous reflection character displaying a progradational geometry represented at the well location by sharply-bounded sand units encased in mud.

To the south, logs from wells along seismic line CNST 82-3 on the Western Platform reveal about 80 meters of sandy, upward-fining Upper Hordaland in the

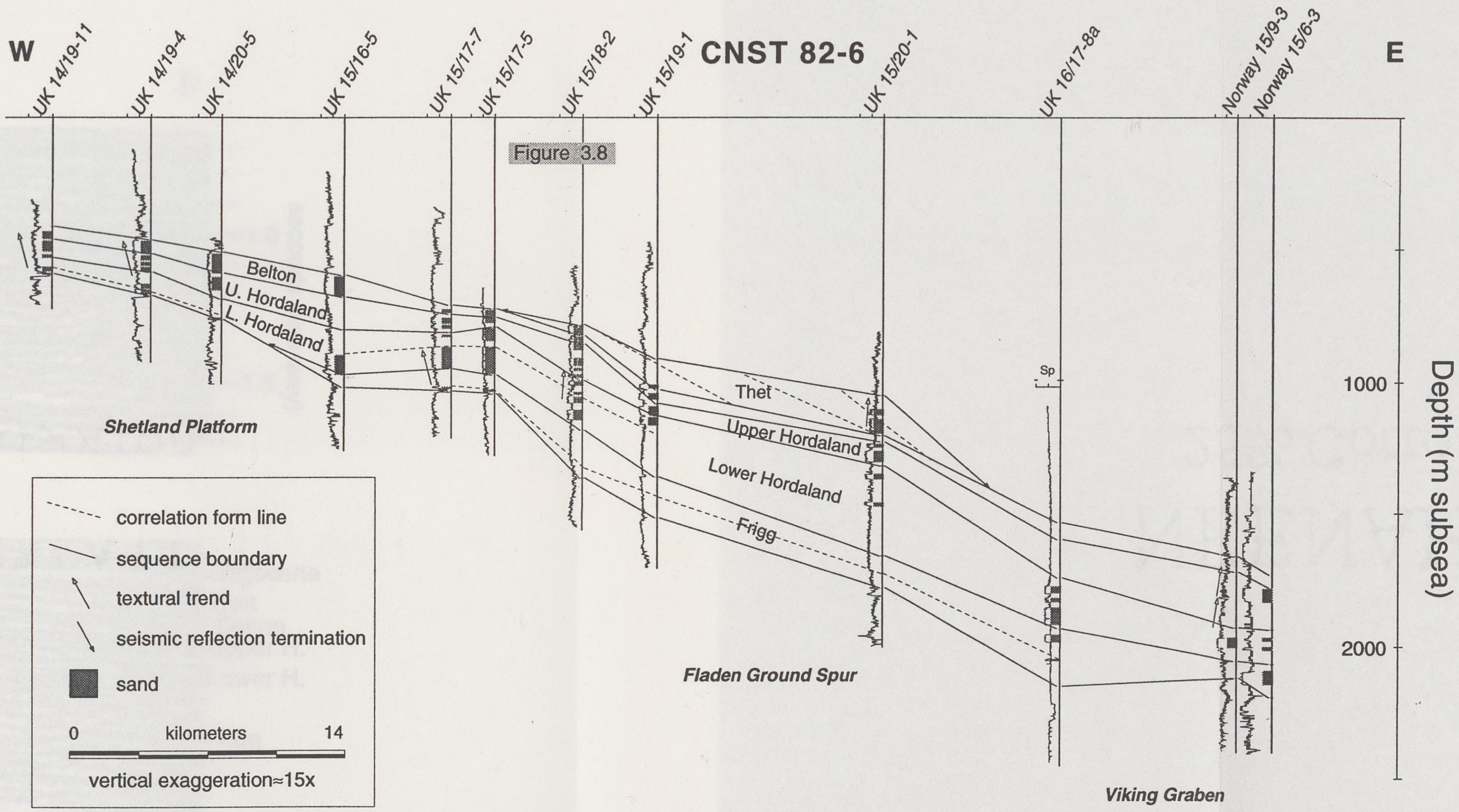

Figure 3.7. Log cross section along seismic line CNST82-6. See Figure 3.5 for location. Shaded rectangle indicates extent of the portion of seismic shown in Figure 3.8. A sandy shelfal section is equivalent to mud-prone basinal sequences in which isolated sand bodies display blocky log patterns. Westernmost wells include upward-coarsening progradational units. The Frigg sequence can be subdivided in by a hemipelagic mud in some wells. Thet progradation is apparent on seismic.

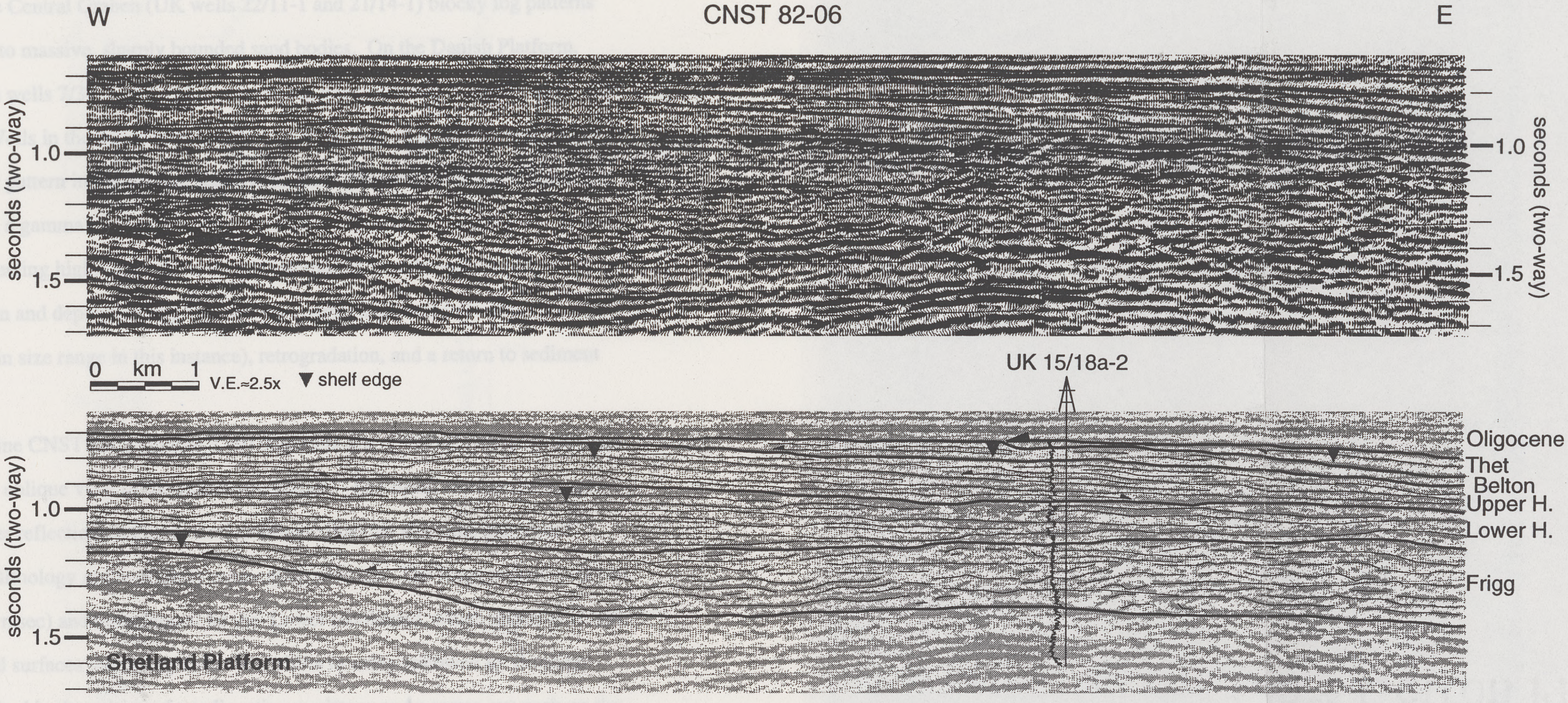

Figure 3.8 A portion of seismic line 82-06 in the Moray Firth. See Figure 3.5 for location map. Mid-dip position includes most Eocene sequences at an outer shelf position with the shelf to the west (left) and basin to the east (right). Arrows indicate reflection terminations, such as the downlap of the Upper Hordaland onto the Lower Hordaland, and the onlap of the Belton onto the Upper Hordaland, toplap of intraThet reflections. This line illustrates the transition from good continuity of reflections on the shelf (to left) grading to less continuous reflections basinward (to right).

Central Graben within a mud-dominated section onlapping the Danish Platform to the east (Figure 3.9). The Frigg sequence is thin and muddy, onlapping the basin margin. Hordaland sequences span the basin, and include sand bodies in the upper unit . In the Central Graben (UK wells 22/11-1 and 21/14-1) blocky log patterns correspond to massive, sharply bounded sand bodies. On the Danish Platform, (Norwegian wells 7/3-1 and 17/10-1) serrate log patterns indicate intercalated muds and silts. Wells in the basin, (*e.g.* UK 22/8-1) include good examples of a "bow-shaped" log pattern in the Eocene sequences. Each genetic stratigraphic sequence begins with a gamma high, gradually decreases to a low, then builds back to to a sequence-bounding high. This succession is interpreted as sediment starvation, progradation and deposition of progressively coarser sediment (all within the mud and silt grain size range in this instance), retrogradation, and a return to sediment starvation.

Strike line CNST82-15 (Figure 3.10) intersects line CNST82-6 (Figure 3.8) and displays an oblique view of the stratal geometries. The strike section shows generally higher reflection continuity and amplitude than the 82-6 line and a sand-dominated lithology at this slightly more updip position. The Frigg sequence is thin (about 100 msec) and downlapped by the Lower Hordaland, which includes at least two internal surfaces indicating downward shifts in onlap followed by flooding which resulted in deposition of a radioactive mudstone and gamma-ray peak on the well logs. The thin Upper Hordaland onlaps and downlaps the underlying unit and, at well 15/12-1, is capped by a condensed interval.

Wells along line CNST 82-15 (Figure 3.11) intersect the above three log sections from the Shetland Platform to the Central Graben (Figure 3.5). Shelfal wells indi-

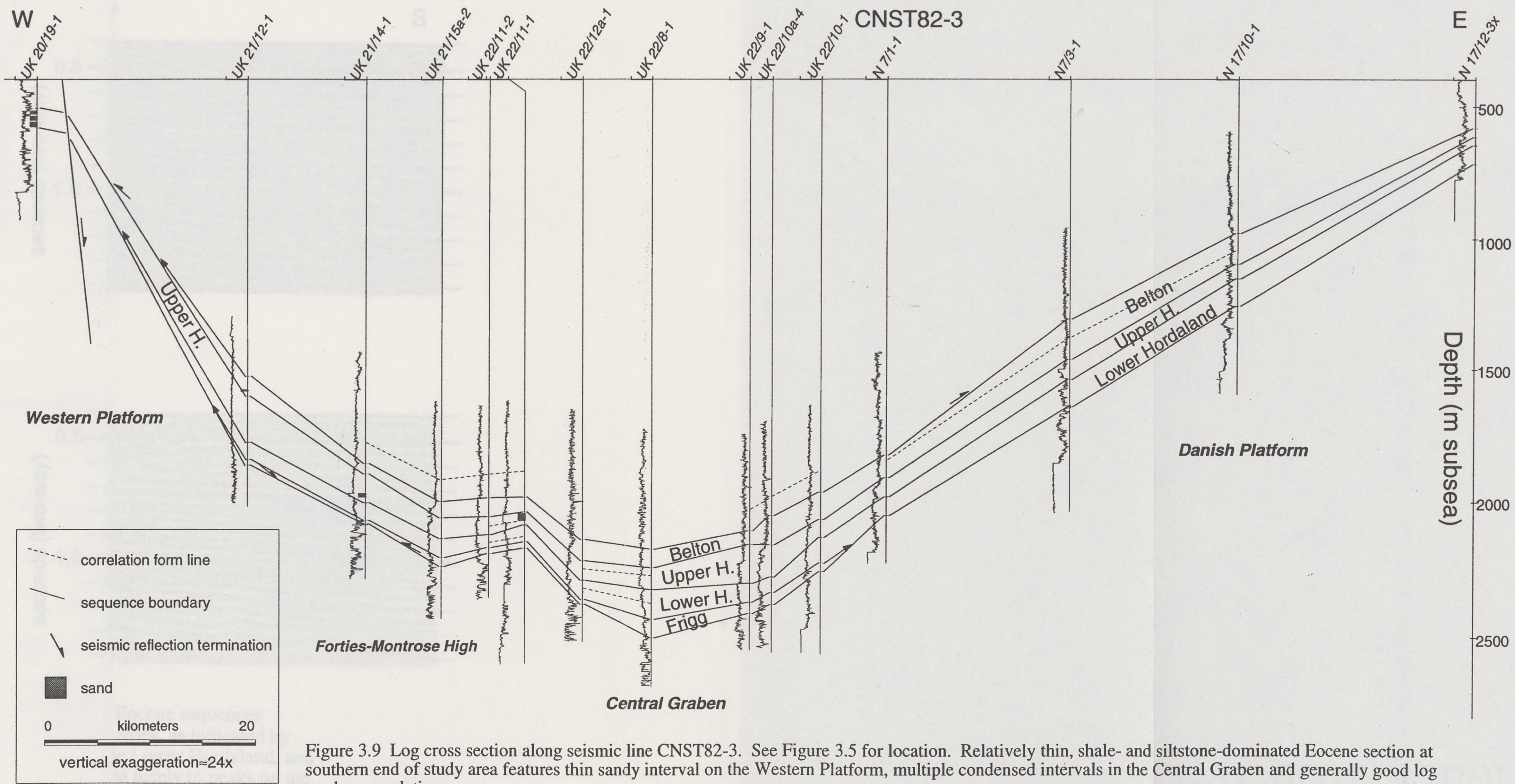

Figure 3.9 Log cross section along seismic line CNST82-3. See Figure 3.5 for location. Relatively thin, shale- and siltstone-dominated Eocene section at southern end of study area features thin sandy interval on the Western Platform, multiple condensed intervals in the Central Graben and generally good log marker correlation.

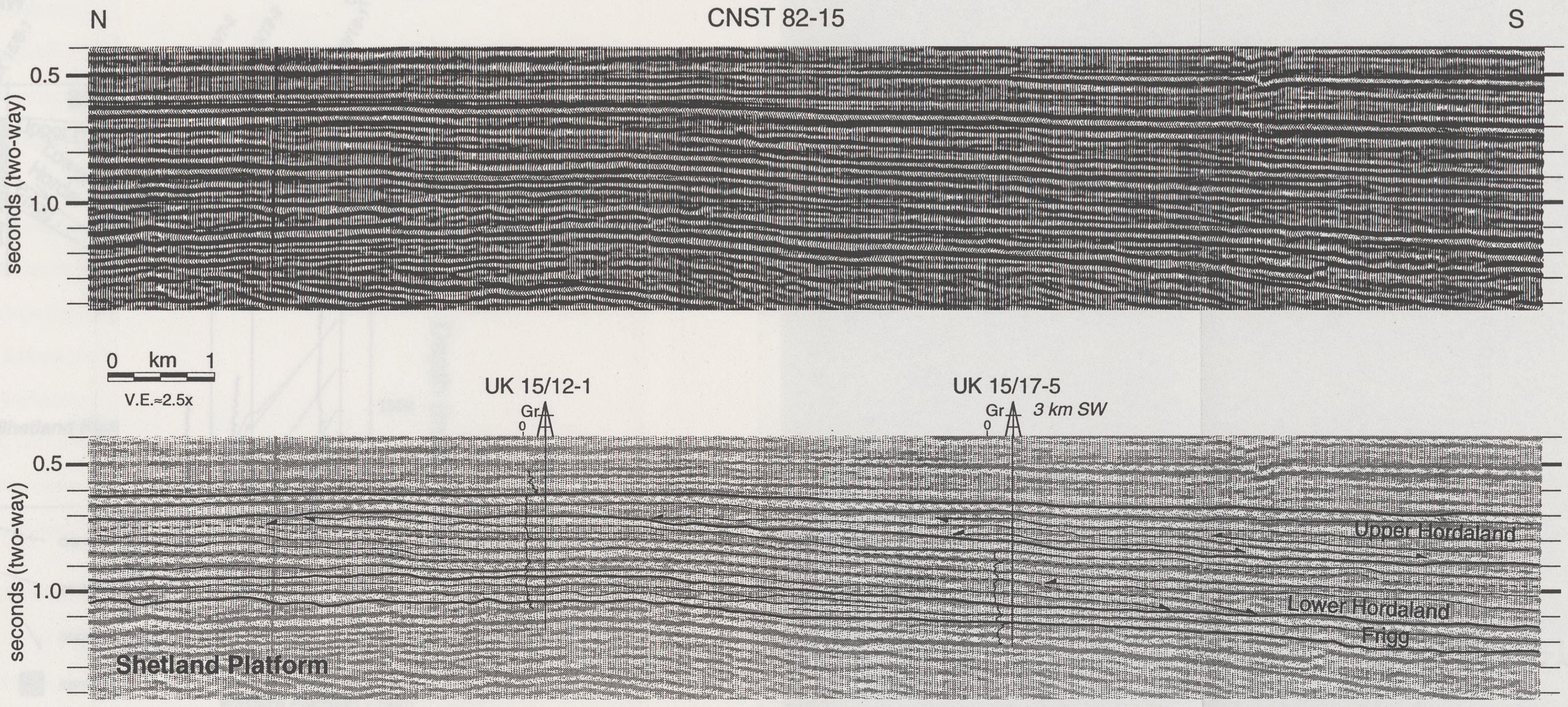

Figure 3.10 A portion of seismic line 82-15 along the southern East Shetland Platform. See Figure 3.5 for location. The three Eocene sequences preserved this far updip are predictably sand-prone, as evidenced by the gamma ray logs from two wells. Detailed stratal geometries, as indicated by arrows marking reflector terminations, include Lower Hordaland downlap onto the Frigg, a minor basinward shift in onlap in the Lower Hordaland, and onlap of the Upper Hordaland onto the Lower Hordaland. Two subregional onlap surfaces within the Lower Hordaland correlate nicely to peaks on the gamma ray logs from both wells.

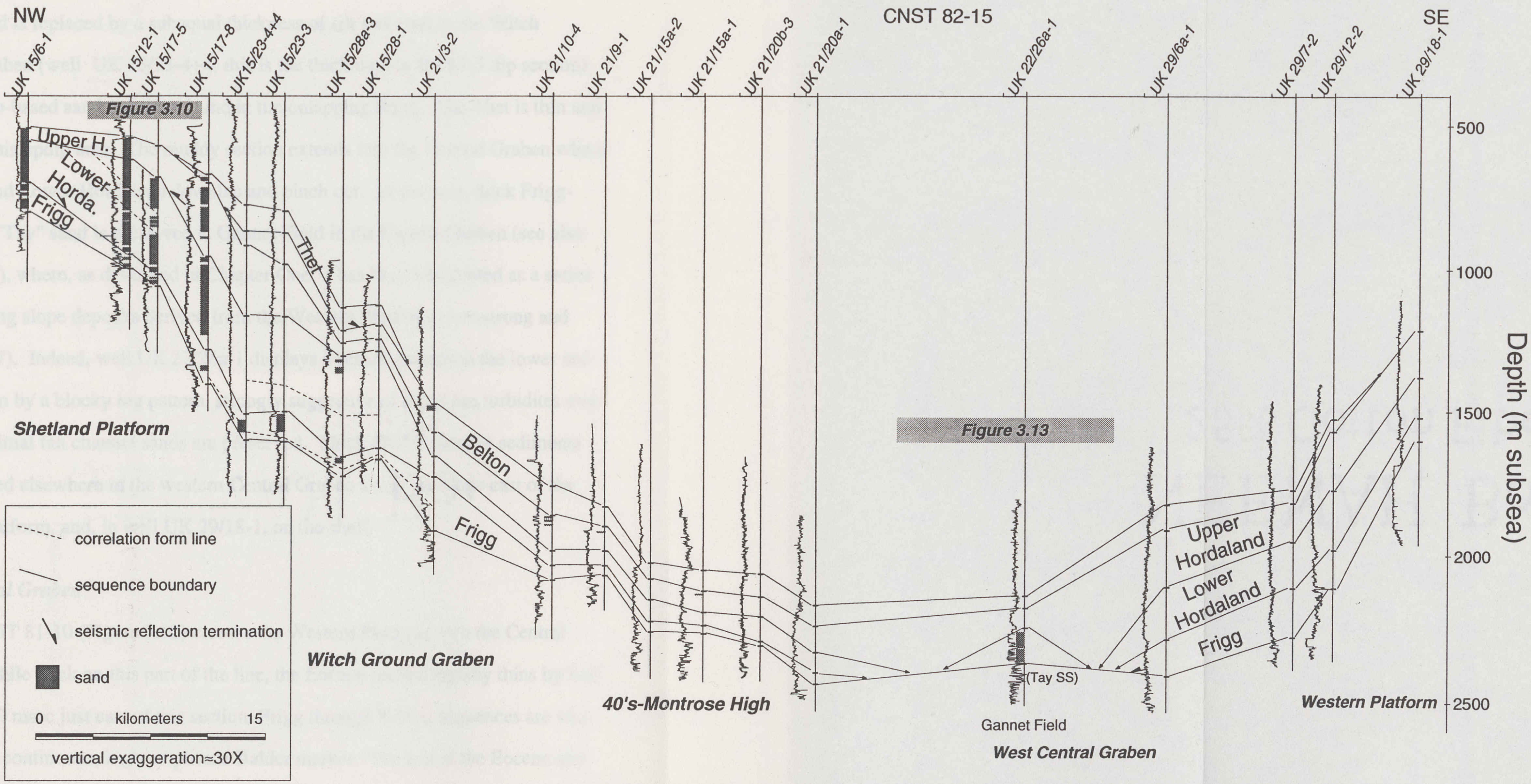

Figure 3.11 Log cross section along seismic line CNST82-15. See Figure 3.5 for location. Despite appearances, this is not a dip section but a strike section. Updip sands to the northwest were transported across the plane of the section. Note the absence of Eocene sand in Witch Ground Graben basinal wells. The Western Platform section is notably argillaceous.

cate a thick (over 300 meters) sand-dominated updip Lower Hordaland, including three local subunits (in wells 15/12-1 and 15/17-5). The sand disappears quite abruptly and is replaced by a subequal thickness of silt and mud in the Witch Ground Graben (well UK 15/23-4+4; this is the thick mud in the 82-5 dip section) where sharp-based sand units are found in the onlapping Frigg. The Thet is thin and muddy in this updip area. The muddy section extends into the Central Graben where the Frigg and Lower Hordaland downlap and pinch out. A discrete, thick Frigg-equivalent "Tay" sand is preserved at Gannet Field in the Central Graben (see also Figure 3.13), where, as described in Chapter One, it has been interpreted as a series of prograding slope deposits derived from the Western Platform (Armstrong and others, 1987). Indeed, well UK 22/26a-1 displays a serrate pattern in the lower section overlain by a blocky log pattern, strongly suggestive of distal fan turbidites over which proximal fan channel sands are preserved. Thick muddy Eocene sediments are preserved elsewhere in the western Central Graben along the slope east of the Western Platform, and, in well UK 29/18-1, on the shelf.

West Central Graben

Line CGT 81-10 (Figure 3.12) crosses the Western Platform into the Central Graben. While thick on this part of the line, the Eocene section rapidly thins by half to about 200 msec just east of this section. Frigg through Belton sequences are visible above a continuous, high-amplitude Balder marker. The top of the Eocene and of the Belton unit is, in typical fashion, characterized by high-amplitude reflections above which is a zone of lower Oligocene sequence low-amplitude reflections. Disruption of the section (basinwide "hydrofracturing" according to Cartwright, 1994) gives the appearance of dipping or shingled, even downlapping reflections

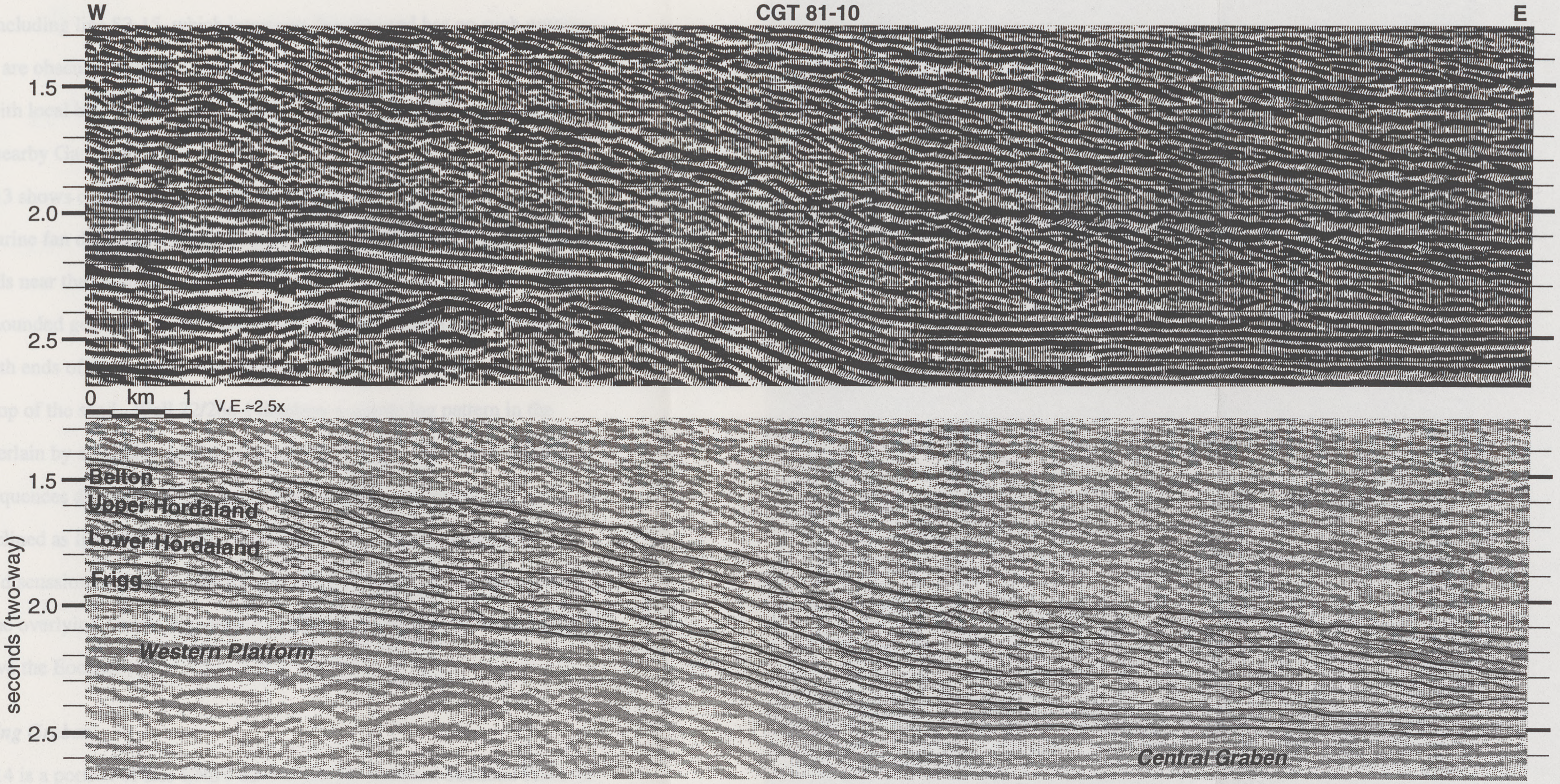

Figure 3.12 Western end of seismic line 81-10 along the Western Platform and slope of the Central Graben. See figure 3.5 for location map. Nearby wells indicate the sediments within these packages, which thin rapidly eastward, are chiefly mud. The Eocene and overlying Oligocene section have been disturbed by faulting, interpreted by Cartwright (1994) as hydrofracturing, which obscures the section.

which pass through the subhorizontal surfaces known to be the actual stratal surfaces. Therefore, sequence-defining stratal surfaces, such as are apparent on the CNST grid (including line 82-15, which intersects this line and has no such processing artifacts), are obscured. Nearby wells indicate a chiefly argillaceous Eocene succession, with local basinal sand bodies found in the Belton and Frigg sequences (the latter at nearby Gannet Field).

Figure 3.13 shows characteristically thin Central Graben Eocene and Frigg sequence submarine fan development at the southern end of line 82-15. Frigg-equivalent Tay[1] sands near the Gannet[2] Field form a classic stratigraphic trap and display seismically mounded geometry. The Balder Tuff seismic marker (visible at the north and south ends of the section) is downlapped by the high-amplitude reflection marking the top of the sand. Well 22/26a-1 displays a serrate log pattern in the lower Tay overlain by a massive sand unit in the upper zone. The Upper Hordaland and Belton sequences display medium amplitude discontinuous reflections, some of which, are inclined as if by differential compaction over the underlying Frigg mound. (For discussion of this complexity, see Timbrell, 1993 and Jenssen and others, 1993.) The overlying lower Oligocene is distinguished by a very low amplitude zone just above the Eocene.

Southern Viking Graben

Figure 3.14 is a portion of line CNST 82-5 along the southern Shetland Platform, a feature known as the Fladen Ground Spur, and east into the southernmost Viking

---

[1] *Tay* is the name of a Scottish firth on the North Sea coast.
[2] Shell U.K. named prospects alphabetically, starting with "A UK". This scheme was abandoned before the sixth prospect and the Auk discovery began a tradition of using bird names. A *gannet* is a large bird that nests on rocky coasts and is related to the tropical booby.

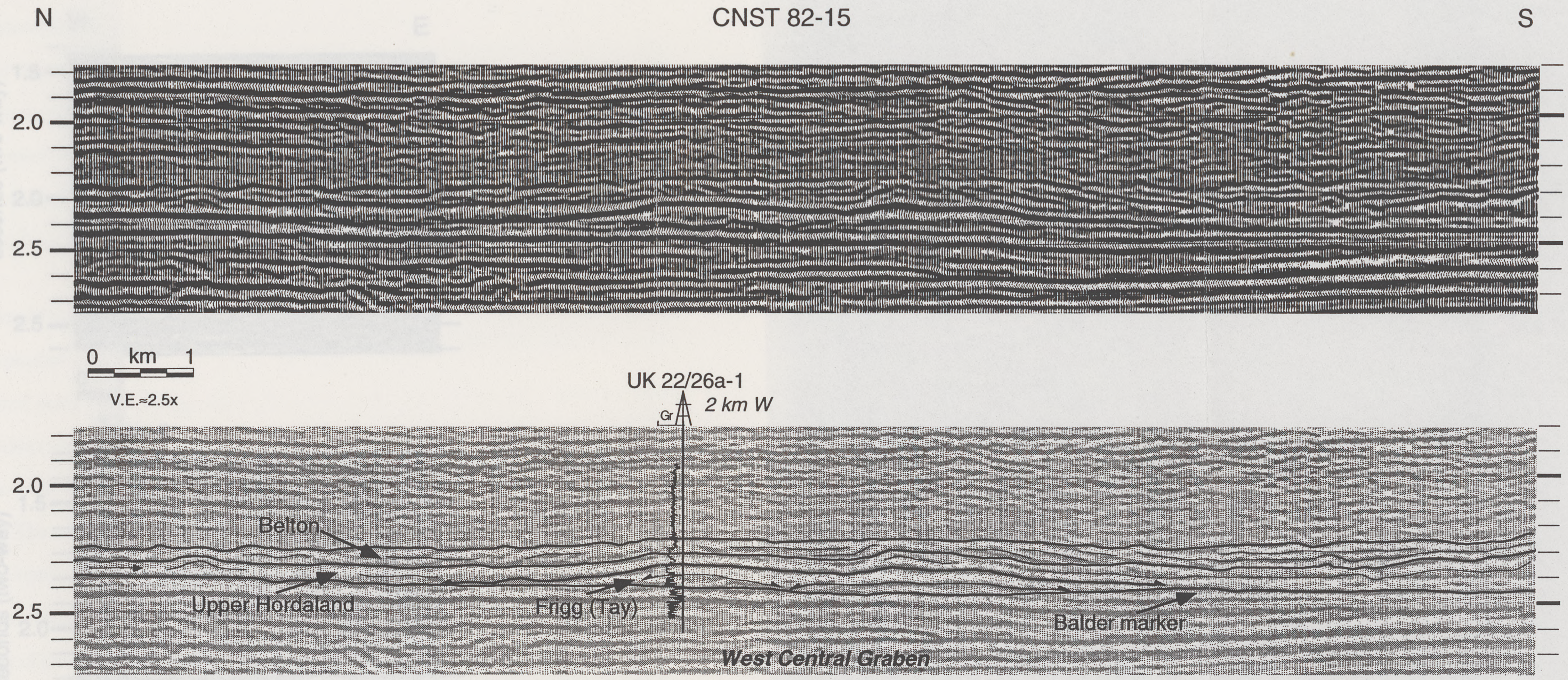

Figure 3.13 A portion of seismic line 82-15 in the west Central Graben (see Figure 3.5 for location), where the Eocene is typically thin (300-500 meters total) and argillaceous. Note the Frigg-equivalent "Tay" sands form a distinctly mounded feature above the Balder marker. The nearby Gannet Field produces oil from this submarine fan sand accumulation sealed by overlying Hordaland and Belton muds. Well U.K. 22/26a-1 shows the gamma log for the Tay sands. (The Hordaland and Belton don't tie well because the well location is two kilometers west of the seismic line.)

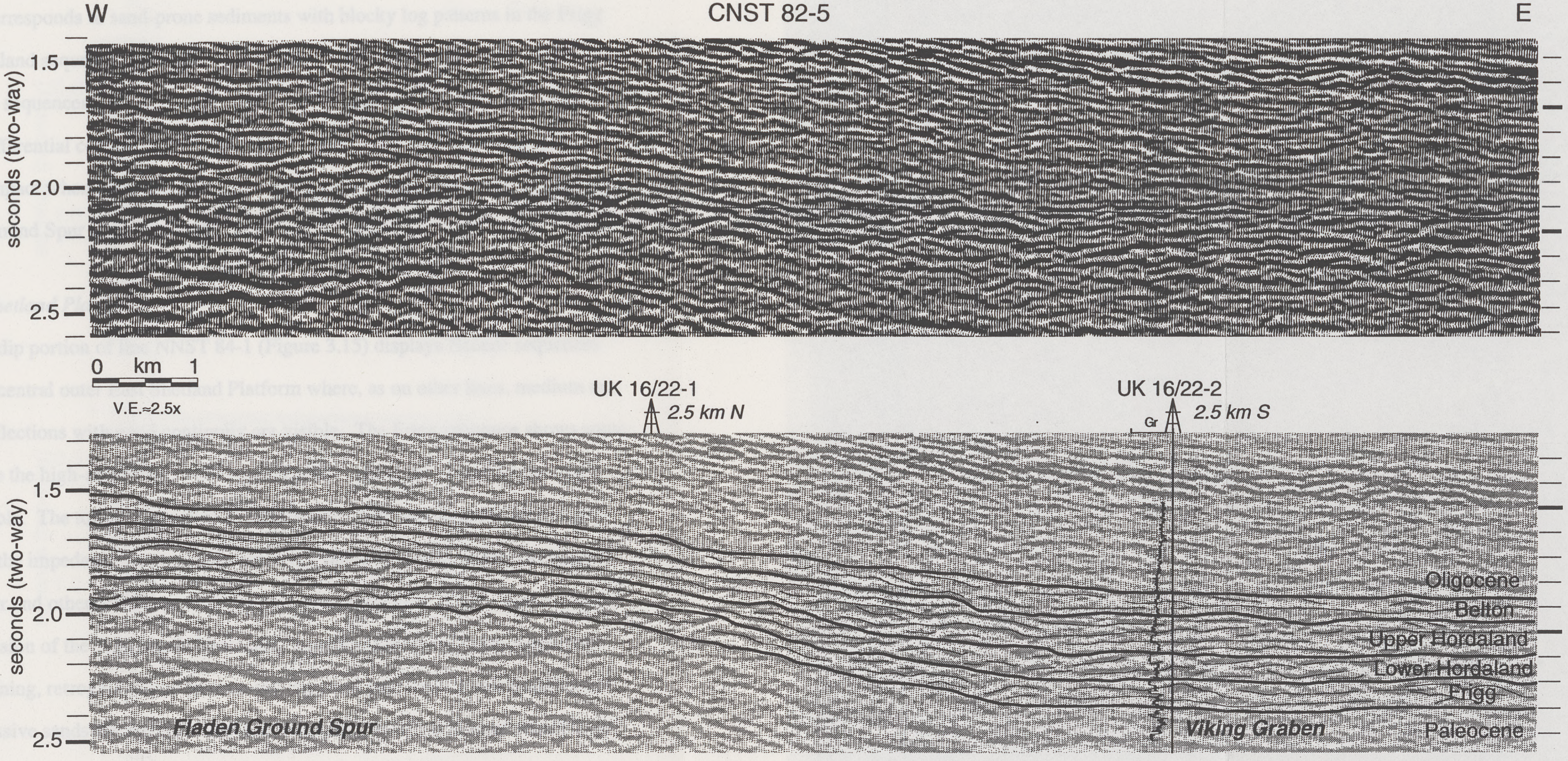

Figure 3.14 A portion of seismic line 82-05 crossing the southern tip of the East Shetland Platfrom (Fladen Ground Spur) and into the southern Viking Graben. see Figure 3.5 for location map. High amplitude, discontinuous seismic reflections in the Viking Graben correspond to sand bodies with blocky log patterns.

Graben. On the uninterpreted line (top) a higher reflection amplitudes characterize the Eocene section relative to the overlying Oligocene. In the Viking Graben this interval corresponds to sand-prone sediments with blocky log patterns in the Frigg and Hordaland sequences, overlain by silts and muds in the Belton and lower Oligocene sequences. The sequences thin onto the platform probably due, at least in part, to differential compaction. The Viking Graben is underlain by sediments which compact when loaded and thus provide greater accommodation space than the Fladen Ground Spur basement high.

Central Shetland Platform

An updip portion of line NNST 84-1 (Figure 3.15) displays Eocene sequences along the central outer East Shetland Platform where, as on other lines, medium amplitude reflections with good continuity are visible. The Frigg sequence shows some onlap onto the high-amplitude double-peak Balder marker but is mostly internally conformable. The top of the section is a continuous high-amplitude reflection produced by the impedance contrast between Frigg sands of the Bruce Fan (as mapped by Heritier and others, 1979) and overlying Lower Hordaland muds. This is a typical expression of the Frigg sand lithofacies. The Hordaland sequences display an upward-fining, retrogradational gamma-ray log trend culminating in a flooding surface. Massive sands are visible in the Thet, including an upper portion which is upward-coarsening as one would expect for this progradational unit.

Central Viking Graben

A downdip portion of the same line (NNST 84-1) is shown from the eastern Viking Graben (Figure 3.16). Reflection continuity in the Eocene and Oligocene

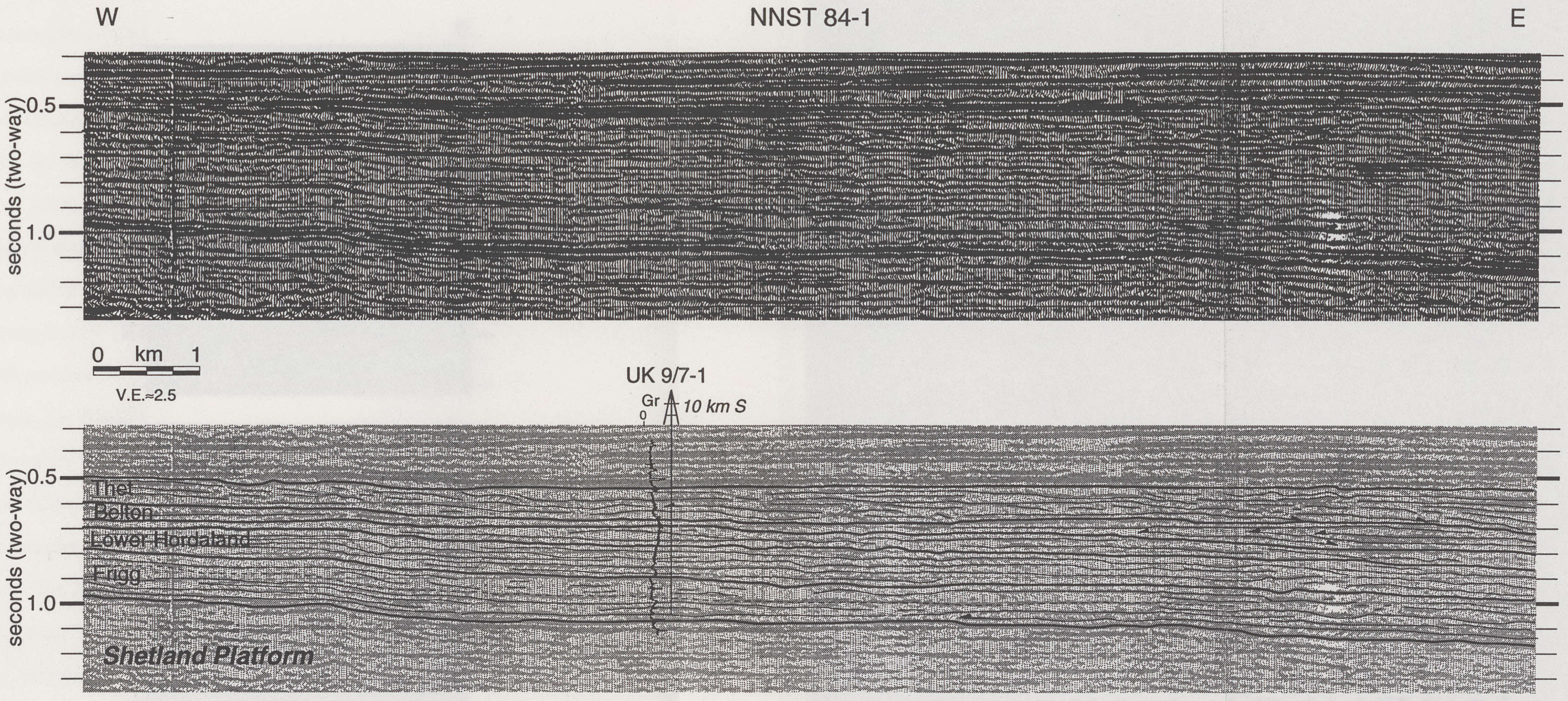

Figure 3.15 A portion of seismic line 84-1 on the Shetland Platform (see Figure 3.5 for location map) where all five Eocene sequences are visible along the margin and reflection continuity is relatively good. The well, located to the south, intersects the sandy Frigg (Bruce Fan), upward-fining Hordaland, thin Belton, and sandy Thet units. Both sand units, as well as the top of the Balder Tuff, are marked by high amplitude reflections.

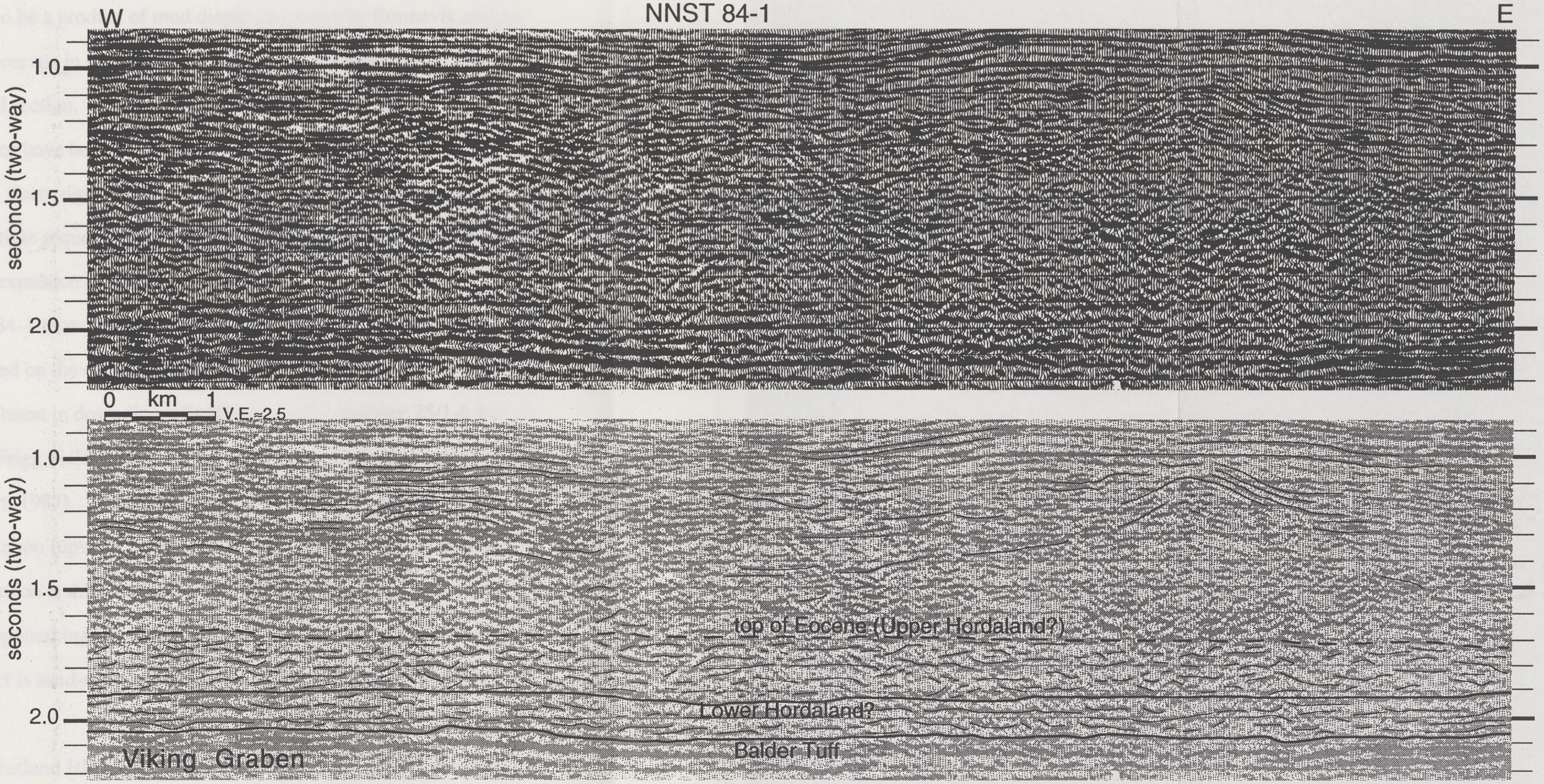

Figure 3.16 A portion of seismic line 84-1 in the northeast Viking Graben. See Figure 3.5 for location map. The Eocene section displays a chiefly chaotic seismic facies with variable amplitudes and very low continuity. Sparse well control in this area indicates a muddy section where correlations are rather tentative. Structures in the overlying Oligocene are suggestive of diapirism that may have been induced as these sediments dewatered during and following rapid deposition of the Miocene Utsira Formation, derived from the Norwegian margin (Garber, in prep.).

section is quite low, approaching a chaotic seismic facies, making differentiation and correlation of units difficult. This same facies is visible on lines to the north and south and is thought to be a product of mud diapirism (noted by Ronnevik and others, 1975) and/or gas escape in the section. Wells are sparse, but gamma logs indicate a mud-dominated section. Gas escape structures and active chimneys from the Jurassic to the sea floor have been reported in the area (Brewster and Jeangeot, 1987; Conort, 1986). Cartwright (1994) showed evidence from three-dimensional seismic data that multiple sequences, including those of the Eocene, underwent hydrofracturing during expulsion of overpressured fluids.

Wells along line 84-1 show massive sand bodies of the Bruce Fan (Heritier and others, 1979) preserved on the outer Shetland Platform and Beryl Terrace in the Frigg sequence, but absent in downdip wells (Figure 3.17). Norway 25/1-6 was, in fact, drilled near the Frigg Field but missed the sand pinchout to the north by about one kilometer (Conort, 1987). The Hordaland units are muddy and onlapping, with evidence of retrogradation (upward-fining) to the west (well UK 9/7-1, as noted in Figure 3.15). The Belton is thick and muddy in the Viking Graben, with a distinct gamma peak at the top marking the condensed section so typical of the top Eocene in the basin. The Thet is sand-rich and progradational, with distinct upward-coarsening trends.

Due east of the Shetland Islands, the Viking Graben begins to broaden to the north (Figure 3.18; Figure 3.1). About 100 meters of Frigg sand forms South Alwyn Fan (Heritier and others, 1979) capped by distinct radioactive mudstones (N 30/7-6) correlatable to the east (N 30/9-1). Predictably muddy Hordaland deposits are

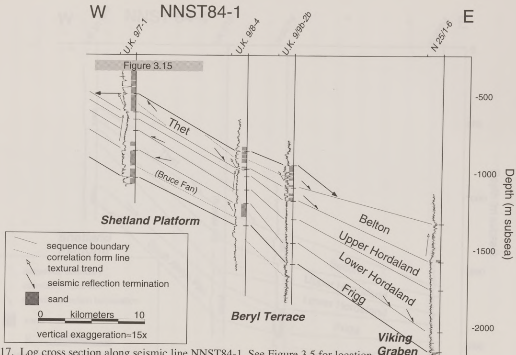

Figure 3.17. Log cross section along seismic line NNST84-1. See Figure 3.5 for location. Shaded rectangle indicates position of seismic example shown in Figure 3.15. Note presence of Frigg and Thet sand bodies on outer Shetland Platform and Beryl Terrace, but chiefly muddy section in Viking Graben. Distinctly retrogradational (upward-fining) Hordaland units lie on the shelf.

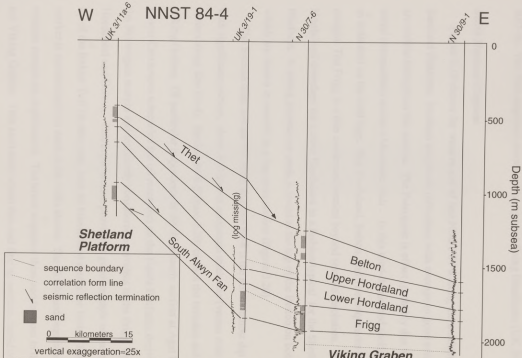

Figure 3.18 Log cross section along seismic line NNST84-4. See Figure 3.15 for location. The Frigg sequence is sandy on Shetland Platform and Beryl Terrace, but is equivalent to mud in the Viking Graben. Sharply-bounded sand bodies in the Belton are on upper slope of the west Viking Graben. Thet is sand-prone updip (Shetland Platform).

overlain by the Belton, which includes local sharp-based basinal sand units (Norway 30/7-6). The Thet sequence shows sandy, upward-fining lithofacies (UK 3/11a-6).

North Shetland Platform

Figure 3.19 shows the western end of line NNST 84-8 along the northern Shetland Platform. Medium amplitude reflections with average to good continuity are visible throughout the section. The Paleogene is offset (probably due to differential compaction) across a Mesozoic fault . In this mud-dominated shelfal section, as indicated on the well logs, thin Hordaland, Belton, and Thet sequences onlap the margin. The Frigg is a thin condensed section beyond seismic resolution. The Upper Hordaland downlaps the Lower Hordaland in a fashion typical for the Shetland Platform. A strong gamma-ray peak is found at the top of the Belton on both logs, which are shown in context in a log cross section (Figure 3.20)

The Eocene thins toward the north and line 84-8 is the northernmost dip line with significant section, about 500 meters maximum thickness (versus over 1000 meters along line 84-4). Section 84-8 (Figure 3.20) crosses the broaden and shallow Viking Graben. Of particular importance is the thick sandy section at Agat Field (a Lower Cretaceous submarine fan oil reservoir) on the Horda Platform, derived from the Norwegian margin and tentatively considered equivalent to the Frigg, Upper Hordaland and Belton. This cross section provides a good example of the continuity of the Balder Tuff (in this case, over 60 kilometers) across the basin. The log marker is unmistakable in each of the wells shown. The Hordaland sequences on the western margin are argillaceous. The lower sequence thins and laps out in the western Viking Graben. Thin sand units which thin and fine up-section, turbidite-style, characterize the Belton on the slope and basin (well 211/27-8, 211/24-5 and 33/12-

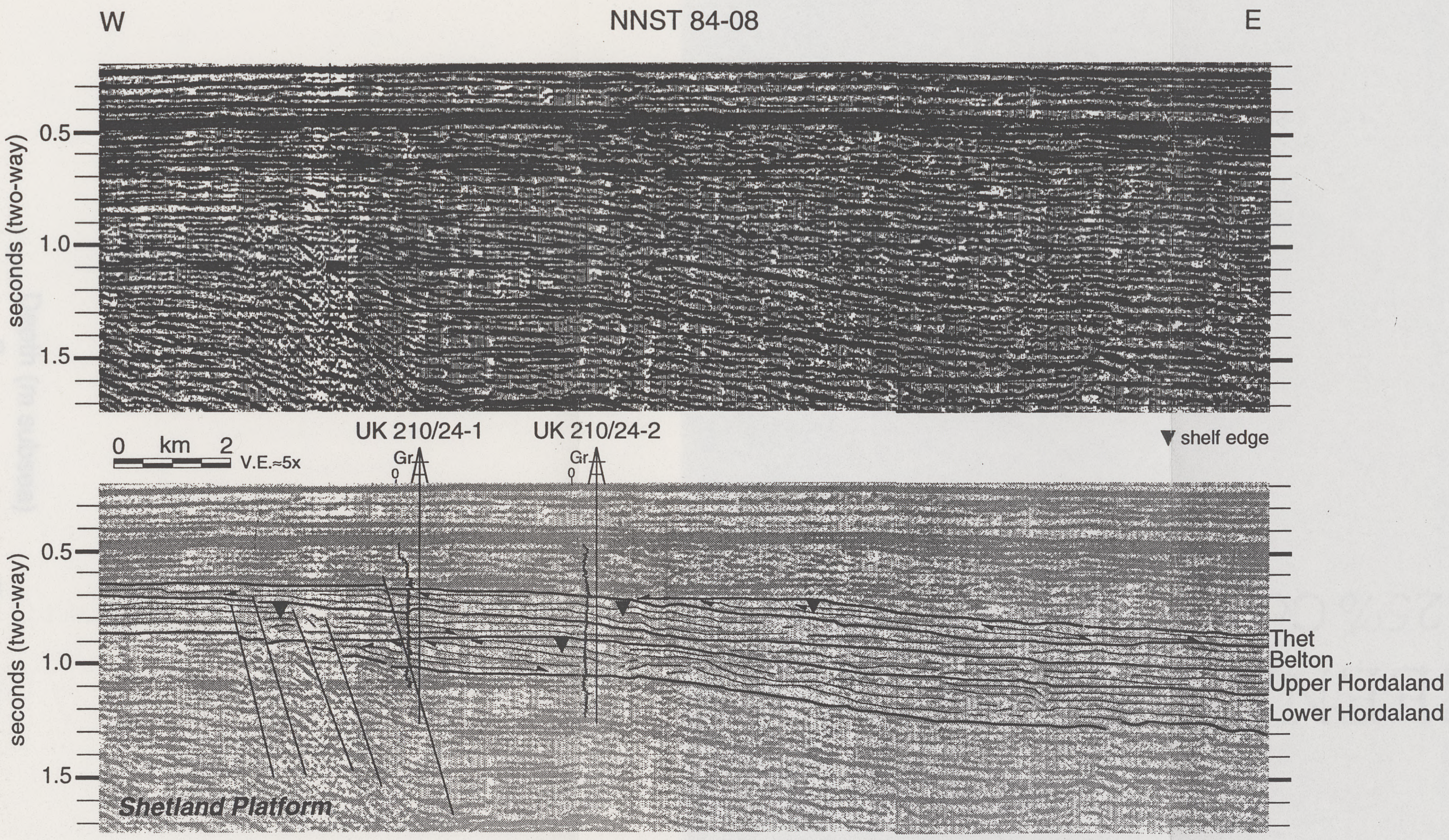

Figure 3.19 A portion of seismic line 84-08 along the northeast edge of the Shetland Platform. See Figure 3.5 for map location. Arrows mark reflection terminations. Even at this relatively updip position, the Eocene section is mud-dominated.

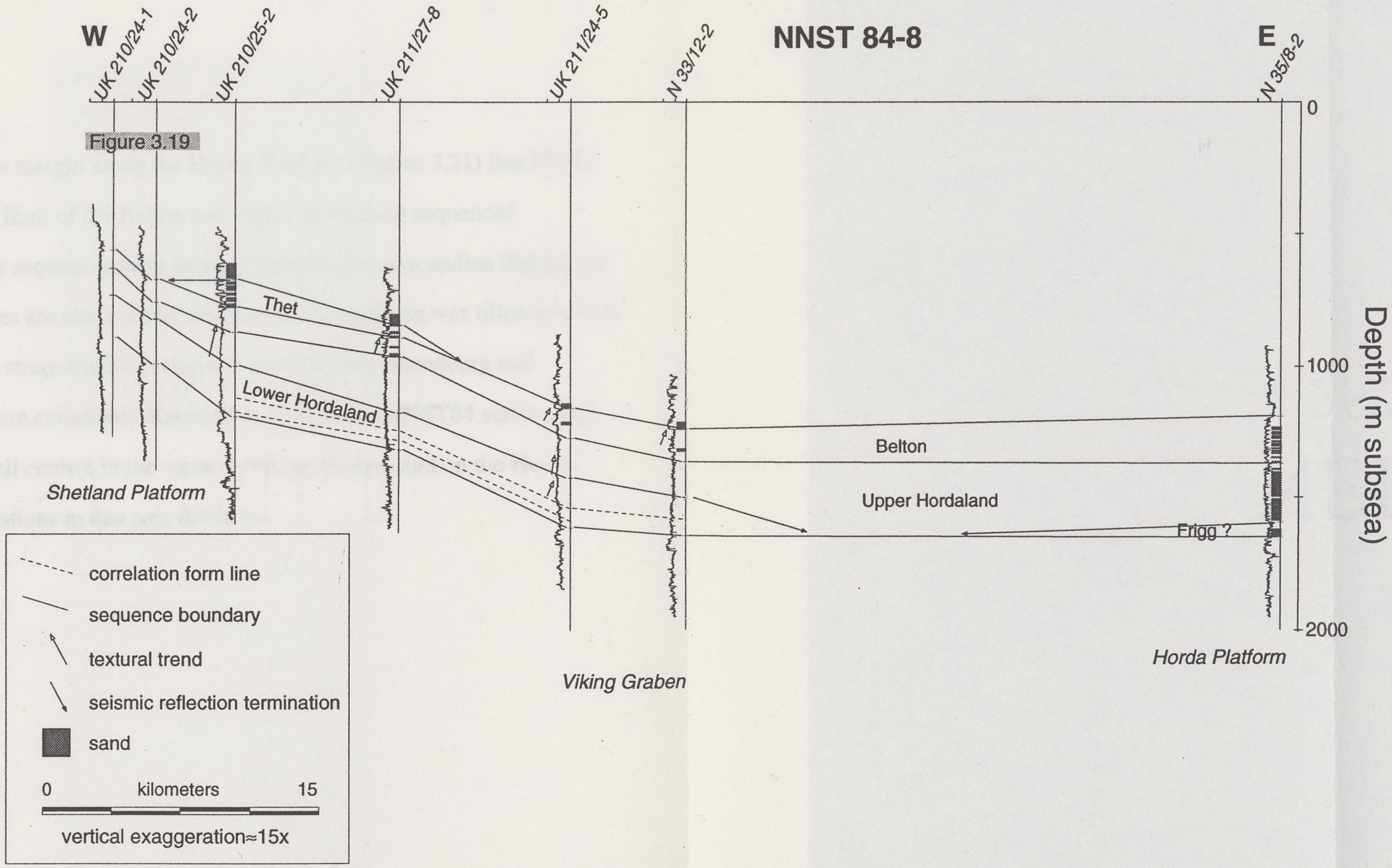

Figure 3.20. Log cross section along seismic line NNST84-8. See Figure 3.5 for location. Shaded rectangle indicates position of seismic example shown in Figure 3.19. This section crosses the northern end of the Thet wedge, which is thin but sandy. Other sequences are mostly mud. The Norwegian platform well (far right) includes sand derived from an eastern source thought to correlate to Hordaland and Belton sequences based on nearby seismic data.

2). Several distinct sand bodies are present in the Thet, which is shows oblique clinoform geometry on seismic interpreted to be a product of progradation (Figure 3.14).

Horda Platform

At the eastern basin margin along the Horda Platform (Figure 3.21) line NNST 84-8 reveals the updip limit of the Belton and Upper Hordaland sequences. Sediments within these sequences were derived from the Fennoscandian Shield, but useful stratal geometries are obscured by structure. The platform was tilted west and Paleocene and Eocene strata eroded during the mid-Pliocene (Rundberg and Smalley, 1989), a feature commonly observed in most of the NNST84 series along the margin. Sparse well control in the western Viking Graben and on the Horda Platform makes correlations in this area difficult.

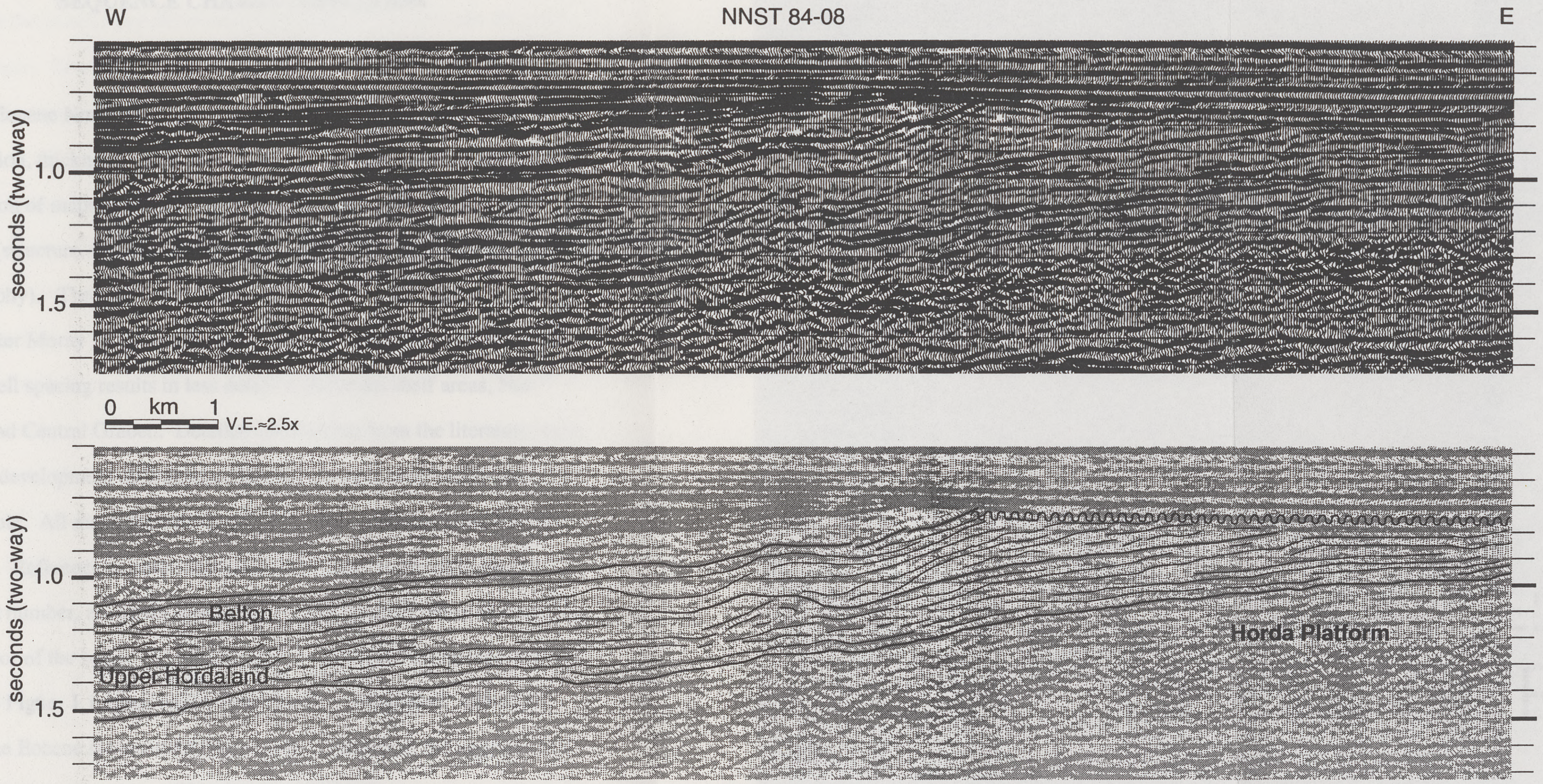

Figure 3.21 Truncation of reflections in the Eocene section is visible on this seismic line (NNST 84-08) across the Horda Platform (see Figure 3.5 for location map). This prism of sediment thins rapidly to the west (basinward) across the shelf. Sparse well control (none near this line) suggests a sandy Eocene section.

Chapter Four

SEQUENCE CHARACTERIZATION

In this chapter Eocene North Sea sequences are characterized by their three-dimensional distribution, thickness, framework sand distribution, and depositional systems. The succession of maps presented for each sequence represents a progression from the objective (structure, isopach, net sand, percent sand) to the interpretive (log motif, paleogeography). The maps show greater detail in areas of denser well control in the of the outer Moray Firth, easternmost Shetland Platform, and Viking Graben. Sparser well spacing results in less detail in the updip shelf areas, Norwegian platform, and Central Graben. Detailed information from the literature, such as field maps from development drilling and 3D seismic, have been incorporated as pertinent and possible. All maps were produced at the same scale in order to facilitate comparisons. Reference to particular geographic areas on these maps is by sector and quadrant number, as shown in Figure 1.10, *e.g.* Q.UK3 refers to Quadrant 3 in the British sector of the basin. Geographic features are used extensively and the reader if referred to Figure 1.1, upon which these features are labeled. The structure at the base of the Eocene is presented first in order to establish the approximate basin configuration before deposition of the Eocene sequences.

4.1 Base Eocene Structure

Structure at the top of the Balder Tuff, constructed from well and seismic data, shows relief of 2,500 meters, from -500 meters on the shallow western side to over

-3,000 meters in the Central Graben (Figure 4.1). Kooi and others (1991) noted that rapid post-Miocene differential subsidence in the Central Graben of over 1000 meters accounts for the present-day difference in structural relief between the Central and Viking grabens. This is important since the differential relief, had it been present during the Eocene, would have focused basinal sedimentation into the Central Graben rather than the Viking Graben, where it occurs. Both troughs are broad features, compared to the sharp, fault-bounded Mesozoic expression shown previously on the tectonic map (Figure 1.1). The deep basin is narrow near the Beryl Terrace (59.3°N), then widens to the north in the Viking Graben, which shows relatively steep slopes on the Shetland Platform (at 60°) crossing to a gentler ramp along the length of the Norwegian Platform. The eastern edge of the Beryl Terrace is not well constrained by available well data and therefore is not expressed as clearly as seismic crossings indicate. The eastern edge of the Shetland Platform shows a headland at about 60°N and wraps gradually south-southwest into the outer Moray Firth area (58°N). Steep slopes are preserved along the Western Platform margin of the Central Graben.

4.2 Sequence Distribution, Lithofacies, and Depositional Systems

Frigg Sequence

The early Eocene Frigg sequence is dominantly a basin-centered, onlapping unit characterized by local sand-rich basin-floor fans in the basin (Figure 3.6, 3.13, 3.17). The sequence is up to 350 meters thick on the Beryl Terrace with secondary depocenters in the Viking and Central grabens (Figure 4.2). The eastern 100 meter

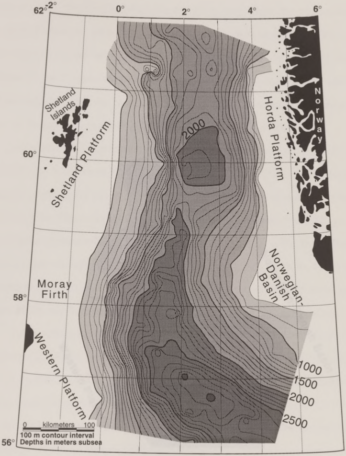

Figure 4.1. Base Eocene (top Balder Formation) structure based on wells supplemented by seismic data. About 2500 meters of relief separate the shallow (-500 m) Shetland Platform from the deepest part of the Central Graben (-3000 m; almost 1000 m deeper than the Viking Graben). The 2000 m contour indicates a wider Viking Graben to the north (60°N) separated from a narrower deep to the south (59°N).

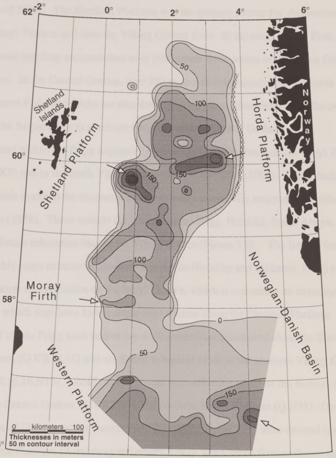

Figure 4.2. Isopach map of the Frigg sequence. Arrows indicate depocenters. Major thicks are apparent on the Beryl Terrace and in the Viking Graben and southern Central Graben. Wavy pattern indicates Frigg erosion on the Horda Platform.

contour follows the trend of the Viking Graben structure (Figure 4.1), narrowing south of 59°N. The Shetland Platform was the primary source for depocenters on the Beryl Terrace and onto the Viking Graben floor. In the outer Moray Firth, a west-east trending accumulation over 100 meters thick occurs in the Witch Ground Graben. In the Central Graben, over 200 meters of Frigg-equivalent sediment occur at Gannet Field and thicks are also developed on the southeastern end of the trough near the Søgne basin (a reentrant along the eastern Central Graben).

Sand within the Frigg sequence (Figure 4.3) is concentrated on the Beryl Terrace (Q.UK9) and in the north Viking Graben (Q.UK10/N25, Q.UK9). These thickest net sands occur in the accumulations previously seismically mapped by Heritier and others (1979). These include the point-sourced Frigg, Heimdal, South Alwyn, Brae, and Ninian submarine fans in the Viking graben (Figure 3.4). The Bruce "fan" is probably more accurately considered an apron (Reading and Richards, 1994) in consideration of its position on the Beryl Terrace, which is essentially an intraslope basin which may have had multiple sand sources along the Shetland Platform.

Thinner Frigg sand bodies (up to 50 meters) are distributed along the Shetland Platform (Q.UK14,15) and are linked to basinal sands in the southern Viking Graben (Q.UK16,16,N15). Localized Frigg sand accumulations occur on the western slope of the Central Graben (Q.UK22) on the northern Horda Platform (Q.N35). Over 200 meters of "Tay" sands at Gannet Field (Q.UK22; Figure 3.13) were derived from the Western Platform (Armstrong and others, 1987). The Central Graben depocenter (up to 250 meters; Figure 4.2) is mud-dominated, as is most of the northern Viking Graben.

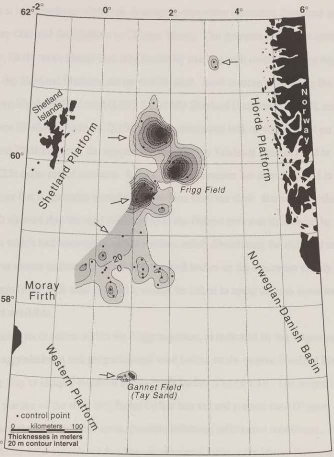

Figure 4.3 Net sand map of the Frigg Sequence. Thickest sands lie along the Shetland Platform, in the Beryl Embayment, and in the north Viking Graben. Previously mapped sand bodies include the Gannet (Central Graben), Frigg, and other fans mapped by Heritier and others (1979).

The northern Frigg sequence fans (Figure 4.4) are locally sand-rich, 80-90% sand, which is in accordance with their description elsewhere (literature discussed in Chapter One and descriptions in Chapter Three). The decrease in percent sand is, in reality, likely more abrupt than was shown by existing well control. Frigg deposits along the Shetland Platform are up to 40% sand. Sand sources were along the southern Shetland Platform (Q.UK15), middle Shetland Platform (Q.UK8), and northern Shetland Platform (Q.UK3). The unfortunate lack of well control on the Western Platform gives the appearance that the Tay Sands (at Gannet Field in Q.UK22) came out of nowhere. In fact, their provenance has been disputed in the literature but is generally thought to have been from the west. Banner and others (1992) showed that the sand distribution in the Gannet area was influenced by salt domes which had contemporaneous seafloor relief, diminishing the utility of sand maps as source indicators. Similarly, the sand bodies on the otherwise muddy Horda Platform (over 30% sand in Q.N35) cannot be linked to updip sources since wells are not available.

Facies successions within the Frigg sequence, as indicated by log responses, include aggradational and progradational sand bodies on the eastern Shetland Platform giving way to sharply-bounded basinal sand bodies (Figure 4.5). The progradational portion of the shelf (log facies D) has less net and percent sand (Figures 4.3, 4.4) than the aggradational areas, possibly reflecting differential subsidence. Paleocene differential subsidence has been documented in the outer Moray Firth (Mudge and Bliss, 1983; Jones and Milton, 1994) and might be expected for the Beryl Terrace as well. Updip sand deposition would have been concentrated in these areas of greatest accommodation space, while sands shed across the structurally higher

Figure 4.4 Frigg sequence percent sand map. Arrows indicate inferred sediment transport directions. This map is similar to the net sand map (Figure 4.3), with the exception of the downdip sands in the outer Moray Firth (Quadrant UK 15), which are low in net sand, but quite clean.

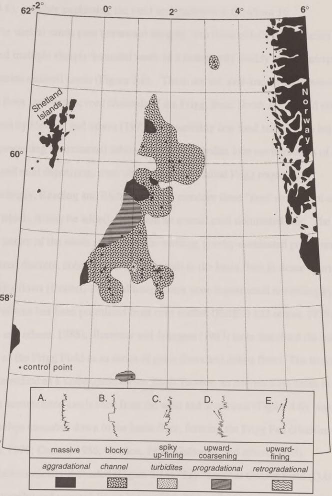

Figure 4.5 Frigg sequence log motif map. Aggradational and progradational areas on the outer Shetland Platform fed sands to blocky deposits the slope and basin floor. Isolated submarine fans of unclear updip equivalents are found in the Central Graben and on the Horda Platform.

Fladen Ground Spur found their way to the shelf edge and into the basin (Figures 3.7, 3.8), possibly explaining the sand accumulation in Quadrant 16.

The shelfal sands pass basinward abruptly into those chiefly of log facies B, single and multiple sharply-bounded sands in a dominantly muddy matrix interpreted as submarine channel sands (Figure 3.6). These are the well-known point-sourced basin floor fans with leveed channels of the Frigg, Brae, South Alwyn and others mapped by Heritier and others (1979). Remarkably few sand bodies with log facies C, representing interchannel submarine fan or turbidite lobe environments of mixed sand and mud deposition, were observed in the basinal Frigg sequence. Accordingly, Reading and Richards (1994) consider these "sand-rich" point-source fans, which, it may be added, are within an overall mud-dominated unit. The fairly clean nature of the sands suggests mass-wasting, gravity-dominated processes which delivered discrete, cohesive, pre-sorted sands to the basin floor in dense debris and turbidity flows (Conort, 1986), although some post-depositional reworking by bottom currents has been postulated from core studies (Heritier and others, 1979; Enjolras and others, 1986). Brewster and Jeangeot (1987) have described the reservoir rocks of the Frigg Field as as series of grain flows and debris flows. The Bruce fan was deposited as a slope apron on the Beryl Terrace, an intermediate break in slope which accumulated sands shed from the west and southwest (Figure 4.6), some of which then cascaded down to the basin floor, forming the Frigg Fan (Heritier and others, 1979; Conort, 1986; Condon, 1988; Galloway and others, 1993).

The seismically-mounded (Figure 3.13) "Tay" sands at Gannet Field (Q.UK22) display spiky and upward-fining log profiles (Figure 3.11), representative of both distal and proximal positions of a sand-dominated prograding slope fan derived from

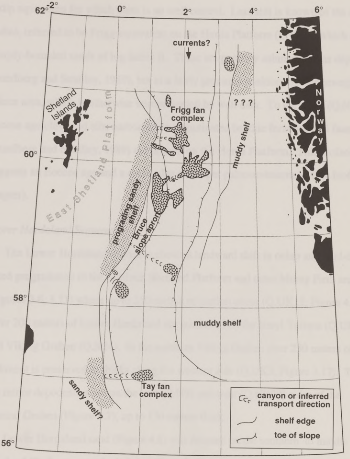

Figure 4.6 Frigg sequence paleogeography. A sand-rich shelf on the Shetland Platform sourced the Bruce Apron on the Beryl Terrace and fan systems in the Viking Graben, some of which may have been reworked by deep marine currents. Tay submarine fan sands at Gannet field were derived from Western Platform. Norwegian Platform was muddy, except at northern extent.

the Western Platform (Armstrong and others, 1987; Banner and others, 1992), the updip equivalent for which there is no well control. Less still is known of the sand bodies, inferred to be Frigg-equivalent on the Horda Platform (Q.N35), which are sharply-bounded sands of log facies B. These are possibly submarine fans deposits (Rundberg and Smalley, 1989), but at a fairly proximal position to the Norwegian source area, which is otherwise unrepresented by well data. To the south (Q.N31) Eocene age clays and silts harboring an agglutinated benthic foraminiferal fauna (Rundberg and Smalley, 1989) are present on the Horda Platform. This biofacies suggests an Eocene age and a shelf-edge or deeper paleoenvironment (see biofacies chapter).

Lower Hordaland Sequence

The Lower Hordaland sequence shows a landward shift in onlap and mud-dominated progradation in the southern Shetland Platform and outer Moray Firth area (Figures 3.6, 3.11) where up to 350 meters of section occur (Q.UK15; Figure 4.7). Over 200 meters of Lower Hordaland are preserved on the Beryl Terrace (Q.UK9) and Viking Graben (Q.N24). In the northern Viking Graben over 250 meters of sediment is preserved in thicks along the western side (Q.UK3; Figure 3.17). There are minor depocenters are on the east (Q.N9) and west (Q.UK29) sides of the Central Graben (Figure 4.7), up to 150 meters thick.

Lower Hordaland sand (Figure 4.8) was focused on the southern to middle Shetland Platform, a marked change from the Frigg sequence sand distribution, which was centered in the north Viking Graben (Figure 4.3). Most of the rest of the Lower Hordaland sequence is muddy, including the 100-200 meter thick sections in the Central Graben (Figure 4.7; Q.N9). Up to 200 meters of sand is present in the

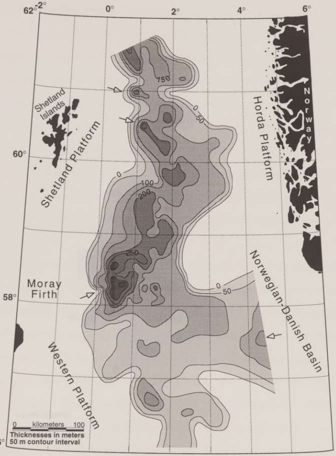

Figure 4.7. Isopach map of the Lower Hordaland sequence. Arrows indicate depocenters in the outer Moray Firth, Viking Graben, and Norwegian-Danish basin.

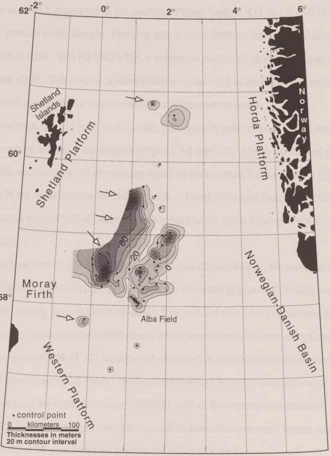

Figure 4.8 Lower Hordaland sequence net sandstone map. Arrows indicate inferred sediment source directions. Maximum sand deposition (over 200 meters) was in the outer Moray Firth Area and Beryl Embayment. Net sand thins over an outer shelf and slope bypass zone to thicker basinal accumulations (over 150 meters) in the south Viking Graben.

outer Moray Firth (Q.UK 15) and Beryl Terrace (Q.UK 9) depocenters. Up to 150 meters of sand is preserved in the southern Viking Graben (Q.UK 16, Q.N15,16) in trends parallel to the margin. Harding and others (1990) report up to 200 meters of net sand at Alba Field (Q.UK15/16), a somewhat surprising amount if it was derived from the shelf. This thicker accumulation of clean sand in the basin, suggests that shelf sand accumulation was limited by accommodation space.

Net sand thins to zero on the slope, indicating bypass of sands in this area, as suggested by the log cross sections (Figures 3.6 and 3.7). Minor shelfal and slope sand lithofacies (up to 75 meters) are found in the northern Viking Graben (Q.UK 3 and Q.N 30) near seismic line NNST 84-6. Local thin sands (less than 10 meters) are present in the Central Graben and in several wells in the Viking Graben (Q.UK9).

Highest Lower Hordaland sand percentages (Figure 4.9) on the southern Shetland Platform (Q.UK15) are updip of the thickest sand (Figure 4.8), which occurs in a chiefly muddy section (10-20% sand). The isolated thin sand in Quadrant 20 in the Buchan Graben is about 90% clean, while sand units in the two other Central Graben areas (Q.UK21,22) are thin and contained in a thicker mud-dominated Lower Hordaland (10% sand). In the north Viking Graben, a western source is inferred from the high percentage (90%) of sand in the western accumulation (Q.UK3) from which sand may have cascaded downslope, across a bypass zone, into the Quadrant 30 accumulation in the north Viking Graben.

Lower Hordaland log characters are similar to those of the Frigg sequence. Massive aggradational sands (log facies A) on the outer Shetland Platform (see western wells in Figure 3.11) pass abruptly over the paleo shelf-edge into thick (up

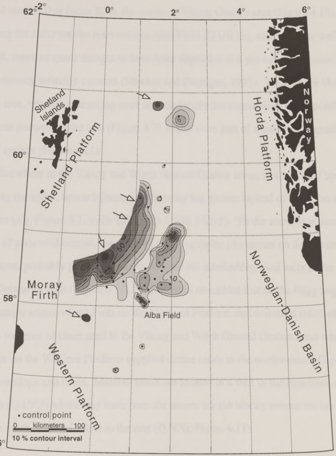

Figure 4.9 Lower Hordaland percent sand map. Arrows indicate inferred sediment sources. Sandiest areas are the Witch Ground Graben, outer Moray Firth and north Viking Graben. Beryl Terrace area with relatively thick net sand (Figure 4.7) only constitutes 40% of the Lower Hordaland section.

to 50 m), sharply bounded sands (Quadrant 16 wells, Figure 3.6) within a mud-dominated section (log facies B) in the southern Viking Graben area (Figure 4.10). Among the latter are the reservoirs at Alba Field (Q.UK16), structureless, well-sorted, massive sands thought to have been deposited in a pre-existing channel by high-density turbidity currents (Newton and Flanagan, 1993). In the outer Moray Firth area, upward-coarsening mud and silt lithofacies successions correspond to the thickest portions of the unit (Figure 4.7) which were part of a muddy, prograding shelf system (Figure 4.11).

Elsewhere in the Viking and Witch Ground Graben areas, isolated sand bodies display the spiky, upward-fining and thinning log pattern typical of distal fan turbidites (*e.g.* Figure 3.7, wells UK 15/20-1, UK 15/6-3). To the southwest, across a zone of poor well control, the massive sand log facies (A) occurs on the Western Platform, probably part of the source of sand for interbedded sand units in the northern Central Graben (Figure 4.11). This pattern resembles that of the Frigg sequence. The major source of sand was on the Shetland Platform and delivered relatively large volumes of clean sand to the Viking and Witch Ground Graben areas while a source on the Western Platform supplied dirtier sands to the northwestern Central Graben slope and basin. Massive sands are located in a well in the East Shetland Basin (Q.UK3) which may have been the source for the blocky submarine fan sands in the north Viking Graben to the east (Q.N30; Figure 4.11).

Upper Hordaland Sequence

The Upper Hordaland onlaps the bounding platforms (Figures 3.1, 3.2) and is distributed over a much larger area than either of the underlying two sequences, extending fully across both the Viking and Central grabens and surrounding shelves

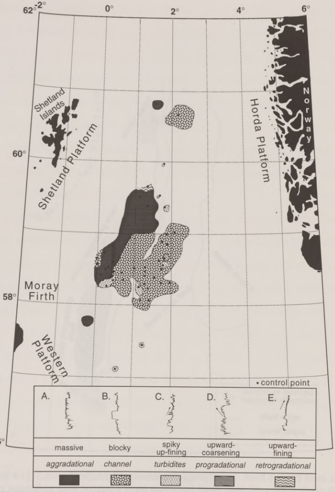

Figure 4.10 Log motif map of the Lower Hordaland sequence. Massive sands on the southeastern Shetland Platform pass downdip into sharply bounded sands encased in mud in the southern Viking Graben and Witch Ground Graben.

Figure 4.11 Lower Hordaland sequence paleogeography. Sand derived from a very sandy aggrading shelf formed a slope apron and basin floor fan system along the southern Shetland Platform margin. A muddy shelf prograded across the outer Moray Firth area. A basin floor fan in the north Viking Graben must have been derived from aggradational shelf sands along the north Shetland Platfrom.

(Figure 4.12). The seismic stratigraphic expression of the unit displays a major landward step in onlap on the Shetland Platform which extends across the basin instead of thinning and pinching out as do the Frigg and Lower Hordaland sequences (Figures 3.1, 3.2). Thickest accumulations, up to 350 meters, are located over the Horda Platform, north Viking Graben, outer Moray Firth, and Central Graben (Figure 4.12). The outer Moray Firth thick (300 meters) is associated with the downlap surface atop the Lower Hordaland (Figure 3.6). Over 250 meters of Lower Hordaland mud in the occur in the Søgne sub-basin area (Q.D3) of the Danish Central Graben. Over 200 meters of Upper Hordaland are present on the Norwegian Platform (Q.N31/35).

Upper Hordaland sand distribution is similar to that of the Lower Hordaland sequence, including bimodal concentration of sand along the southern Shetland Platform and bypassing or funneling to the southern Viking Graben (Figure 4.13). By comparison, total Upper Hordaland sands is generally thicker (up to 200 meters in the outer Moray Firth, Q.UK15) and mud-free, over 90% sand in updip wells (Figure 4.14). A 20 kilometer-wide sand fairway trends southeast off the Fladen Ground Spur (Q.UK16), including nearly 100 meters of net sand in a sand-dominated (60-80%) section (Figures 4.13., 4.14, 3.6). Over 100 meters of sand are present in the southern Viking Graben (Q.N15) and, based on available control, could possibly be derived from the west across the bypass slope or from the southwest along the shelf-connected sand trend. Up to 70 meters of sand occur along the Western Platform margin and onto the slope of the Central Graben (Figure 4.13). A kidney-shaped accumulation up 45 net meters comprising 80% of the section in the northwest Central Graben (Q.UK21/22) may have been derived from western or northwestern

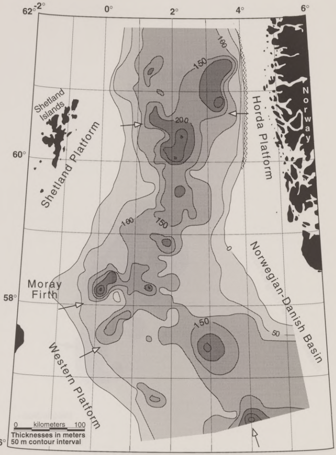

Figure 4.12. Isopach map of the Upper Hordaland sequence. Arrows indicate depocenters in Moray Firth, north Viking Graben, Horda Platform and near the Søgne sub-basin in the Danish Central Graben.

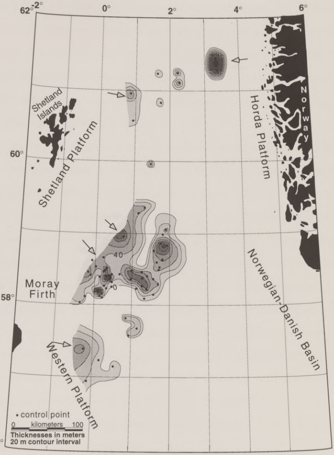

Figure 4.13 Upper Hordaland sequence net sand map. Major sand accumulations are in the outer Moray Firth and southern Viking Graben areas. Limited input occurred along the Western Platform and northern Viking Graben, and localized but thick sand bodies are found on the Horda Platform.

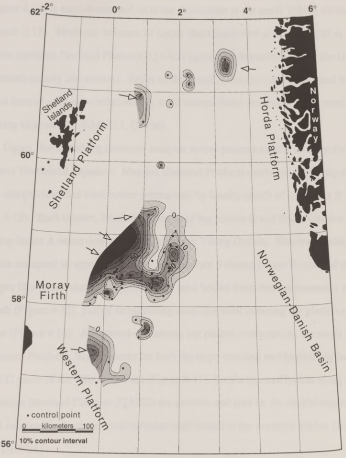

Figure 4.14 Percent sand map of the Upper Hordaland sequence. Arrows indicate sediment sources along the southern Shetland Platform where the sequence is up to 90% sand. A clean sand fairway links updip sands to Viking and Witch Ground Graben sands.

sources. The thick Upper Hordaland section in the southeastern Central Graben (Figure 4.12) is mud-dominated, as is the depocenter in the north Viking Graben (Figure 3.17). Moderate volumes of Upper Hordaland sand are present (50 m net) on the northern Shetland Platform (Q.UK2) opposite substantial sand on the Horda Platform (nearly 200 meters). Either of these updip sources may be invoked for local basinal sand accumulations (up to 45 meters thick) occurring in the north Viking Graben (Q.UK3/9/211, Q.N34).

Upper Hordaland log character analyses reveal patterns similar to those for the Lower Hordaland sequence. Massive Shetland Platform sands pass downdip into the sharply-bounded sand bodies represented by blocky motifs of log facies B (Figure 4.15). Both thinner, interbedded sands of log pattern C and thick, massive sands of log facies A occur downdip in the southern Viking Graben. Whereas shelfal sands occupied an apparent headland in Quadrant 9 during Lower Hordaland time, Upper Hordaland massive, aggradational sand bodies form two promontories to the south (Figure 4.15), part of an aggrading sand-rich shelf covering the platform at this time (Figure 4.16). An upward-coarsening log pattern characterizes the sands on the Western Platform, likely sources for both the slope-attached and basinal log facies B and C sands of the Central Graben (Figure 4.16). Similarly, sand bodies along the northern Shetland Platform (Q.UK2) are massive and may be the shelfal equivalents and sources for the three small turbidite sand bodies in the northern Viking Graben (Q.UK3/211).

Massive sands in the seismic unit which thins westward across the Horda Platform (Figure 3.21) are thought to correlated to the Upper Hordaland (Q.N35). A shallow marine environment has been interpreted for these sands, which include

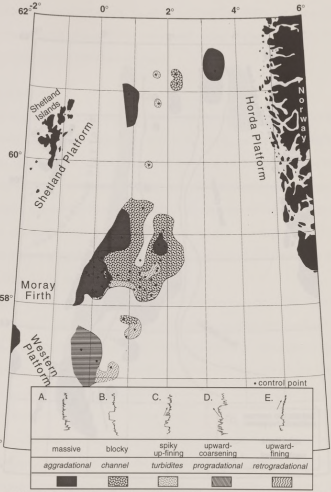

Figure 4.15 Log motif map of the Upper Hordaland sequence. Aggradational sands of the Shetland Platform are related to sand bodies with blocky log motifs in the Witch Ground Graben area. Progradation from the Western Platform shed sandy turbidites onto the up-per slope and basin in the northern Central Graben. Minor shelf sands along the northern Shetland Platform may be related to localized sand bodies in the north Viking Graben.

Figure 4.16 Upper Hordaland sequence paleogeography. A sand-rich shelf along the Shetland Platform delivered sands to a slope apron and basin floor submarine fan deposits along the Viking Graben. A prograding shelf along Western Platform sourced Central Trough submarine fans.

glauconite, shell and plant debris (Rundberg and Smalley, 1989). As noted previously, their distribution is speculative since well control is sparse, but wells in the next quadrant south (Q.N31) are sand-poor.

Belton Sequence

The regressive Belton sequence is distributed over nearly as much of the basin as the underlying Upper Hordaland, but is generally thinner, particularly on the basin margins (generally less than 50 meters) and in the Central Graben (Figure 4.17). The thickest Belton section (up to 300 meters) is centered in the Viking Graben (Q.UK9/3), associated with low-continuity, high-amplitude reflections which distinguish it seismically from underlying and overlying units. The thick but areally restricted Eocene in the Stord Basin on the Horda Platform (Q.N31) is thought to include some Belton age sediments.

Sand distribution within the Belton sequence is similar to that of the Upper Hordaland with less distinction between shelf, basin, and slope sands perhaps reflecting the gradual decrease in differential topography as the basin filled with sediment (Figures 4.18, 4.19). A depocenter near the Beryl Terrace (Q.UK3/9; Figure 4.17) is mud-dominated, as are two thicks in the Central Graben (Q.N2/3, Q.N8). Up to 100 meters of net sand are present on the outer shelf of the Shetland Platform (Q.UK14/15/9) linked to deposits in the Viking Graben which are up to 100 meters thick (Figure 4.18). Other Belton net sand accumulations include up to 80 meters in the western Central Graben (Q.UK22), an inferred source along the northern Shetland Platform (Q.UK3) with over 45 meters, and the 130 meter thick sands on the Horda Platform (Q.N35) which may be linked to deposits in the Viking Graben (Figures 4.18, 4.19). Because these wells are isolated on the shelf, it is not clear if a

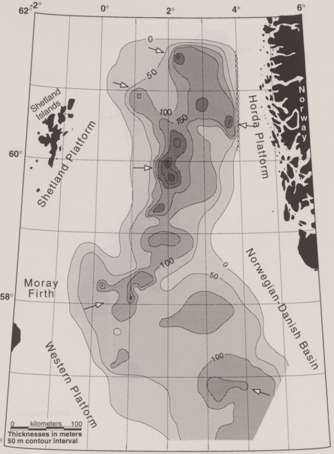

Figure 4.17. Isopach map of the Belton sequence. Arrows indicate depocenters. The unit is thin over much of the basin, particularly the Central Graben area. Thickest accumulations are in the Viking Graben (up to 250 meters). Wavy pattern indicates erosional truncation of Belton sequence on the Horda Platform.

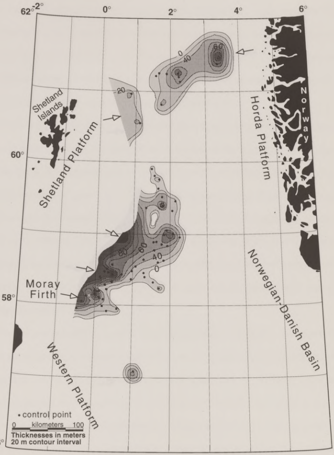

Figure 4.18 Belton sequence net sand map. Sand accumulations lie along the southern Shetland Platform and in outer Moray Firth area. Secondary accumulations are found in the northern Viking Graben, possibly derived from the Horda Platform.

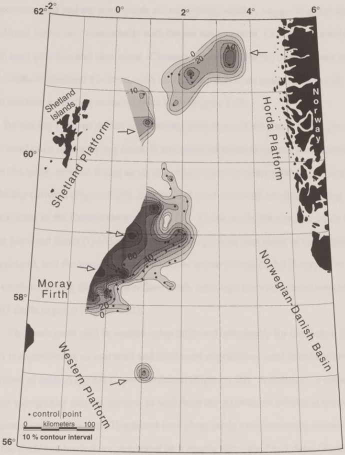

Figure 4.19 Belton sequence percent sand map. Arrows indicate sources on the northern and southern Shetland Platform and Horda Platform. Cleanest section is indicated on southern Shetland Platform and outer Moray Firth.

sand fairway existed between them and the basinal sands in Quadrants 34/33. Belton percent sand and net sand trends are remarkably similar, suggesting that the sand/mud ratios vary consistently with the net sand amount, *i.e.* high net sands have high sand percents and vice versa. Cleanest sand units (>90%) occur in two areas on the southern Shetland Platform, with secondary projections outlined by the 60 percent contour extending eastward from them (Figure 4.19).

Belton log patterns differs substantially from those of the preceding sequences in that sand units of blocky log facies B are restricted to the slope and pass basinward into the spiky, upward-fining sands thought to represent deep water deposition via turbidity currents (Figure 4.20). Interbedded sand units with similar spiky log patterns occur in the Central Graben (Q.UK22). To the north, the massive sands in the East Shetland Basin (Q.UK3) extend over a larger area than those of the Upper Hordaland, and the massive shelfal (shallow marine) sands (Q.N35) may have sourced northern Viking Graben basin-floor sands (although the well control west of the shelf sands is poor) (Figure 4.21).

The basinward shift in coastal onlap indicated seismically for the Belton (Figure 3.1) is expressed as an eastward and northward migration of sand lithofacies relative to those of underlying the Upper Hordaland (Figure 4.20). A decrease in differential basin topography may be inferred as well from the distribution of Belton sediments. Whereas during Frigg and Hordaland time clean sands were bimodally distributed on the shelf and basin floor, separated by a muddy outer shelf and slope (Figures 4.13, 4.18), massive Belton sand bodies extend onto the slope and grade into thinner, turbidite sand bodies toward the basin center (Figure 4.21).

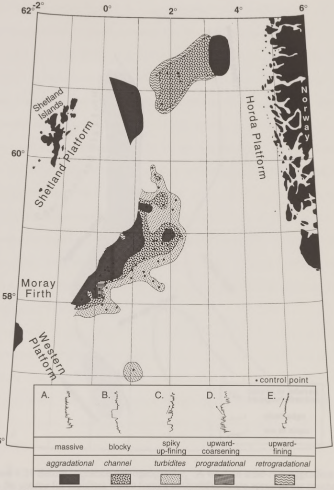

Figure 4.20 Belton sequence log motif map. Massive sand bodies on the south-eastern Shetland shelf are updip of sharply-bounded sands on the slope and thin, interbedded upward-fining sands on Viking Graben basin floor. Shelf sands from the Norwegian Platform may have sourced basinal deposits characterized by blocky log patterns in the northern Viking Graben.

Figure 4.21 Belton sequence paleogeography. A western sand-rich aggrading shelf was the source for tubidites which form a heterolithic slope apron in the southern Viking Graben and Witch Ground Graben. Sandy shelves are inferred updip of basinal sands in the north Viking and Central troughs.

Thet Sequence

The Thet sequence forms a regressive foreshelf wedge which follows the trend of the margin to the southwest into the outer Moray Firth area (Figure 4.22) . The unit ranges up to 260 meters thick just south of the Beryl Terrace (well UK 9/28-1a) , and has a secondary depocenter (>200 m) in the outer Moray Firth. Because the seismic interpretation of this unit suggests that it was related to a fall in relative sea-level which forced sand-rich shelfal deposition seaward (Figures 3.1, 3.2), the distribution ought to be constrained more by accommodation space than by sediment input. If the top of the Thet was constrained by lowered sealevel to be a flat, wave-base graded surface (Swift and Thorne, , then thicks ought to represent bathymetric lows atop the Belton which allowed greater accumulation of sediment. Figure 4.23 shows the top Belton structure, which confirms this hypothesis. Along the 1000 meter contour there are several promontories (indicated by arrows) which correspond to thinner Thet, which presumably prograded rapidly to the slope, beyond which thicker Thet is preserved.

Thet sands are concentrated in several distinct lobes which are separated along strike by intervening passes with thin or absent sand (Figure 4.24). These are actually filled with silt, not mud, but distinctly finer than the sands shown on the map. The lobes correspond approximately to the thickest accumulations of Thet (Figure 4.22). A northern accumulation includes over 120 meters of sand (Q.UK3). A thick up to 200 meters is centered along the bend in the Shetland Platform (Q.UK9/16), and secondary isolated thicks up to 80 meters occurs in the outer Moray Firth (Q.UK15). The sand trends for percent sand are similar, with sandiest intervals

Figure 4.22. Isopach map of the Thet sequence. Note different scale from other maps. Arrows indicate depocenters. Unit is a wedge perched on the outer Shetland Platform. Arrows indicate thickest accumulations, possibly related to local variations in accomodation space during deposition of this regressive sequence.

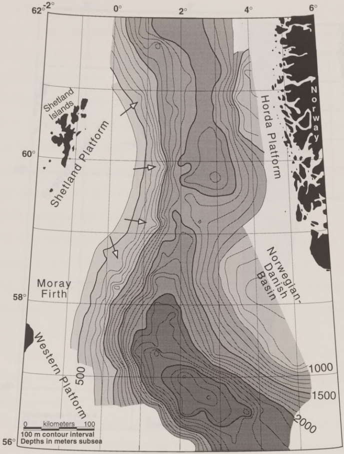

Figure 4.23. Structure atop the Belton sequence. Arrows indicate headlands which may have influenced deposition of the overlying Thet sequence.

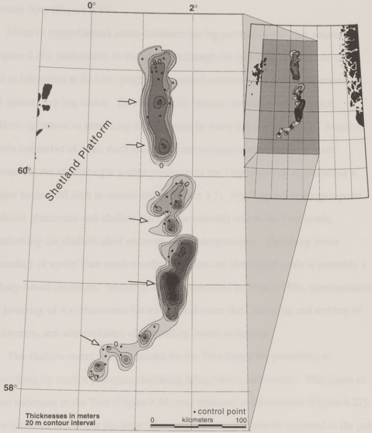

Figure 4.24 Thet sequence net sand map. Thickest sands are on the southeastern Shetland Platform in several distinct lobes (arrows), corresponding to the thickest portions of the Thet wedge.

(over 80% sand) found in along the north Shetland Platform and over the Fladen Ground Spur (Figure 4.25).

Massive aggradational sands dominate the log patterns in the Thet sequence (Figure 4.26), particularly to the south. Although the unit displays seismic offlap and is interpeted to be have prograded, upward-coarsening is poorly expressed on the gamma-ray log facies. This is probably because the unit is so sand-rich, reflecting extensive reworking of sediments by wave and current action. Massive sands indicative of inner shelf and shorezone environment of deposition are consistent the shelf margin wedge geometry of the Thet sequence representing a major basinward shift in coastal onlap (Figure 3.1). Mud log and cuttings reports indicate glauconite and shallow marine macrofossils within the Thet sands, reinforcing the shallow shelf environmental interpretation. The sharp lower boundary of updip Thet sands overlying Belton and Hordaland muds is probably a "sharp-based shoreface" feature of the sort described by Plint (1988), representative of lowering of wavebase onto the middle and outer shelf, scouring and erosion of sediments, and accumulation of prograding coarse sediments.

The shallow water depth indicated for the Thet brings the possibility of reworking by marine processes, including tides, waves, and storms. The passes of finer sediment in the Thet (Figure 4.24) may represent tidal channels (Figure 4.27). The mo-dern North Sea has large tidal ranges so these would be expected in the past. Con-don and others (1992) documented Eocene tide-dominated deltaic deposits on the updipmost East Shetland Platform. Houthuys and Gullentops (1988) found tidal sand ridges in the Eocene of the far southern North Sea (Belgium). Active currents

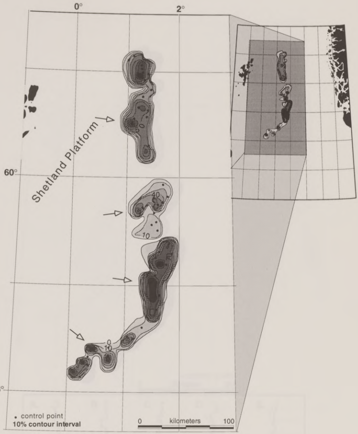

Figure 4.25 Thet sequence percent sand map. Sandiest sediments are in several distinct zones (indicated by arrows of inferred transport direction) along the Shetland Platform.

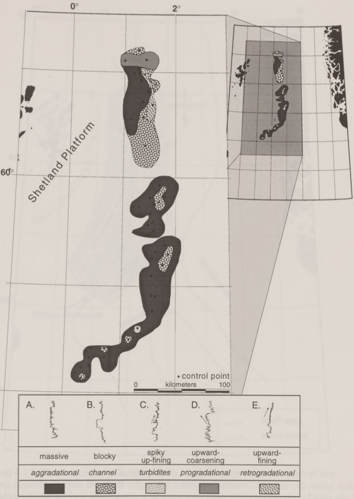

Figure 4.26 Thet log motif map. Dominantly massive sand bodies characterize the unit, with some blocky and progradational components.

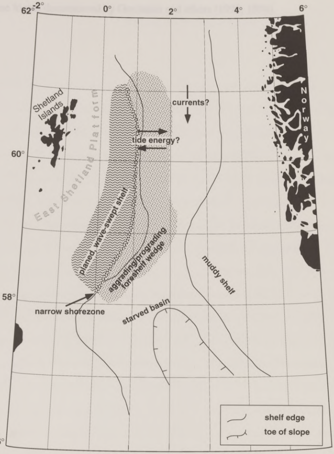

Figure 4.27 Thet sequence paleogeography. Late Eocene relative sealevel low forced deposition over the shelf-edge. An erosional surface is preserved updip and a hiatal/erosional surface basinward. Currents may have scoured the deep basin while tidal energy may account for silty areas along strike.

may have swept through the basin and moved or eroded sediments forming the late Eocene hiatus documented by Gradstein and others (1992, 1994).

Chapter Five

CHRONOSTRATIGRAPHY

Estimation of chronostratigraphic ages is an important part of sequence stratigraphy in order to compare their occurrence with that of other local, regional, and global geological events. Numerical ages also make possible calculations of rates of processes, such as sediment accumulation and subsidence. The construction of numerical times scales is an intricate, iterative process in which enormous quantitities and varieties of data must be reconciled. Numerical time (geochronology) is determined from the measurement of ratios of radioactive isotopes of differing known rates of decay. Because radiometric dating is not possible or feasible for all rocks, ties and interpolations to radiometrically dated rocks are necessary. The most direct tie is a magnetostratigraphic tie, since magnetozones are considered to be globally isochronous. Less precise and less strictly synchronous, but easier and more uniquely identifiable, are biostratigraphic events and zones. In the best case, rocks contain index fossils which are recognized as part of a global biostratigraphic scheme, such as the Paleogene calcareous nannofossil (NP) zonation of Martini (1971) or planktic foraminiferal (P) scheme of Blow (1969), both which have been tied to magnetostratigraphic and chronostratigraphic scales (*e.g.*, Hardenbol and Berggren, 1978; Harland and others, 1990). Although a few of these "index" fossils appear in the North Sea Tertiary section, they do not occur commonly enough to be useful. As a result, indirect ties to lower latitude sections containing fossils from the P and NP zonations are necessary.

North Sea strata can be indirectly tied in to global chronostratigraphies in several ways. Although radiometric and paleomagnetic dates are not available, the fossils which occur in the Tertiary are also found in outcrops in northwest Europe for which there are good radiometric, magnetostratigraphic, and/or global biostratigraphic control. Furthermore, many of the outcrops are among the earliest and most-studied anywhere, including the type sections for European stages, originally defined lithostratigraphically, which have been adopted worldwide as chronostratigraphic units (Harland and others, 1990). For example, the type section of the Ypresian stage is in Belgium, and contains fossils common to those in North Sea wells as well as calcareous nannofossils of zones NP11 and NP12 (Hay and Mohler, 1967; Martini, 1971). Bujak and Mudge (in press) have erected a dinoflagellate cyst zonation for the North Sea Eocene which includes many taxa also found in these onshore localities.

Of the several numerical time scales in use, that of Harland and others (1990) is considered the most applicable to North Sea Tertiary deposits and will be employed here. The Harland time scale emphasizes European stratigraphy and stage boundaries and is commonly used by Northwest European geologists, stratigraphers, and petroleum companies. Another commonly used time scale is that of Haq and others (1988), which includes a global succession of depositional sequences and their bounding surfaces. It is important to note that these two time scales differ significantly in the Eocene (Figure 5.1). For example, Haq and others (1988) place the base of the Eocene near the NP9/10 boundary, low in magnetozone C24, at 54 Ma, whereas Harland and others (1990) put the Paleocene/Eocene boundary within NP10, also low in magnetozone C24, but at 56.5 Ma, a difference of two and one-

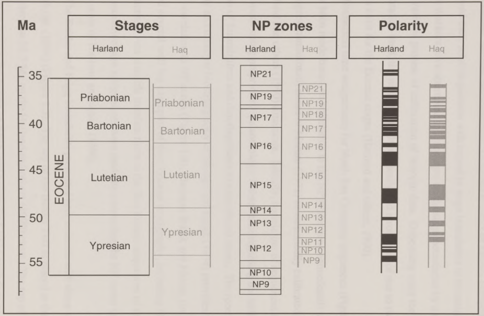

Figure 5.1 Side-by-side comparison of two numerical time scales. Note great differences in the ages assigned nannofossil (NP) zones and polarity chrons of the Eocene from Harland and others (1990) and Haq and others (1988).

half million years. These differences are attributable to several factors. Actual numerical designations of the biozones referenced are not provided by the time scales in question. Instead, the occurrence of fossils in rocks of known European stage has allowed their relative position with regard to stage boundaries to be assigned. Time-scale workers have attempted to place ages on the stage boundaries by a complex and variable process of calibration of isotopic data. Depending upon the method of calibration used, the results vary dramatically and errors bars of one to two million years exist for the Eocene stages (Harland and others, 1990).

Numerical time assignments for North Sea Cenozoic sequences (Figure 5.2) have been made based on correlation to the NP (Paleogene nannofossil) and NN (Neogene nannofossil) zones of Martini (1971) as numerically calibrated on the Harland and others (1990) time scale. Initially, correlation of sequences to NP zones was made using proprietary paleontologic information regarding the indirect correlation of foraminifera and dinoflagellates to nannofossil zones. The recent stratigraphy and dinocyst biostratigraphy of Mudge and Bujak (1994) provides a more direct correlation to NP zones (Figure 1.8). Because Bujak and Mudge (in press) provided several well log examples of their Eocene stratigraphy, including NP zone correlations, it was possible to relate them to the five Eocene sequences of this study. The numerical age assignments were made by converting the NP zones using the time scale of Harland and others (1990).

The Balder and Frigg boundaries presented here coincide with those of Mudge and Bujak (1994) (Figure 1.5). The top of the Balder Tuff is placed at the NP10/11 boundary, at 55.7 Ma on the Harland and others (1990) chart. The top of the Frigg sequence falls in the middle of NP15, just below the P10/11 boundary, at 47.2 Ma.

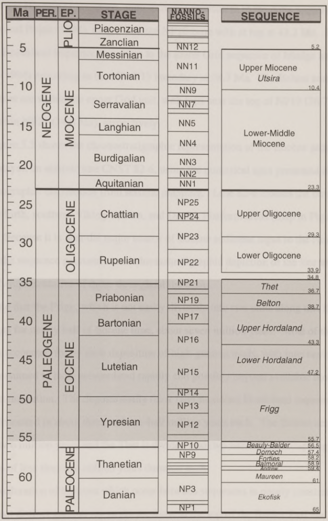

Figure 5.2 Cenozoic North Sea chronostratigraphy (sequences from this study are shaded). Linear time scale of Harland and others (1990). Some Eocene sequence age calibration from Mudge and Bujak (1993). Paleocene sequences of Liu (in prep.), Oligo-Miocene sequences of Garber (in prep.). See also Galloway and others, 1993.

The Lower Hordaland sequence, approximately equivalent to the Alba sequence of Mudge and Bujak (1994), ranges into the NP16 zone with at top at 43.3 Ma. The Upper Hordaland sequence correlates to the lower Grid sequence of Mudge and Bujak (1994) extending to the NP17/19 boundary at 38.7 Ma. The Belton and Thet sequences are within the upper Grid unit, with tops near the top of NP19 (36.7 Ma) and within NP21 (34.8 Ma), respectively.

Figure 5.3 shows the chronostratigraphic representation of the Eocene sequences as displayed on seismic line CNST 82-6, using the numerical ages presented above and geographic distribution from seismic mapping. Line 82-6 crosses the outer Moray Firth, southern Viking Graben, and Danish Platform areas (map in Figure 1.10). Because it is near the major source of Eocene sediment input to the North Sea basin, the sequence geometries and chronostratigraphic depiction of the line are *broadly* representative of those throughout the basin.

Note that the Frigg, which is not easily divisible into two units along this line, accounts for nearly half of Eocene time, about seven million years. Most of this time is accounted for by slow deposition of high-gamma muds, with intervening sands assumed to have accumulated rapidly and possibly beyond available biostratigraphic resolution. The depositionally thick (and muddier) Hordaland sequences were deposited in about three and one-half million years each. The Belton occupies about two million years and the Thet is divided into two successive offlapping wedges of less than one million years duration each.

The duration of hiatuses which occur between sequences is poorly constrained. The most distinct gamma-ray peaks are those at the top of the Balder Tuff and top of the Belton. Neal (1992) presents a Central Graben Eocene chronostratigraphy based

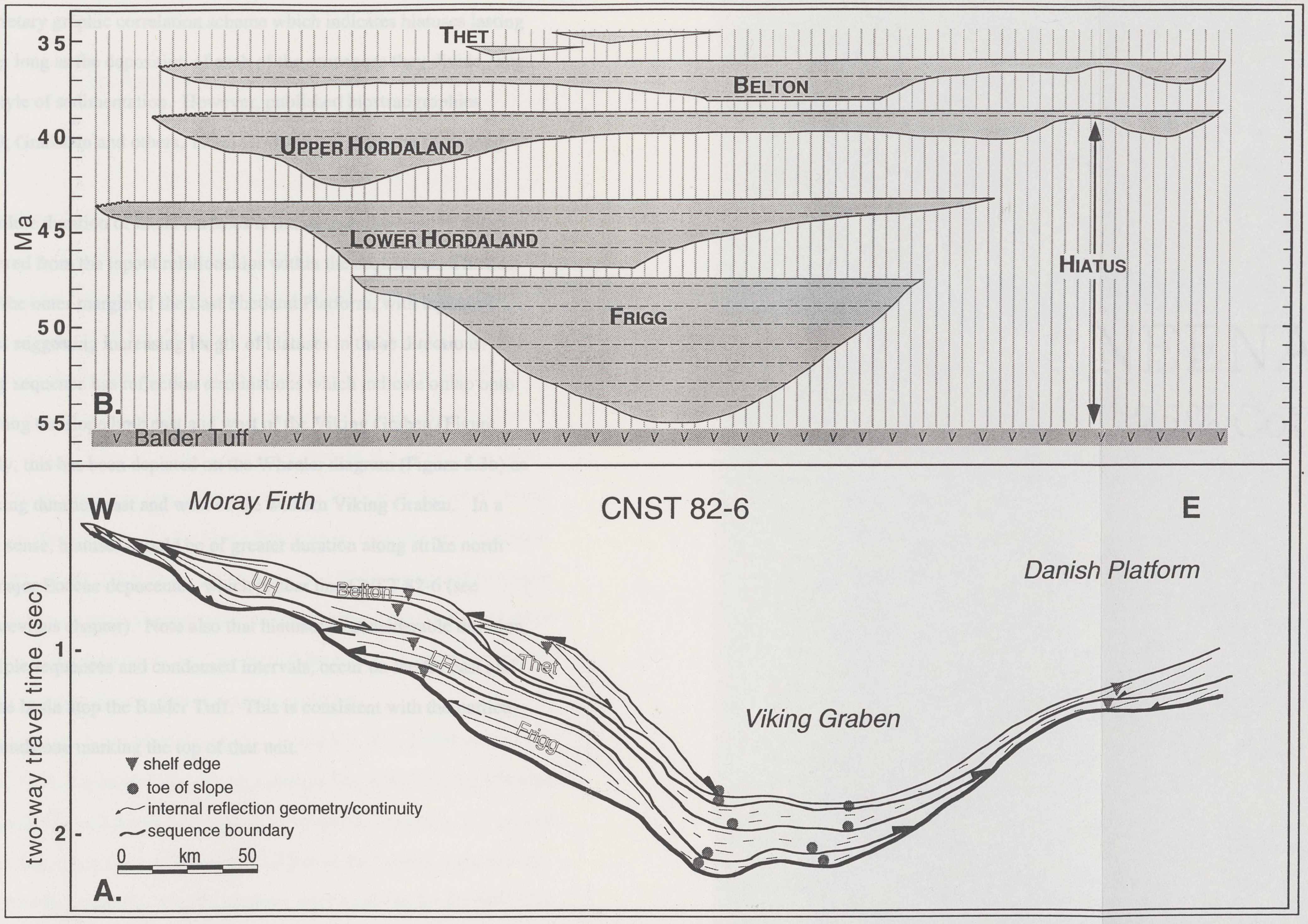

Figure 5.3 A. Seismic interpretation of line CNST 82-6. B. Chronostratigraphic (Wheeler) diagram of line 82-6 Eocene sequences showing lateral distribution on horizontal axis and geologic time on vertical axis. Lengths of hiatuses between sequences are poorly constrained.

on Amoco's proprietary graphic correlation scheme which indicates hiatuses lasting five to ten times as long as the deposition of each of the sequences they divide, suggesting a pulsed style of sedimentation. However, published biostratigraphies (King, 1981, 1989; Gradstein and others, 1992, 1994) do not show the same long hiatuses.

While the absolute duration of hiatal surfaces is intractable, the relative duration of hiatuses is inferred from the lapout relationships within the sequences. Thickest section occurs on the outer margin of the East Shetland Platform, with lapout of units west and east suggesting increasing length of hiatuses in those directions. For example, the Frigg sequence has reflection terminations which indicate onlap onto the Balder Tuff along the slope both east and west of the Viking Graben (Figure 5.3a). Accordingly, this has been depicted on the Wheeler diagram (Figure 5.3b) as a hiatus of increasing duration east and west of the western Viking Graben. In a three dimensional sense, hiatuses should be of greater duration along strike north and south of the major Eocene depocenter, which is near line CNST 82-6 (see isopach maps in previous chapter). Note also that hiatuses of considerable duration, representing multiple sequences and condensed intervals, occur on the far east and west margins of the basin atop the Balder Tuff. This is consistent with the particularly radioactive mudstone marking the top of that unit.

Chapter Six

FORAMINIFERAL BIOFACIES ANALYSIS

6.1 Introduction

This chapter presents data and interpretations from foraminiferal study of a well on the Beryl Terrace. The intention is to show how the objectively and subjectively evaluated foraminiferal biofacies relate to and impart additional understanding of the sequence stratigraphy presented in the previous chapters. As discussed above (Chapter One), North Sea biostratigraphies which are useful for purposes of correlation have been proposed. These typically emphasize use of marine dinoflagellate cysts (Bujak and Mudge, in press) which apparently evolved at a particularly rapid rate in the early Eocene and thus providing a correspondingly high degree of resolution in that section (Figure 1.8). Earlier North Sea work on foraminifera (Gradstein and Berggren, 1978; King, 1981; Gradstein and others, 1988) emphasized two main components of the fauna: agglutinating and calcareous forms, with the former occurring preferentially in the deep basin and the latter on the surrounding shelves, each providing a relatively low degree of stratigraphic resolution.

The well selected for biostratigraphic study, Unocal UK 9/12-2, was chosen for several reasons. First, it is located directly on a seismic line, CNST 82-10, allowing an accurate tie between well depths and seismic travel times. Secondly, it is located on the Beryl Terrace, a key area, and intersects all five of the Eocene sequences described in the preceding chapters. Finally, samples were available for the well from the operator, Unocal UK Ltd, in sufficient volumes to extract meaningful quantities of foraminifera. Well logs, including gamma-ray, resistivity, sonic, travel times from the integrated sonic log, and a digitized log converted to time domain were available. Correlation of these data to surrounding wells and seismic lines, completed before the ditch cutting samples were obtained, allowed confident placement of the Eocene sequence boundaries on the seismic section and well log.

Figure 6.1 shows the location of the well and seismic line under discussion and others in the area overlain on Mesozoic structural features. UK 9/12-2 is located on the Beryl Terrace, an intermediate structural feature between the outer Shetland Platform and Viking Graben along which Eocene sands were funneled to the basin floor. A portion of seismic line CNST 82-10 (Figure 6.2) shows the location of the well and expression of the sequences about ten kilometers east and west thereof. The normal fault left of center marks the boundary between the Shetland Platform and Beryl Terrace. Displacement on this fault of Paleogene strata is probably attributable to differential compaction, but could possibly be strike-slip based on the upper Paleocene anticlinal feature just west of the fault. The Frigg sequence is relatively thick (over 200 msec) with the distinctive Balder seismic marker at the base and a high-amplitude reflection at the top of the Bruce fan sands (Heritier and others, 1979) which show a massive clean sand on the gamma-ray log. The Lower Hordaland sequence onlaps the Frigg sands and is muddy. The gamma-ray shows upward-fining overlain by upward-coarsening textural trends indicative of the retrogradation followed by progradation. A strong gamma-ray peak marks the top of the Lower Hordaland and correlates to a continuous, high-amplitude seismic reflection. The Upper Hordaland, muddy and slightly upward-fining according to the gamma-ray curve, thins updip, and displays medium-amplitude reflections of average continuity. The Belton sequence has a highly variable, spiky gamma-ray re

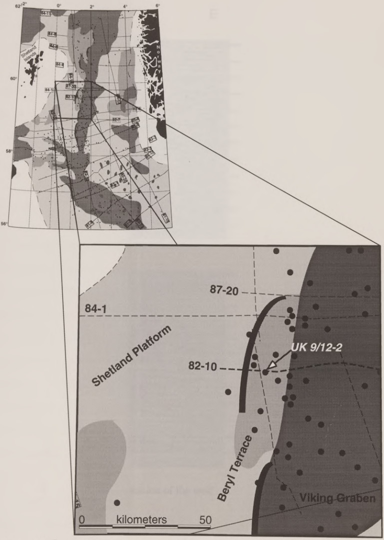

Figure 6.1 Location map indicating position of well UK 9/12-2, seismic line CNST 82-10. Shading of Mesozoic structure after Figure 1.1.

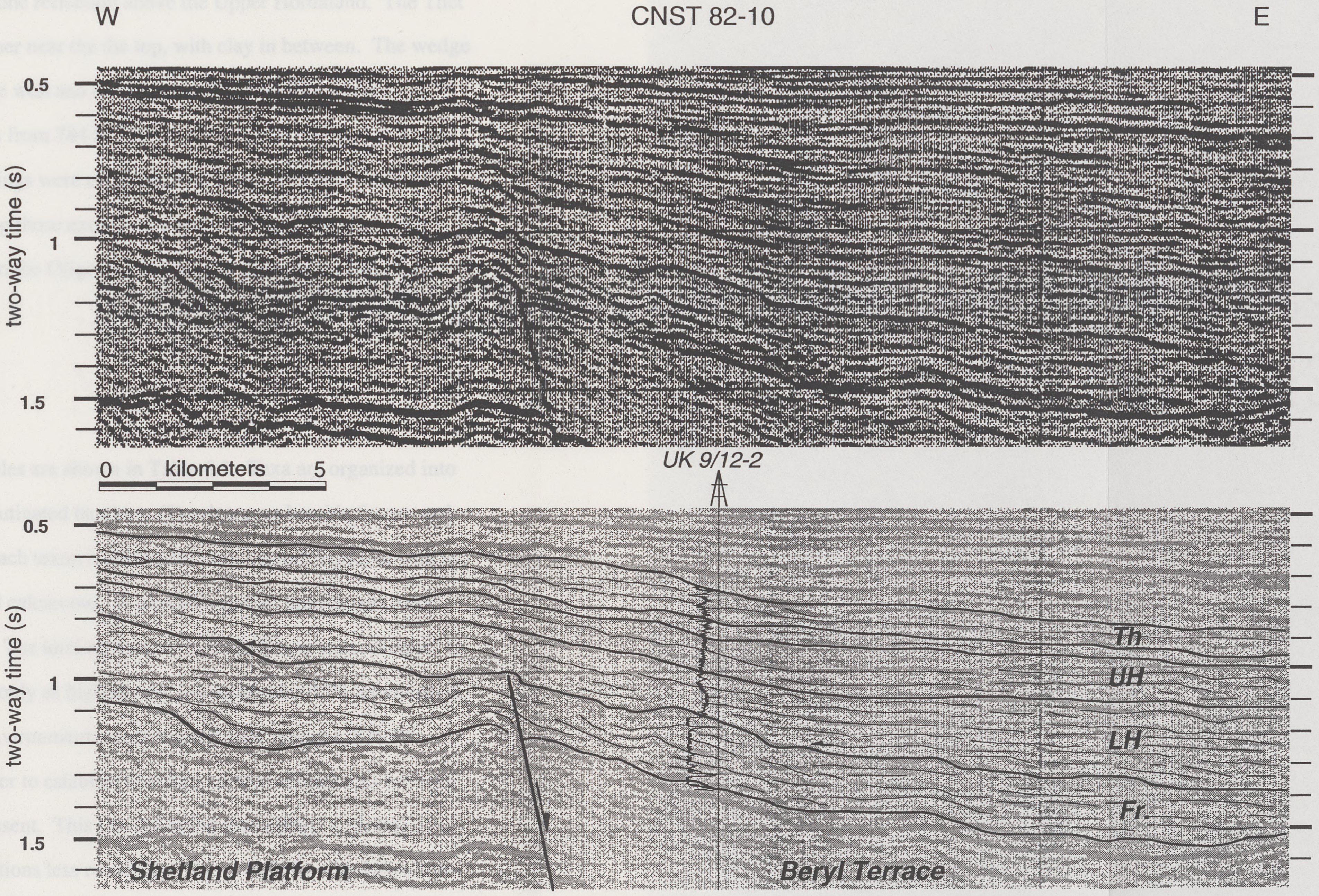

Figure 6.2 A portion of seismic line CNST 82-10 showing expression of Eocene sequences passing through the location of the well in which foraminiferal samples were studied.

sponse and is thin, lying about one reflection above the Upper Hordaland. The Thet has a sand at the base and another near the the top, with clay in between. The wedge is thickest just to the west of the well and thins up and downdip from there.

The Eocene section extends from 784 to 1363 meters in well UK 9/12-2, a total of 579 meters, from which cuttings were obtained at 10 meter intervals. A total of 69 samples were used, including those extending about 50 meters down into the Paleocene and 50 meters up into the Oligocene sections in order to compare their biofacies with the Eocene.

6.2 Data

The raw counts of the samples are shown in Table 6.1. Taxa are organized into three principle groups: (1) agglutinated benthics, (2) calcareous benthic forms, and (3) planktics. The number of each taxon is shown for each sample depth, as well as the totals of all agglutinants, all calcareous, all planktic, and all three forms (total foraminifera) for each sample. The total number of foraminifera in most samples is relatively low: as few as none, only as high as 165, averaging about 50 foraminifera. Standard procedure for paleoenvironmental analysis typically requires 200-300 foraminifera per sample, in order to establish accurate relative abundances between the tens of species typically present. This impoverished assemblage with low overall abundance makes interpretations less robust than they would be with larger samples.

Twenty-eight agglutinated forms were recognized, with primary genera including *Cribrostomoides*, *Cyclammina*, *Haplophragmoides*, and *Rhizammina* tubes. Only *Cyclammina* and *Haplophragmoides* were considered sufficiently abundant to

DEPTH (meters)	Ammodiscus spp.	Ammosphaeridina spp.	Bathysiphon spp.	Bathysiphon spp. A (flat)	Cribrostomoides spp.	Cyclammina amplectens	Cyclammina paupera	Cyclammina placenta	Cyclammina rotundidorsata	Dorothia spp.	Glomospira spp.	Haplophragmoides eggeri	Haplophragmoides tetruseptus	Haplophragmoides walteri	Hormonsina	Hyperammina spp.	Kerreriella spp.	Praecystammina spp.	Psammosphaera spp.	Recurvoides spp.	Reophax spp.	Reticulophragmium spp.	Rhizammina spp.	Saccammina spp.	Spiroplectammina spp.	Spirosigmoilinella spp.	Trochammina spp.	Textularia spp.	Urnulina spp.	TOTAL AGGLUTINANTS
759										2																1				3
768										1															5	2				8
777																														0
786																										1				1
796																								1						1
805																		1			1				2	1				5
814																								1		1				2
823																					1			1		1				3
832																										1				1
841																														0
850														1												1				2
860			1																											1
869																										1				1
878																														0
887																														0
896																														0
905																					4					1		1		6
914																														0
924																									1					1
933																														0
942												1								1			1	3			1		5	12
951			1							1							1													3
960						1				1					1										1					4
969					2				2	1	1							1												7
978					5	3	1		7		2	1	1	1		1		4					37		2		1	2		68
988					7				3		1	1										1	14					1		28
997					5		8			1	2	1	1	2	3			1		1			13		3					41
1006					2				10			1		1			1	1		3			24		2	1				46
1015			1		1				11			1					1						7							22
1024			1			1			4	1		12		1			1			2			12		2	1	1			39
1033		3			43	2			25			1		2		1				1			35		2	1				#
1042			1		2				1			2								1			7		1		1			16
1052			1		11				11	1				4			1			2			12		5	1	4			53
1061					2				5			4		1					1	3		1	11		1					29
1070					4									8			1						7		2					22
1079					5				8		1	4								1			9		2					30
1088					7	1			13	1				3									11		1		1			38
1097			3		9	1	2		10			3		1			1						13	1		1				45
1106					4	3			3			8		6									19					1		44
1116					1	1			1			2									1		1				1			8
1125			1		3	1			4						1								14		1					25
1134	1		4		5	4	1		8			3									1		10	2	2	1	1			43
1143					4	5			6			4		4									22	3	1					49
1152			1		12	5			5			4		1									17				2			47
1161					3										2								6							11
1170	1				3	1			1	1		1		2								2	16	1	1		1			31
1180					1	1			1											1	1		4	1	1					11
1189						2			2												1		4	2						11
1198						1	1	1	2														3							8
1207						4			8			2		1				1		1	1		12		2		3			35
1216						1		1	2											1			4			1	1			11
1225						2			1			1		2	1							2	1	1						11
1234	1					2						2		1									7				1			14
1244			1		2				1										3				1		1					9
1253									1			1											1			1				4
1262	1				2	1																	5							9
1271																														0
1280					1	1			6					2													2			12
1289					1				1		1			1											1	1				6
1298					1																		4		1		1			7
1308									2		1	1		1						2			5				1			13
1317														1									3							4
1326					1	2																	1							4
1335			2		1	1								3			1					2	2							12
1344	1				2	2														1			5	1						12
1353	1																					1	8							10
1362	1		1	5		2						4									1		1							15
1372						3															1		1							5
1381											2									1			1				2			6
1390	2																										1			3
1399	1						2																				2			5

DEPTH (meters)	Bulimina spp.	Cassidulina spp.	Cibicidoides spp.	Dentalina spp.	Eponides spp.	Epistomina spp.	Epistominella spp.	Fissurina spp.	Gavelinella spp.	Glandulina spp.	Globocassidulina spp.	Gyroidina spp.	Hoeglundina spp.	Lenticulina spp.	Marginulina spp.	Nodosaria spp.	Nonionella spp.	Nuttallides spp.	Oridorsalis spp.	Osangularia spp.	Pararotalia spp.	Planulina spp.	Pullenia spp.	Virginulina spp.	Uvigerina spp.	TOTAL CALCAREOUS	Catapsydrax spp.	Globigerina spp.	Globorotalia spp.	Subbotina spp.	Radiolaria	TOTAL PLANKTIC	TOTAL FORAMINIFERA
759	1		8	8					5			3		3				5					3	1		37						0	40
768	6	5	14	13					5		2	3				1	1		2			1			1	54						0	62
777	4	3	6	10		2			3			1					3						1			33						0	33
786		2	2	4	1		1				1	2				4							1			18						0	19
796		1	7	1								1				3						1	1			15						0	16
805			2	2	1				1		1			1									1			9						0	14
814		1	1		2											2							1			7						0	9
823		2	2	2	1								1			1										9						0	12
832	1	1	1	2								1		2												8						0	9
841	1	1		2	1							1														6						0	6
850		2	1		1				1										1				1			7						0	9
860		1	2		1							1														5						0	6
869		2	4							1				2		3						1				13						0	14
878																										0						0	0
887		1																			1					2						0	2
896																										0						0	0
905	1	2	1	6																			1			11						0	17
914		2	4	1				1								4										12	1					1	13
924				1		2										2							1			6						0	7
933			7	5					2					1		6							1			22	2		1	1	3	4	26
942	2	12	24	12	7				2			5								2		1	1		1	69	24	20	5		19	49	130
951	1		5	8					1					2					1				1			19			1		5	1	23
960	3	3	16	7	2				2		1								1				1			36	6	14	6		15	26	66
969	2	5	7		4							2		4		1							1			26	4	11	4		1	19	52
978		3	3	1	3						1															11	1	3		1	1	5	84
988																										0				1	2	1	29
997		6	3	2	2																	1				14					1	0	55
1006		6	7	4	2						1	1		1			1									23	1	1	2	2	5	6	75
1015		2		1																						3	1			2		3	28
1024		3	6	6	2									1									1			19		2			4	2	60
1033		2	4	14		1			4					10	3	1	3					1				43		4	2			6	165
1042				1																						1	1		1		5	2	19
1052		8	6	5	3							1		1		3								1		28	1				3	1	82
1061		4	1									2														7					2	0	36
1070	1	2	2	2												2										9	1		1			2	33
1079			2																							2	3		2	5		10	42
1088		5	4	2	1							1				1										14				1		1	53
1097		2	2		3																		1			8				1	2	1	54
1106		2	2											1												5					3	0	49
1116	1	1		1																						3				1		1	12
1125			3	4																						7	2					2	34
1134		1	2		1									1												5					26	0	48
1143				1										1		1										3					40	0	52
1152		2	2	2	2							2														10			1		22	1	58
1161				1																						1					10	0	12
1170												1		2	1											4					27	0	35
1180																										0						0	11
1189		2																								2				1	12	1	14
1198		1												1												2					61	0	10
1207												3										1				4	1	1			66	2	41
1216		1												2										1		4					13	0	15
1225															1											1					66	0	12
1234																										0					30	0	14
1244														1	1											2					16	0	11
1253																										0				1	1	1	5
1262															1											1					2	0	10
1271																										0						0	0
1280					1																					1					6	0	13
1289	1														1											2					21	0	8
1298																										0						0	7
1308														1												1					23	0	14
1317																										0		1			12	1	5
1326			1																							1					3	0	5
1335																										0					4	0	12
1344			1	1																						2					15	0	14
1353																										0						0	10
1362		1																								1					2	0	16
1372																										0						0	5
1381																										0						0	6
1390																										0						0	3
1399																										0						0	5

Table 6.1 Checklist of microfossils identified and counted in samples from well U.K. 9/12-2.

divide into species; the rest of the agglutinants were only identified to genus. Twenty-seven calcareous genera were identified, dominated overall by *Cassidulina*, *Cibicidoides*, and *Dentalina* (calcareous tubes), among which division into species was not considered useful. Four planktic foraminiferal genera were present in subequal fractions, *Catapsydrax*, *Globigerina*, *Globorotalia*, and *Subbotina*. Radiolarians (spherical planktic silica microfossils) were present in some samples and were counted. They all appear to be of the genus *Cenosphaera*, as described by King (1983), who noted their maximum abundance in NP13 time (late Ypresian).

It is apparent from consideration of Table 6.1 that there is variation among the foraminifera as a function of depth in the well. A crude biostratigraphic subdivision may be recognized simply by considering the obvious divisions in the table, at 3810 and 3120 feet. In order to consider the variability further, the foraminiferal abundances have been plotted as a function of depth alongside the well log and the sequence interpretations overlain (Figures 6.3-6.5). As noted earlier, the sequences were interpreted long before the foraminiferal samples were studied, and the boundaries shown are essentially unchanged.

The graph of the total number of several key genera of agglutinated foraminifera (Figure 6.3) shows least three Eocene units reflected in their variation. Agglutinants are rare in the Frigg sand, common in the Hordaland sequences, and very rare to absent in the overlying Belton and Thet units. Information for selected calcareous benthic foraminifera (Figure 6.4) indicates a nearly symmetrical trend with respect to depth. Calcareous forms are rare or absent in the Frigg sequence, abruptly more common in the Hordaland and Belton, and in low abundance in the Thet sequence. Summary information (Figure 6.5) shows the total foraminifera

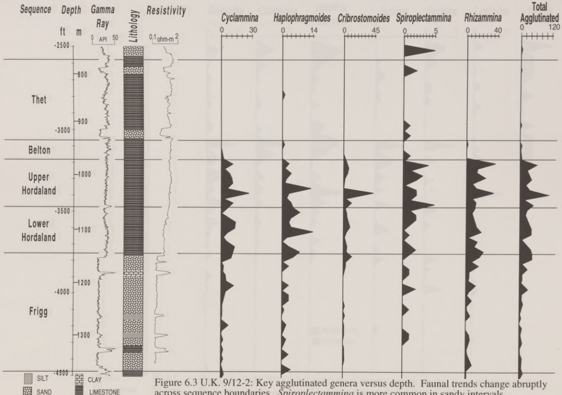

Figure 6.3 U.K. 9/12-2: Key agglutinated genera versus depth. Faunal trends change abruptly across sequence boundaries. *Spiroplectammina* is more common in sandy intervals.

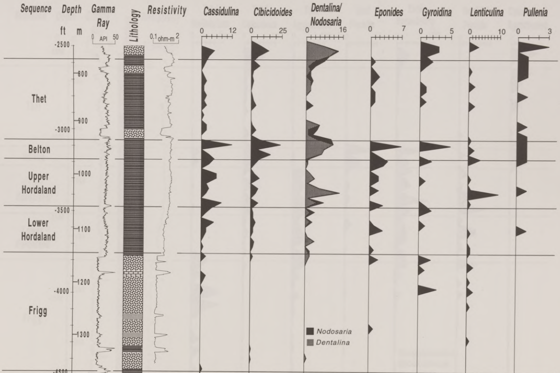

Figure 6.4 U.K. 9/12-2 key calcareous genera versus depth. Low numbers in the Frigg increase up-section. Highest numbers in the Belton and Oligocene.

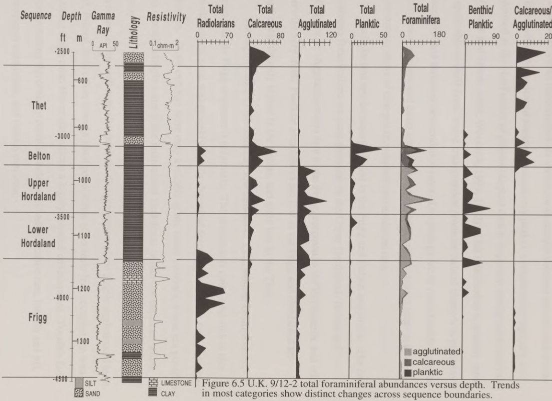

Figure 6.5 U.K. 9/12-2 total foraminiferal abundances versus depth. Trends in most categories show distinct changes across sequence boundaries.

abundance peaks (uncorrected for variations in sample volume) are not well correlated with the condensed sections (gamma-ray peaks), a relationship typically espoused as the chief utility of paleontological data in sequence stratigraphic analysis (Loutit and others, 1988; Wornardt, 1989, 1992). This relationship is actually most applicable to shelf areas where transgression produces radical changes in paleoenvironment and sediment accumulation rates. Deepenings are of considerably less consequence in slope and basin areas where they do not produce such large paleoenvironmental shifts or changes in sediment accumulation rate.

Radiolarians are dominantly found in the Frigg and Belton sequences. The calcareous foraminifera are most abundant in the Upper Hordaland, Belton and Oligocene. Agglutinants are rare in the Frigg, common in the Hordalands, and otherwise very rare. Planktic abundances are low in the Frigg and Hordaland sequences, abruptly higher in the Belton, and quite low in the Thet.

The significance of the distinctly low number of foraminifera, or impoverishment, in the Frigg sequence is enigmatic. The sequence is quite sand-rich in this well and the sand was probably rapidly deposited thereby diluting the fossil concentration. Since cuttings were only available at ten meter intervals, it was not possible to directly sample some of the intercalated mudstones within the sequence which may have much higher foraminiferal concentrations. The sand within the Frigg sequence in this well may also promote disaggregation of the fragile agglutinated tests. If, indeed, lower than average sized populations of foraminifera occupied the area during Frigg time, this might indicate a highly stressed environment. Possible factors stressing the ecology could include rapid sedimentation rate, low Eh and pH, restricted circulation, and limited nutrients.

In summary, the Frigg sequence is characterized by an impoverish agglutinated foraminiferal assemblage supplemented by radiolaria. Radiolaria vanish and agglutinants and calcareous forms are more abundant in the Lower and Upper Hordaland. Agglutinants disappear across the Upper Hordaland/Belton boundary and the Belton is conspicuously enriched in calcareous and planktic forms. Finally, the Thet is dominated by calcareous benthics in moderate numbers. This subjective analysis of the biofacies present in the well does suggest distinct breaks within the section which correspond to four of the five sequence boundaries previously identified. The Hordaland succession is not divisible, suggesting the lower and upper sequences do not reflect a change in factors would have influenced the foraminiferal biofacies, chiefly paleoenvironment.

6.3 Q-Mode Cluster Analysis

In order to more objectively consider the biofacies, a quantitative technique called cluster analysis was performed. Cluster analysis, one of many multivariate techniques commonly applied to quantitative micropaleontologic datasets, is a method for grouping samples or variables based on some measure of similarity (Park, 1974). The mode of cluster analysis applied, Q-mode cluster analysis, is the grouping of samples based upon the similarity of the fauna contained in each sample. In contrast, R-mode cluster analysis groups variables, which in this instance would be foraminifera, based on their co-occurrence in samples. The basic steps involved in cluster analysis are: (1) obtaining a data matrix, (2) computing a similarity matrix, (3) clustering samples, and (4) computing a "cophenetic correlation coefficient". The similarity matrix is derived using simple matrix algebra to produce a number which represents the degree of similarity between each sample and every other sample. There is a variety of mathematical formulas for computing the similarity, the choice of which is determined by the type of raw data. The Bray-Curtis coefficient (Bray and Curtis, 1957) is generally considered particularly applicable to faunal percentage data. Clustering of samples is typically done by connecting the two most similar samples, treating them as a single sample, recomputing the similarity between this new sample and the remaining samples, and repeating the process until values of all the samples are graphically connected in a *dendogram.* The cophenetic correlation coefficient is a number which indicates the degree of distortion in the cluster analysis introduced by the averaging of samples in the clustering procedure. A value of 1 indicates identical starting and finishing matrices (no distortion), whereas values from 1 to 0 indicate decreasing similarity (increasing distortion).

The data matrix used was a derivation of the data matrix shown in Table 6.1. The raw counts were converted to percentages of the total number of foraminifera in each sample, thus eliminating bias introduced by the fact that each sample had a different number of foraminifera. Next, taxa which did not average over one percent of the total fauna were removed because they are considered insignificant and only add noise to the data (this was verified by performing a preliminary cluster analysis with the rare forms included). Barren samples were omitted from the data matrix, since they provide no biofacies information (they are, however, significant in other ways). The final data matrix included the percentages of 29 taxa in 68 samples. Clustering was performed using a method referred to as Weighted Pair Group Averaging, a common algorithm in which no correction is made for the fact that the weight of each sample added to the cluster increases since each is compared to an average of the previously clustered samples. The necessary arithmetic computations were performed using BioStat™ software on an Apple™ Macintosh™ computer.

The dendogram produced by the cluster analysis is shown in Figure 6.6. Samples are on the vertical axis indicated by sample depth and shaded bars indicating which Eocene sequence they fall within and similarity is shown on the horizontal axis. The cophenetic correlation coefficient for this cluster analysis is 0.73. This means that there is a modest amount of distortion of the data caused by the averaging of similarities in the clustering process.

By subdividing the dendogram at the similarity level shown by the dashed line (about 0.75), distinct clusters emerge, which are closely related to the sequences, along with a few outliers at the bottom of the dendogram. The two most similar samples are at 1262 and 1344 meters in the Frigg sequence. The sample from 887 meters is dissimilar from most of the rest of the samples, probably explained by the fact that it only has two calcareous foraminifera, distinguishing it from both other samples with low numbers, which are chiefly the agglutinated biofacies, and other samples with calcareous forms, which typically have a wider variety of taxa. The Frigg falls into two cluster groups which include one Upper Hordaland sample (1042 m). Two other Frigg samples, 1280 and 1372 meters, are outliers (for no reason apparent in the data), as are the two samples from the underlying Balder . Three Frigg samples cluster with the Hordaland samples (1143, 1152, and 1207 m) possibly because of their enrichment in *Rhizammina*. The Hordaland comprises one group, an idea supported by the stratigraphy and subjective consideration of the paleontologic data, with many of the Lower Hordaland samples falling within a mixed

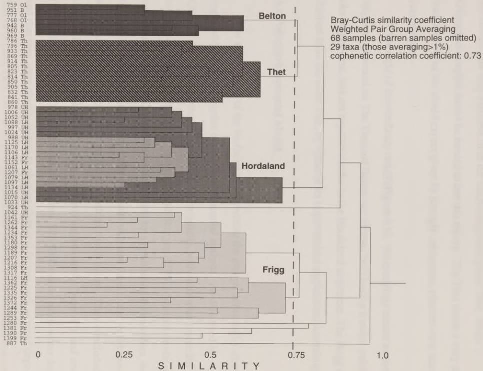

Figure 6.6 Dendogram of Q-mode cluster analysis of foraminiferal samples from well UK 9/12-2.

subcluster. The Belton forms a distinct cluster that includes two samples from the Oligocene, which we might interpret to support the idea that these two muddy units are similar and very different from the intervening sand-prone Thet. More Oligocene samples would be needed to test this theory. The Thet forms a very distinct cluster, as we would expect given its strongly calcareous, planktic-free faunal component.

To the right of the similarity cutoff (Figure 6.6), the groupings cluster as they might be expected to. The Thet and Belton are similar, both having a major calcareous component, and are together similar to the Hordaland sequences. The Frigg is distinct from the other four, by virtue of its impoverished agglutinated assemblage.

6.4 Paleoenvironmental Model

The significance of the biofacies characterizing the groups indicated by clustering is addressable by means of paleoenvironmental analysis. As discussed in Chapter One, agglutinated foraminifera are enigmatic, with somewhat uncertain paleoenvironmental significance. Gradstein and Berggren (1981) reported on the occurrence of microfossil assemblages dominated by agglutinating foraminifera, from the North Sea and Labrador Sea Paleogene and compared them to the well-known so-called "flysch facies" in the Alpine-Carpathian flysch basins. They concluded that the biofacies represented by large, coarsely agglutinating ("type A") and small, fine-grained ("type B") agglutinants range from 200-4000 meters paleo-water depth and that they were chiefly related to physico-chemical factors such as rapid deposition of organic-rich, carbonate-poor clastics under conditions of restricted bottom water circulation.

The agglutinants in UK 9/12-2 are chiefly in the lower Eocene and vanish quite abruptly in the Belton. While it is unlikely that this study, in its limited scope, will solve the riddle of the paleoenvironmental significance of agglutinants, we may speculate. Agglutinating faunas are commonly regarded as indicating lack of carbonate in the water for benthic calcareous forms to construct their tests. However, benthic calcareous forms do occur in low but steadily increasing numbers from the base of the Frigg to the top of the Upper Hordaland (Figures 6.4, 6.5). It is possible that these microfossils are non-indigenous and were transported downslope or are the result of contamination in the well. If so, one would expect to see abrasion of the tests or possibly sorting by size, neither of which were typically observed. Test dissolution of the calcareous benthics or planktics was not observed either, as might be expected if the carbonate compensation depth (CCD) were shallow. Furthermore, there is a 20 meter thick micritic limestone bed at 1175 meters in the Frigg sequence (Figure 6.5) which suggests that carbonate was readily available in the water. In summary, there is not any concrete evidence to support a paleoenvironmental interpretation, or carbonate availability signal, of the agglutinants which differs from that of Gradstein and Berggren (1981). However, it may be possible to refine the paleobathymetric range of agglutinants, which they proposed was 200-4000 meters.

Jones (1988) presented analyses of Late Paleocene flysch fauna in six North Sea wells thought, by virtue of their structural position relative to one another, to represent a transect along paleoslope from the outer shelf to basin floor. In his paleoslope transect approach, he assumed a 200 m water depth for the shelf edge and calculated a 1500 meter water depth for the basin center based on trigonometric reconstructions assuming a particular dip along the slope from the shelf edge to the basin floor (following methods of Nyong and Olsson, 1984). His paleobathymetric model is only as accurate as his not insignificant assumptions regarding these water depths, the dip of the slope, and the position of the shelf edge and basin floor. While his water depths may have error, the position along the transect is well-constrained such that the differing foraminiferal assemblages he found within contemporaneous rocks probably represent shelf, slope, and basin settings. Alternatively, the variation in foraminiferal assemblages along the transect could reflect paleoenvironmental factors not necessarily related to water depth, such as substrate type or oxygen content.

Jones (1988) found delicate, fine-grained tubular agglutinants of *Rhizammina* genus, thought to prefer fine-grained, low-energy environments (Schafer and others, 1983; Schröder, 1986) preferentially on the basin floor. On the middle slope occurred more robust, coarse-grained tubes along with *Recurvoides*, *Psammosphaera*, and *Rhabdammina*, thought to prefer higher energy areas, possibly turbidity current-influenced, with coarser sediments. The upper slope wells were populated by fewer coarse-grained tubes and relatively more common *Haplophragmoides walteri*. Figure 6.7 is a table of the environmental preferences of various agglutinating taxa, including groups of tubes related by size and texture. Radiolarians are thought to be most abundant in the open ocean (Ingle, 1980), partly due to the dissolution of carbonate tests below the calcium compensation depth (CCD).

Eocene deepwater calcareous benthic foraminifera have been described for the North Sea only briefly. King (1983, 1989) named an "outer sublittoral - epibathyal" biofacies, comprised chiefly of *Bulimina, Gyroidina, Pullenia, Uvigerina, Valvulinerina, Bolivina,* and *Nodosaria,* which he assigns a water depth of 50 meters to "over 200" meters, which is not very precise. Tjalsma and Lohmann (1983)

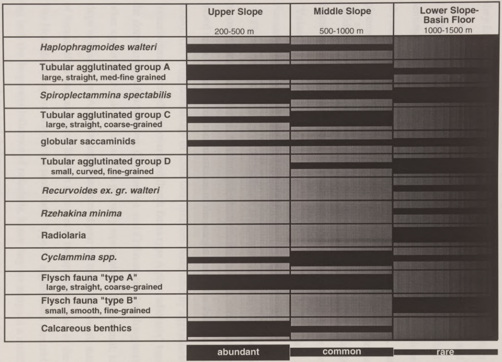

Figure 6.7 Table of relative abundance of taxa on the upper, middle and lower slope (modified after Jones, 1988; additional interpretation from Ingle, 1980, Gradstein and Berggren, 1981, and Tjalsma and Lohmann, 1983).

studied Paleocene and Eocene bathyal and abyssal benthic foraminifera in the Atlantic and circum-Atlantic. Among the species identified relevant to this study, they found *Cassidulina, Cibicidoides,* and *Gyroidina* representative of deeper (abyssal) depths and *Lenticulina* at shallower (bathyal) depths. Berggren and Aubert (1975) described two Atlantic benthic biofacies: a shelfal fauna distinguished by lenticulinids, vaginulinids, textularids, and polymorphinids, and a lower slope and abyssal plain assemblage of *Nuttallides, Gaudryina, Dorothia, Gyroidina, Bulimina,* pleurostomellids and stilostomellids. The shallower biofacies is referred to as "Midway-type" after its description in the Midway Group of the Gulf Coast (e.g. Plummer, 1927; Kellough 1959, 1965) while the deeper water assemblage is called "Velasco-type" following early publications illustrating it from the Velasco Formation of Mexico (Cushman, 1925, 1926).

Figure 6.8 is a summary of the biofacies assignment and interpreted paleoenvironment for each sequence. Absolute paleobathymetries are less certain as they are based upon the geometric reconstruction of the margin during the Paleocene (Jones, 1988). The Frigg assemblage of small total numbers dominated by agglutinated foraminifera is termed "impoverished flysch fauna type A plus radiolaria" based on the dominance of *Rhizammina, Cyclammina,* and *Cribrostomoides,* along with a few other agglutinants and radiolaria. This probably represents the deepest unit: lower slope to basin floor. A shallowing is interpreted near the top as the overall numbers of foraminifera and calcareous fraction increases in the uppermost sand of the Frigg. The Hordaland sequences share the same basic "type A" agglutinated assemblage, but lack the deepwater influence of radiolaria, hence they are assigned a middle slope association. A gradual shallowing throughout Hordaland time is inferred from

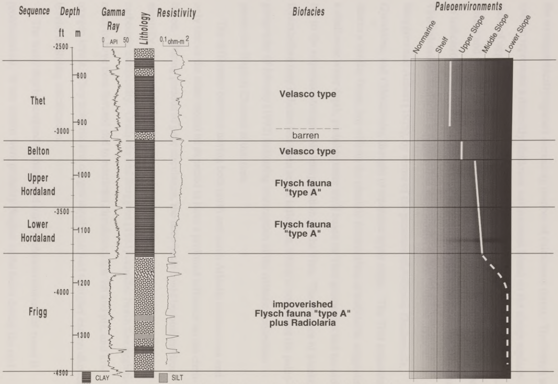

Figure 6.8 Summary of Eocene biofacies and interpreted paleoenvironments

the stratigraphically-upward increasing number of calcareous forms. The Belton sequence represents a distinctly shallower environment based on the abrupt replacement of agglutinants by a calcareous benthic assemblage with an increase in radiolarians and planktics. The influx of radiolarians and planktic foraminifera could be an indication of increased oceanographic connection to the Atlantic during this time. This calcareous biofacies is regarded as most similar to the "Velasco" type of Berggren and Aubert (1975), by virtue of the presence of *Pullenia, Oridorsalis, Gyroidina,* and *Cibicidoides,* thought to represent upper slope. The Thet sequence shares a similar fauna, but without the planktic foraminifera or radiolaria, suggesting a shallower water depth, probably outer shelf based on Thet geometries and according to the sequence stratigraphic interpretation for the Thet. The absence of planktic foraminifera may indicate less open ocean influence, which is consistent the paleogeography of Murray (1992) indicating interruption of the Atlantic connection across the English Channel at this time.

The difference between having both north and south Atlantic connections and only one or the other would be expected to have a profound influence on the circulation. During periods of poor circulation, the deep basin could become environmentally adverse, with low oxygen, poor nutrient supply, and possibly decreased carbonate availability. Gradstein and Berggren (1981) consider North Sea agglutinants to have been favored due to restricted circulation, low Eh and pH, and low oxygen levels. They note that low oxygen supply can lead to higher carbon dioxide levels, inhibiting calcification.

The water depths assigned to these (and many) paleoenvironmental zones is problematical. Water depths were probably deepest in the basin during the mid-

Paleocene interval (about 60 Ma) studied by Jones (1988). Furthermore, while his transect included wells in the basin (the Viking Graben), the structural position of UK 9/12-2 on the Beryl Terrace precludes a "basinal" environmental interpretation. Finally, the depths must be geologically reasonable. Given that the Frigg contains a biofacies most similar to what Jones (1988) found in the lower slope and basinal areas, we might assign the Frigg his paleobathymetric range of 1000-1500 meters. The problem with this is that the present day structural top of the Frigg is at 1143 meters, requiring that either the basin stopped subsiding post-Frigg or has undergone considerable uplift, neither of which seems a tenable conclusion. Instead, a modification of the paleobathymetries represented by the shelf and slope environments is in order. The Frigg is assigned to the lower slope (reserving the basinal environment for the Viking Graben to the east) adjusted upward to 600-900 meters. The Hordaland middle slope environment is regarded as 300-750 meters. The slightly shallower upper slope Belton falls in the 200-500 meter range, and the shoaling outer shelf Thet, 100-200 meters.

Overall, the paleobathymetric trend for the Eocene sequences at this well location is reasonable within the constraints of what is expected from the sequence stratigraphic analysis. In the broadest sense, the seismic stratigraphy suggests filling of the basin and reduction of differential topography compatible with gradual shallowing. The abrupt shoalings for the Belton and Thet are compatible with the sequence interpretations that suggest each represents a basinward shift in coastal onlap, that for the Thet being rather dramatic. The biofacies patterns and their abrupt change at sequence boundaries indicates that, with the exception of the Lower/Upper Hordaland boundary, the sequence boundaries represent significant changes in paleoenvironment as well as changes in paleobathymetry. The change from dominantly agglutinated to calcareous fauna at the Upper Hordaland/Belton boundary is the most dramatic change in biofacies. It is interesting that samples in the Belton include planktic foraminifera and radiolaria, which may indicate a better paleoceanographic connection to North Atlantic surface waters at this time. If so, the improved basin circulation, and consequent increase in oxygen and nutrient levels, may be responsible for the disappearance of the agglutinated foraminifera thought to represent a "stressed" environment.

Chapter Seven

SUBSIDENCE ANALYSIS

This chapter examines the subsidence history and rates of sediment accumulation of a well on the Beryl Terrace. This type of information is useful in elucidating relationships which may have been important in sequence development, such as changes of sediment supply rate or in creation of accommodation space. Although primary interest is on the Eocene section, the younger rocks must be stripped off in order to determine their contribution to subsidence. Similarly the underlying Paleocene and Mesozoic strata need to be backstripped in order to document the space made available by their compaction before and during Eocene loading. The older and younger units are not as well-constrained in either age or water depth as the Eocene.

7.1 Data Input

The tectonic subsidence and other information derived from subsidence analysis is only as valid as the data used in the computation. Detailed geologic information is required, including the age, lithology, porosity, paleo-water depth and thickness of each unit, as well as the duration of any hiatuses and/or thickness of section eroded. Numerical ages were assigned following the time scale of Harland and others (1990) and, for the Cenozoic, the chronostratigraphy in Figure 5.2. Figure 7.1 provides a graphic summary of some of the information which was input for UK 9/12-2. The

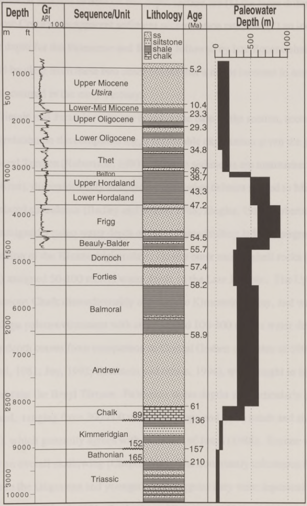

Figure 7.1 Summary of well U.K. 9/12-2, information used in subsidence analysis. Thickness, lithology, age, and interpreted paleowater depth are plotted. Numbers near unconformities indicate age of rocks lying above unconformity.

fundamental features to note on this depth section are (1) the large difference in pre- and post-Cretaceous apparent sediment accumulation rate, and (2) an increase in water depth for the Paleocene and Eocene, followed by late Eocene shallowing. It should be clear from these two observations that a major increase in accommodation space occurred in the early Tertiary.

Triassic and Jurassic rocks are found at the base of the section, according to the interpretation on the composite log, a reasonable expectation given the geology of the Beryl Terrace (Robertson, 1993). Triassic sediments are nonmarine (fluvial and lacustrine), disconformably overlain by Bathonian deltaics related to Middle Jurassic rift-related subsidence (Badley and others, 1988; Ziegler, 1982; Robertson, 1993), both assigned a paleo water depth of zero. Downfaulting led to transgression and deposition of the Kimmeridgian clays, chiefly outer marine shelf rocks (Robertson, 1993) assigned 50-100 meters water depth, in the Late Jurassic. The Upper Cretaceous Chalk disconformably overlies the Kimmeridge clay, and was deposited in a slope paleoenvironment with an estimated 100-400 meters water depth. The water depth comes from comparison to Central Graben estimates of 100-600 meters (Wood, 1981; Joy, 1992; Gradstein and others, 1994), which ought to have been deeper than the Beryl Terrace. Paleocene water depths are particularly poorly constrained, ranging from 300-600 meters for slope and basin sands and shales (Wood, 1981), which generally agrees with estimates of Jones (1988). Eocene water depths show an overall shallowing (Chapter Six). The dominantly calcareous foraminiferal fauna in the Oligocene and younger strata suggests they were deposited in shelfal water depths (Wood, 1981; Gradstein and Berggren, 1981), estimated to range from

50-200 meters at this position. Ages for the Cenozoic sequences are from the chronostratigraphy presented in Chapter Five.

North Sea sediment porosities are anomalously high, a fact not overlooked by the petroleum industry. Much of the Tertiary is undercompacted and uncemented. Paleocene and Eocene age sands are unlithified with porosities as high as 30% and permeabilities up to 5 Darcies (*e.g.* Alba Field (Mattingly and Bretthauer, 1992), Frigg Field (Mure, 1987)). Harris and Fowler (1987) present a porosity versus depth relationship extending into the Jurassic for the southern Viking Graben (Figure 7.2), although this probably reflects higher than average sandstone porosities since only reservoir rocks are plotted. The subsidence program of Bond and Kominz (1984) defines porosities as exponential curves. In order to reflect the higher porosities in North Sea rocks, the clean sandstone porosities were revised upward based on the work of Harris and Fowler (1987) to 40% at the surface, 30% at 2000 meters, and 10% at 4000 meters burial depth.

The data input for the subsidence program is shown in Table 7.1. Stratigraphic units and unconformities are shown in the first column. The thickness of each unit, measured from the well log, is in column two. Unconformities are recorded as 10 centimeters thick (small, but nonzero, a requirement of the program). Densities were calculated based on the fractional lithologies within each unit and assuming densities of 2.65, 2.68, 2.71, and 2.75 for sand, siltstone, shale, and carbonate, respectively. Sands are presumed to be very clean, based on their description from cores (*e.g.*, Harris and Fowler, 1987; Milton and others, 1990) and their expression on the gamma-ray log. No externally derived cement was interpreted and very little

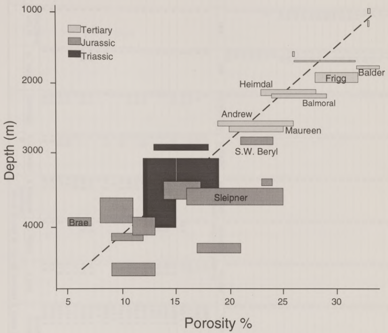

Figure 7.2 Porosity versus depth relationship for hydrocarbon-bearing reservoirs in the North Sea (modified after Harris and Fowler, 1987) illustrating anomalously high porosities, a factor taken into account during backstripping.

North Sea; well UK 9/12-2; age at bottom is estimated 225 Ma; no external cement										
22					LITHOLOGY					
name	thickness	density	shale %	micrite %	sandstone %	calcarenite%	siltstone%	siltinite %	ss type	
	(m)	g/cm2							4=cl;1=dirty	
Triass	290	2.6942	0.6	0	0.26	0.1	0.04	0	4	
Unc1	0.1	2.6942	0.6	0	0.26	0.1	0.04	0	4	
Bathon	101	2.6528	0.15	0	0.8	0.01	0.04	0	4	
Unc2	0.1	2.6528	0.15	0	0.8	0.01	0.04	0	4	
Oxford	38	2.6659	0.37	0	0.63	0	0	0	4	
Kimmer	126	2.6858	0.34	0.01	0.06	0	0.55	0.04	4	
Unc3	0.1	2.6858	0.34	0.01	0.06	0	0.55	0.04	4	
Chalk	94	2.75	0	1	0	0	0	0	4	
Andrew	476	2.6422	0	0	0.98	0.02	0	0	4	
Balmoral	313	2.703	0.9	0	0.1	0	0	0	1	
Forties	134	2.6492	0.1	0	0.88	0.02	0	0	4	
Dornoch	131	2.6427	0.03	0	0.95	0	0.02	0	4	
Balder	78	2.6799	0.42	0	0.23	0	0.35	0	4	
Frigg	210	2.6463	0.07	0	0.91	0.01	0.01	0	4	
Lower	95	2.7087	0.95	0.02	0.03	0	0	0	4	
Upper	80	2.7087	0.95	0.02	0.03	0	0	0	4	
Belton	49	2.7087	0.95	0.02	0.03	0	0	0	4	
Thet	146	2.6984	0.75	0	0.16	0.04	0.05	0	4	
LoOligo	152	2.689	0.6	0.05	0.3	0	0.05	0	4	
UpOligo	27	2.6707	0.35	0	0.55	0.04	0.06	0	4	
LoMio	61	2.6555	0.1	0	0.75	0.05	0.1	0	4	
Utsira	283	2.6525	0.1	0	0.85	0.05	0	0	4	
			% externally derived cement							
name	density	shale	micrite	sandstone	calcarenite	siltstone	calcisiltstone	age	wd1	wd2
Triass	2.6942	0	0	0	0	0	0	210	0	0
Unc1	2.6942	0	0	0	0	0	0	165	0	0
Bathon	2.6528	0	0	0	0	0	0	157	0	50
Unc2	2.6528	0	0	0	0	0	0	152	0	0
Oxford	2.3949	0	0	0	0	0	0	145	0	50
Kimmer	2.5758	0	0	0	0	0	0	136	50	100
Unc3	2.5758	0	0	0	0	0	0	89	0	0
Chalk	2.75	0	0	0	0	0	0	59.1	100	400
Andrew	2.6422	0	0	0	0	0	0	58.9	300	600
Balmoral	2.703	0	0	0	0	0	0	58.2	300	600
Forties	2.6492	0	0	0	0	0	0	57.4	250	500
Dornoch	2.6427	0	0	0	0	0	0	55.7	250	500
Balder	2.6799	0	0	0	0	0	0	54.5	300	750
Frigg	2.6463	0	0	0	0	0	0	47.2	600	900
Lower	2.7087	0	0	0	0	0	0	43.3	500	750
Upper	2.7087	0	0	0	0	0	0	38.7	500	750
Belton	2.7087	0	0	0	0	0	0	36.7	200	500
Thet	2.6984	0	0	0	0	0	0	34.8	100	200
LoOligo	2.689	0	0	0	0	0	0	29.3	50	200
UpOligo	2.6707	0	0	0	0	0	0	23.3	50	200
LoMio	2.6555	0	0	0	0	0	0	10.4	50	200
Utsira	2.6525	0	0	0	0	0	0	5.2	50	200

Table 7.1 Input file detailing values used in backstripping program.

cementation of any kind was noted in the mud log description. Minor local cement is derived internally from dissolution of shell debris.

7.2 Results and Discussion

Plotted in Figure 7.3 are selected results of the backstripping procedure. A gradual increase in total sediment column thickness in the Mesozoic was followed by a dramatic increase at about 61 Ma (indicated by the arrow). This period of rapid deposition coincides with the Andrew sequence (Figure 7.1). About 500 meters of sand was deposited in just over one million years, as contrasted with the underlying 100 meters of Cretaceous chalk which accumulated slowly over about 30 m.y. High accumulation rates continued through the Paleocene, were moderate during the Eocene, and leveled off in Oligocene time. Decompacted sediment thickness mimics the first curve but with correspondingly thicker section.

The amount of space between the seafloor and sea-level, regardless of eustatic effects, is the amount of space available for sediments to accumulate, also referred to as "accommodation space" (Jervey, 1988). The portion of the accommodation space accounted for by sediments is shown on the curve with black squares in Figure 7.3. The actual accommodation space is calculated by adding the water depth to this curve, and is indicated by the shaded band on Figure 7.3, which extends from the minimum to maximum water depths. The most dramatic changes in accommodation space are coincident with the inflection points on the subsidence curve: in the early Paleocene and late Eocene.

The paleobathymetric shallowing of about 500 meters for the Thet and Belton sequences (indicated by the arrow in Figure 7.3) requires a tectonic uplift of several

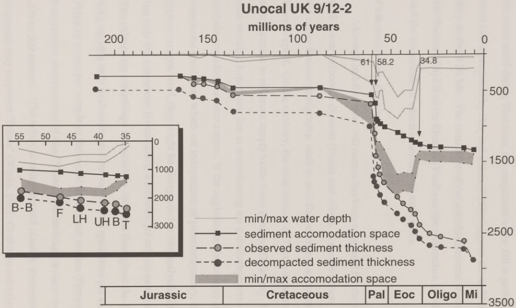

Figure 7.3 Subsidence curves for well UK 9/12-2. Inset box shows enlargement for Eocene curves. Major changes in subsidence (inflection points) are indicated at the beginning of the Paleocene (61 Ma), middle Paleocene (58.2), and end of Eocene (34.8). Major changes in accommodation space occur in the early Paleocene and late Eocene.

hundred meters and/or a eustatic fall. Although either is consistent with the sequence stratigraphic interpretation of relatively low sea-level forcing deposition to the outer shelf during Thet time, the magnitude of the fall is problematical. The sea-level curve proposed by Haq and others (1988) suggests about 50 meters of eustatic drop at about 36 Ma. The remainder of the paleobathymetric shallowing requires 450 meters of uplift of the Shetland Platform, the mechanism of which is unknown and the magnitude of which is unlikely in most cases.

Paleobathymetry Revisited

Although uplift of over 500 meters has been suggested for the tilting associated with lower Paleocene deposits (Nadin and others, in review), there is not evidence in the upper Eocene stratigraphy, such as an influx of coarse sediments, to support Eocene uplift. On the contrary, the total volume of Thet sediment suggests a significant decrease in sediment supply to the basin (Liu and Galloway, 1993). An alternate working hypothesis lies in re-evaluating the paleobathymetric estimates, which include considerable error ranges. If the agglutinated fauna represents paleoenvironmental conditions which are independent of paleobathymetry, such as substrate type or oxygen level, they might be disregarded in this analysis. Instead, considering only the calcareous foraminifera, a different paleobathymetric story emerges. The calcareous assemblage is essentially the same throughout the Eocene (Figure 6.4), varying only in abundance, from one or two specimens per sample in the lower Frigg to scores per sample in the rest of the Eocene section (Figure 6.5). The paleobathymetric interpretation of this "Velasco" assemblage is outer shelf to upper slope, 200 to 500 meters. The influx of radiolaria and planktic foraminifera in the Belton sequence may represent "floods" (Wood, 1981; Gradstein and others, 1992) indicative of a paleoceanographic change which allowed greater circulation of open marine waters during that time, of no paleobathymetric significance. In this case, a water depth of 200-500 meters throughout the Eocene still requires a shallowing of 100-300 meters between the Thet and the Oligocene. While more reasonable than a 500 meter shallowing, this interpretation still requires a significant tectonic component beyond the maximum attributable to eustasy (50 meters) as suggested by Haq and others (1988).

This analysis shows that there is considerable uncertainty in interpreting the paleobathymetric significance of foraminifera, particularly agglutinants, of the North Sea Paleogene flysch. Examination of the entire UK 9/12-2 well might better constrain the paleobathymetries of the underlying Paleocene and overlying Oligocene and Miocene, thus placing the Eocene in a firmer context relative to these apparently deeper and shallower sections, respectively. However, consideration of the Cenozoic in many North Sea wells (Gradstein and Berggren, 1981; Gradstein and others, 1992, 1994; King, 1983, 1989) has not provided any particular refinement of the slope and basin paleobathymetries.

Subsidence Mechanisms

Rapid Paleocene subsidence represents the downdip extent of the tilting of the East Shetland Platform (Jones and Milton, 1990; Milton and others, 1990), which some have postulated was caused by a plume related to the Iceland hotspot (White, 1988; Nadin and others, in review). Nadin and others (in review) postulate, further, that following the uplift and tilting during the Paleocene, collapse of the plume led to strong regional subsidence. This, combined with post-rift thermal subsidence, is thought to account for strong Eocene subsidence (also noted by Joy, 1992, and

Armentrout and others, 1993). The onset of spreading between Greenland and Svalbard to the north (and resulting ridge-push forces) and the earliest Alpine compression to the south may have influenced the basin in the late Eocene, accounting for the inflection point at 34.8 Ma on the subsidence curve. Kooi and others (1991) showed that such tectonic events may produce intraplate stresses which are felt over a large area capable of influencing subsidence patterns. Joy (1992) loosely postulates that the transition from an intracratonic setting to one adjacent to an opening ocean basin constitutes a major tectonic change which ought to be manifested in the sedimentary record in the basin.

Depositional Rates

Sediment accumulation rates, calculated by division of the uncompacted sediments thicknesses by their duration, are shown in Figure 7.4. Rates were about 30 meters per million years in the Mesozoic, then increased dramatically in the Paleocene to as high as 700 m/my during deposition of the Balmoral sequence. The Beauly-Balder sequence accumulated at 106 m/my, which is consistent with the overall higher Paleocene rates of deposition but not representative the much lower rates expected for the condensed section atop the Balder Formation.

Eocene sequences show moderate accumulation rates (Figure 7.4 inset) of 30-50 m/my for the first four units with the Thet sequence topping out at 115 m/my. High rates of deposition for the Thet are consistent with the sequence stratigraphic interpretation of a relative drop in sea-level which shifted deposition basinward and focused it on the outer shelf, in the area of study. Oligocene rates were low, with a minor increase in the Upper Miocene with Utsira Formation deposition.

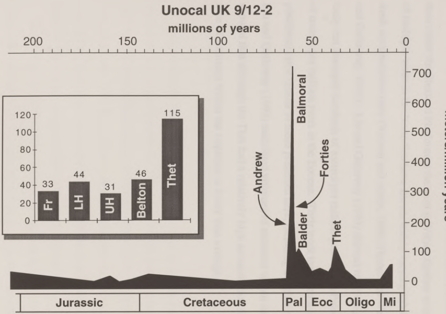

Figure 7.4 Sedimentation rates of uncompacted sediments for well UK 9/12-2. Paleogene peaks are in the Andrew, Balmoral, Forties, Beauly-Balder, and Thet sequences. Inset details depositional rates for Eocene sequences.

Both the subsidence and accumulation rates presented must be considered representative only of well UK 9/12-2. The subsidence is probably extrapolatable across the Beryl Terrace, a discrete structural element, but with a different subsidence history than either the Shetland Platform to the west or Viking Graben to the east. Studies of multiple wells in the North Sea have shown widely varying subsidence and sediment accumulation rates (Nielsen and others, 1986; Thorne and Watts, 1989; Liu and Galloway, 1993). Liu and Galloway (1993) showed rates which varied spatially but averaged hundreds of meters per million years in the Paleocene versus tens of meters per million years in the Eocene. Their work indicated average Eocene depositional rates similar to those presented here, including a higher rate for the Thet. Liu and Galloway (1993) calculated volumes of sediment within the basin and showed that although the Thet had a relatively high accumulation rate, the total volume of sediment within the sequence is lower than average.

Chapter Eight

SYNTHESIS AND CONCLUSIONS

The previous chapters document and interpret the Eocene sequence stratigraphy of the North Sea basin using an integrated approach combining seismic and well log data, localized foraminiferal biofacies analysis, tectonic subsidence history and depositional rate analysis. Because these several chapters present sometimes disparate perspectives of the stratigraphy, this chapter summarizes and reconciles the results and incorporates pertinent information from the literature, including that on regional climate, paleoceanography, tectonic history, and eustasy. Techniques applied and their utility are discussed, and the major conclusions are reviewed at the end of the chapter.

8.1 Remarks On Analytical Techniques

The methods applied in this study have individual strengths, weaknesses, and limitations with regard to unraveling the North Sea Eocene sequence stratigraphy. The regional approach taken necessarily applies a broad brush to the geologic picture, which may include significant sub-regional variation. Conversely, the localized evaluation of one well for biofacies and subsidence analysis brings a very local focus which may not apply sub-regionally, much less regionally.

The regional grid of reflection seismic data interpreted was useful for identifying basin-scale sequence development, but not localized geometries which only occurred on one or two lines within the grid. Furthermore, the displayed scale of regional seismic data is such that relatively small but important sequence stratigraphic features, such as basin floor fans and submarine channels and levees, are beyond the resolution of the data. Because of the high degree of structural heterogeneity in the North Sea, it is not possible to make confident well correlations or evaluate geometries more than a few kilometers from a seismic line, such that seismic data gaps can not be adequately filled using well data. At the same time, without nearby well data, as is the case for large parts of the Norwegian Platform, seismic sequences cannot be confidently lithostratigraphically interpreted.

Distinct reflection lapouts within the seismic data, particularly near the shelf margin on the Shetland Platform, make the North Sea Eocene an excellent candidate for seismic stratigraphic analysis following the methods of Mitchum and others (1977). However, it was not possible to correlate any of the seismic sequence boundaries to shelfal erosion events nor was clear evidence of coastal deposits indicative of coastal onlap present in any of the wells. Well distribution on the inner shelf, however, is quite sparse. Correlation of sequence boundaries in the well log data set was possible only by way of peaks on the gamma-ray log which are chronostratigraphically significant and widely correlatable sediment starvation surfaces. This combination of Exxon-type and Frazier-type sequence identification and correlation worked very well, partly because North Sea transgressive deposits are quite thin such that seismic sequence boundaries nearly coincide with overlying maximum flooding surfaces.

Biostratigraphy as an aid to correlation in this project could have been strengthened had the robust, high -resolution dinoflagellate cyst zonations of Bujak and Mudge (in press) been available for many wells. This would have greatly increased the confidence of sequence interpretations on wells distal from seismic lines. The data and interpretations used, chiefly of a foraminiferal nature, provided lower resolution than the palynological data. Sequence age estimates were possible only to within the resolution of the NP zones (1-2 m.y.) to which they were correlated and it was not possible to estimate the duration of condensed intervals.

The utility of foraminiferal biofacies analysis and the pertinent paleoenvironmental and paleobathymetric constraints it provides was well-demonstrated for the single well studied. One of the most important results of the biofacies analysis was that significant, objectively verified changes in the microfauna occurred at the sequence stratigraphic boundaries, suggesting major changes in paleoenvironment during those times. Greater confidence in the paleoenvironmental interpretations would have been achieved had it been possible to examine more of the Cenozoic section and extend the study to more wells. Furthermore, larger sample sizes would have provided greater numbers of foraminifera which would have added confidence to interpretations by increasing the signal strength and perhaps shed light on the calcareous versus agglutinated assemblages and the nature of impoverishment.

The tectonic subsidence in the well studied, which may represent the Beryl Terrace area as a structural element is well-constrained. The subsidence and accumulation rate information, even if only locally applicable, provides useful insights on sequence evolution. More precise paleobathymetric information would have enabled a more defensible interpretation of the magnitude of late Eocene relative uplift, which was almost certainly chiefly tectonic in origin.

8.2 Tectonics

Galloway and others (1993) documented four North Sea Cenozoic mega-sequences correlated with and thought to have been a product primarily of tectonic phases in and around the basin. These *tectonosequences* correspond to the Paleocene, Eocene, Oligocene, and Miocene, a finding not surprising given the shared regional tectonics and proximity of the North Sea to many of the northwest European outcrops where these subdivisions were historically defined. Each tectonosequence spans tens of millions of years and is comprised of shorter sequences spanning millions of years. Major tectonic events, such as uplift of the Shetland Platform or the onset of seafloor spreading in the North Atlantic and phases of the Alpine orogeny, affected both the sediment source areas and basin configuration and are thought to control tectonosequence development. The Eocene section constitutes one tectonosequence and some of the Eocene sequences may be related to regional tectonic phases as well as to eustatic variations.

Figure 8.1 summarizes northwestern European and Atlantic tectonics and oceanography in relation to the Eocene sequences. Atlantic rifting has been a persistent factor in North Sea evolution, a direct influence during Mesozoic rifting and a peripheral influence thereafter. Although indirect, regional tectonics have been assigned a growing sphere of influence in recent years through such mechanisms as intraplate stresses which can effect subtle vertical and horizontal motions far afield from active deformation fronts (Cloetingh, 1986; Cloetingh and others, 1987; Kooi and others, 1989) . The three most important tectonic processes which may have influenced the North Sea Paleogene are North Atlantic seafloor spreading to the west

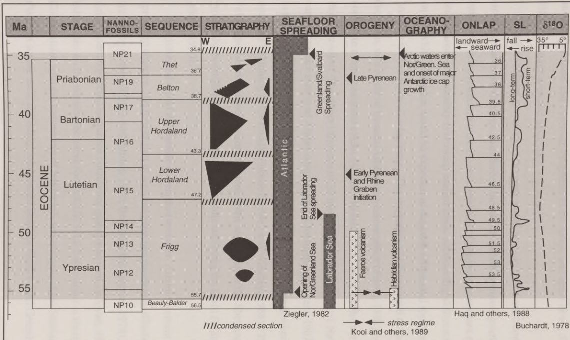

Figure 8.1 Overview of North Sea Eocene sequences and timing of regional geologic events which may have influenced sequence development (modified after Galloway and others, 1993). Onlap and sealevel curves of Haq and others (1988) and North Sea oxygen isotope paleotemperatures of Buchardt (1978) provided for reference.

and north, Alpine and Pyrenean orogenies to the south, and uplift of the Shetland Platform source area and associated volcanism.

Atlantic seafloor spreading to the west would be expected to exert compressive stress on the basin via ridge-push forces, but as the spreading moved north of the basin, the stresses exerted were more extensional. Compressive stresses may uplift source areas and possibly downwarp basinal areas, accentuating differential topography, while extension would be expected to diminish differential topography and possibly lead to regional subsidence. The orogenies which occurred to the south of the basin, as a result of Eurasia/Africa plate convergence (Frisch, 1981), would also constitute a compressional stress, but one oriented more nearly north-south, rather than east-west. The direct influence of 35 megaPascals (MPa; 1 Pa=1 Newton pressure per square meter) of Alpine compression (Cloetingh and others, 1987) is visible in the southern North Sea in the Hampshire Basin and Sole Pit areas where inversion occurred beginning in the middle Eocene (Dewey and Windley, 1988). The late Paleocene Hebridean volcanism produced uplift and tilting of the Shetland Platform, raising the Scottish Highlands source area while subsiding the basin (Milton and others, 1990).

The base and top of the Eocene correspond to major Atlantic-domain seafloor spreading changes, the former part of a global plate reorganization affecting many spreading centers (Hayes and Pitman, 1970; Rona and Richardson, 1978), potentially producing tectonosequence boundaries globally as well (Schwan, 1980). Inflections on the subsidence curve for well UK 9/12-2 also occur at these times. Concomitant with the outpouring of Balder ash and collapse of the Shetland Platform source area, spreading commenced between Norway and Greenland

(Pitman and Talwani, 1972; Ziegler, 1982), to which Kooi and others (1989) partially attribute their calculation of 1 kbar regional NW-SE compressional stress in the Early Eocene. The earliest phase of the Pyrenean orogeny began about this time as well (Srivastava and Tapscott, 1986), producing N-S oriented compression to the south. All of these tectonic reorganizations and stress reorientations serve to differentiate the Paleocene tectonic setting of the North Sea region from that of the Eocene (Galloway and others, 1993).

In the Late Eocene, spreading commenced between Greenland and Svalbard, producing an W-E extensional regime (Le Pichon, and others 1988; Kooi and others, 1989), which persisted throughout Oligocene time. This fundamental change from early Eocene regional compressive to late Eocene extensional stress regime proposed by Kooi and others (1989) agrees with the observations which show the Eocene as partly representing a transition from Paleocene to Oligocene sedimentation and stratigraphy. The Frigg style of sedimentation, emphasizing coarse sediment bypassing to the basin center, is more similar to the Paleocene (Liu, in prep.), while the increasing introduction of shelf and slope mud and onset of Norwegian sources during the Hordaland and Belton time has more in common with the overlying Oligocene (Garber, in prep.).

With regard to intra-Eocene sequence development, the compressive stress regime postulated by Kooi and others (1989) and the resulting enhanced differential topography from basin margin to center is consistent with the early Eocene Frigg sequence in which discrete sands from a high-energy shorezone were fed across a relatively steep shelf to pond in the basin center and intervening lows (*e.g.* the Beryl Terrace). A variety of regional and global events occurred near the Frigg/Upper

Hordaland boundary, including cessation of volcanism in the Faeroe Trough (Knox and Morton, 1988) and the end of spreading in the Labrador Sea (Pitman and Talwani, 1972). The result must have been to relax compression, reduce differential topography between basin margin and center, and possibly shift source areas from one favoring sand to another favoring mud.

Clear tectonic influences within the region are not apparent during Hordaland and Belton time, although extension in the Rhine Graben (Dewey and Windley, 1988) and early phases of Pyrenean orogeny occur during Lower Hordaland time (Ziegler, 1982). The Belton/Thet sequence boundary coincides with a late stage in the Pyrenean orogeny. As discussed in Chapter Seven, the Thet relative sea-level fall must have had tectonic and probably eustatic components.

8.3 Climate and Eustatic Considerations

North Sea Eocene climate varied over a range of about twenty degrees, according to oxygen isotope analysis (Buchardt, 1978; Figure 8.1). An early Eocene warming trend peaked at about 30°C by the end of Frigg sequence time. Gradual cooling became abruptly more rapid in late Belton time, with terminal Eocene temperatures of about 5°C. Eocene climate is relevant to source area weathering and to glacially-induced eustatic fluctuations.

Late Eocene cooling, often interpreted to be have accompanied (or caused) polar ice buildup, would explain, in part, the eustatic fall thought to contribute to the Thet sequence downward shift of onlap. The absence of Thet age sediment elsewhere in the basin, documented by seismic and biostratigraphic evidence (Gradstein and others, 1992), may be related to strong bottom current activity related to the encroachment of Arctic waters which entered the Norwegian-Greenland Sea at this time (Ziegler, 1988; Rea and others, 1990). The relative shallowness of the basin, enhanced by a eustatic low, would have favored axial ocean current development capable of transporting suspended sediment and possibly eroding as well. Currents were not, however, sweeping all through the basin as the English Channel was disconnected from the North Sea basin by an intervening high at this time (Murray, 1992).

The Frigg sequence fan sands at Frigg Field have been linked to a large (110 m) Ypresian eustatic fall (Haq and others, 1988) by McGovney and Radovich (1979) and Heritier and others (1979). However, this is about two million years after the age proposed for the Frigg sands by Bujak and Mudge (in press), who place them in the NP12/13 range. Furthermore, mechanisms for eustatic variations of that amplitude and frequency are not widely agreed upon during this non-glacial period of, in fact, warm climate. The fact that coastal onlap cannot be demonstrated for the Frigg interval makes it unlikely that even a stratigraphically significant relative fall in sea-level occurred at this time. It appears, instead, that the last vestiges of the uplifted source area, tapping Jurassic sandstones, rapidly shed sand into deep water at this time. This is consistent with the concentration of Hordaland depocenters (Figures 4.7-4.16) to the south of those of the Frigg sequence (Figures 4.2-4.6), since the northerly Shetland sources are considered sand-prone while Moray Firth area sources in the Scottish Highlands are chiefly metamorphic basement (Morton, 1979).

The major change from large-scale, basin-centered sand deposits to prograding muddy platforms at the Frigg/Hordaland sequence boundary suggests a change in the source area. This coincides with the onset of cooling (Buchardt, 1978; Figure 8.1), which may have favored arid chemical weathering of Scottish Highlands rocks into clays rather than the mechanical weathering of Orkney-Shetland Paleozoics (Morton, 1979, 1981) into sand. Furthermore, the wide variety of tectonic changes discussed above probably contributed to the change in source area, perhaps by uplifting it, which in itself could have contributed to local orographic climatic changes. The large relative increase of silty mud to the basin during Hordaland time is suggestive of temperate glacial activity, but this may not be compatible with the interpreted paleotemperatures, and, in any case, is not substantiated by any coeval glacial deposits. It is not known if the silts, clays, and muds of the Hordaland resemble glacial flour or not but core examination might resolve the matter.

The onset of Antarctic ice accumulation is generally agreed to be late Eocene or early Oligocene (Barron and others, 1981). This is expected to have influenced eustatic sea-level by a lowering of about 50 meters (Miller and others, 1987; Prentice and Matthews, 1990), which is in general agreement with the 36 Ma fall of 50 meters proposed by Haq and others (1988). However, as noted above, the relative sea-level fall interpreted to produce the Thet shelf-margin wedge was well over this, suggesting a major tectonic component to that fall.

The Haq and others (1988) sea-level and onlap curves (Figure 8.1) do not bear close resemblance to the sequences described herein. If the Haq and others curve does reflect global eustatic variations, it might be concluded that eustasy is not a controlling factor in the North Sea Eocene and that other factors, such as sediment supply or tectonics over-rode eustasy. It is interesting to note that the low-order variations on the Haq and others (1988) curve do roughly correspond to changes in the North Sea. For example, during Frigg time many sequences occur on the onlap curve, while during Hordaland time there was less apparent eustatic variation. Higher frequency appears to return in the late Eocene.

The timing of the condensed sections observed in the North Sea do not consistently correspond to major condensed intervals on the Haq and others (1988) curve. In any case, the average duration of events on the onlap curve, about 1.5 million years, is about the same as the potential error in estimating the age of North Sea Eocene sequences by indirect correlation of NP zones. Thus, individual events on the onlap curve, with their apparent 100, 000 year precision, can neither be refuted nor supported with the present age control.

8.4 Conclusions

1. The Eocene of the northern North Sea consists of five regionally mappable stratigraphic sequences. Four of the sequences are bounded by widely correlatable radioactive mudstones representing relative sediment starvation and one is bounded by erosional surfaces. The pulse of deposition represented by each unit reflects a unique quantity, texture, and source of sediment as well as varying accommodation space.

2. The early Eocene Frigg sequence includes deposits of a high-energy shore-zone along the Shetland Platform which fed clean sands across a relatively steeply sloping shelf to the floor the Viking Graben and intervening Beryl Terrace. A subsidiary sediment source on the Western Platform delivered discrete pulses of sand to

the Central Graben slope and basin into discrete slope fans (Tay sands, Gannet Field).

3. Middle Eocene Lower and Upper Hordaland sequences record a thick, mud-dominated progradation focused on the southern Shetland Platform and outer Moray Firth with clean sands bypassing the inner shelf to basin floor via debris flow and high-density turbidity currents, such as those at Alba Field in the Witch Ground Graben.

4. A basinward shift in coastal onlap marks the late Eocene Belton sequence, a thin, basin-centered unit reflecting decreased differential basin topography with shelf, slope, and basin sands arranged in logical succession east of the Shetland Platform source area, rather than bimodally concentrated on the inner shelf and basin floor as in the early and middle Eocene sequences. Norwegian sources which previously delivered sand to a restricted area on the Horda Platform may have reached the north Viking Graben during Belton time.

5. Coincident with the eustatic fall accompanying the onset of Antarctic glaciation in the latest Eocene, the sand-prone Thet sequence was deposited in a shelf margin wedge geometry occupying the length of the outer East Shetland Platform. The upper Eocene is otherwise quite thin or missing in the basin, possibly as a result of bottom current scouring related to Arctic Ocean water encroachment from the Norwegian-Greenland Sea.

6. Foraminiferal biofacies analyses of well UK 9/12-2 on the Beryl Terrace show a stepwise evolution from an early Eocene fauna dominated by agglutinated foraminifera representing a lower slope environment to a late Eocene outer shelf calcareous benthic assemblage. Q-mode cluster analysis confirms that a distinct biofacies is associated with four of the five Eocene sequences, and changes coinciding with the sequence boundaries. Paleoenvironmental analysis suggests abrupt shallowing and/or rapid changes in basin circulation and connection to the Atlantic occurred coincident with the sequence boundaries, consistent with their geometric indication of onlap variation.

7. Subsidence analysis of the Mesozoic and Cenozoic section for the same well shows a pronounced increase in subsidence rate of the basement in the Early Paleocene, moderate late Paleocene through the Eocene subsidence, and low subsidence during the Oligocene and Miocene. Decompacted sediment accumulation rates for the Eocene average about 37 meters per million years for the first four sequences, but increased to 115 meters per million years for the Thet sequence, presumably due to the rapid, focused deposition which occurred when baselevel lowered.

8. Intraplate stresses related to North Atlantic seafloor spreading to the west and the Africa-Eurasia Alpine collision to the south have exerted primary influence on long-term sequence development in the basin, defining an Eocene tectonosequence. Initiation of Greenland/Norway spreading and major, effusive basaltic volcanism mark the early Eocene while Greenland/Svalbard spreading and Alpine pulses oc-

curred in the late Eocene. Within the Eocene, the strongest link between the observed sequences and regional tectonic influences is at the Frigg/Hordaland boundary, corresponding to the end of Labrador Sea spreading, a time of one of the largest proposed global eustatic falls. Although the direct relationship between these geographically separated areas is unclear, it is thought that intraplate stress of the sort described by Cloetingh and others (1986) contributed to uplift and downwarp of sediment source areas, basin margins, and areas of sediment deposition.

Appendix

Sequence Tops in North Sea Wells

measured in meters from mean sea level

WELL	LATITUDE	LONGITUDE	B	Fr	LH	UH	Be	Th
Norwegian Sector Wells								
1/5-2	56°34'42.0000"N	02°38'30.2000"E	2802	2719	2664	2616	2564	
1/6-4	56°44'52.0590"N	02°42'23.6430"E	3075	2978	2901	2835	2762	
1/9-1	56°24'05.0700"N	02°54'06.4900"E	2849	2752	2682	2604	2564	
1/9-5	56°29'27.6900"N	02°57'55.2700"E	2945	2865	2783	2705	2643	
2/1-3	56°54'41.3900"N	03°06'30.3900"E	2768	2728		2584	2396	
2/3-1	56°53'09.5000"N	03°51'38.3000"E	2105		1945			
2/4-10	56°40'41.5000"N	03°13'21.6000"E	2976	2759	2589			
2/5-6	56°34'13.3400"N	03°37'16.5700"E	2883	2755		2631	2588	
2/6-2	56°30'48.9000"N	03°42'39.6600"E	2991	2822		2655	2485	
2/8-2	56°29'52.8530"N	03°28'33.6380"E	2795	2683		2550	2468	
2/8-3	56°18'31.0000"N	03°26'54.0000"E	2684	2536		2403	2285	
2/8-7	56°26'50.6000"N	03°36'48.3000"E	2479	2383		2311	2245	
2/9-2	56°20'56.7000"N	03°56'00.6000"E	2905	2740		2411	2277	
3/5-2	56°32'34.4560"N	04°23'22.0730"E	2541	2346		2221	2032	
3/7-1	56°27'43.5000"N	04°00'07.8000"E	2661	2382		2151	2030	
7/1-1A	57°47'52.0000"N	02°09'56.0000"E	2051		1984	1929	1822	
7/3-1	57°50'35.7000"N	02°44'57.1000"E	1658		1536	1457	1306	
7/9-1	57°20'37.1000"N	02°51'21.0000"E	2039	1966	1889	1582	1520	
7/11-1	57°04'15.6000"N	02°26'24.4000"E	2839	2757	2721	2639	2567	
8/3-1	57°59'13.0000"N	03°40'13.0000"E	881		815	775	671	
9/4-2	57°41'11.0000"N	04°02'35.0000"E	1111	1076	982	854	791	
9/4-3	57°36'54.5000"N	04°18'57.7000"E	1063	1030	863	789	677	
9/4-4	57°42'01.4800"N	04°13'20.7900"E	1039	1006	879	779	725	
9/8-1	57°20'34.0000"N	04°20'13.0000"E	1089	1062	962	857	814	
9/12-1	57°11'40.0000"N	04°57'21.0000"E	962	905	761	637	537	
15/2-1	58°45'19.7500"N	01°35'40.5400"E	2036	1910	1650	1494	1387	
15/3-1	58°50'55.0000"N	01°43'13.0000"E	2124	1973	1752	1545	1388	
15/3-2	58°59'00.5000"N	01°47'12.6000"E	1947	1736	1503	1421	1227	
15/3-4	58°49'05.2800"N	01°52'59.8200"E	2208	2085	1902	1656	1532	
15/5-1	58°35'00.7000"N	01°39'11.0000"E	2028	1901	1817	1734	1622	
15/6-3	58°30'16.6800"N	01°42'36.5217"E	2181	2065	1928	1774	1724	
15/6-4	58°37'30.9700"N	01°48'19.1800"E	2156	2033	1930	1794	1653	
15/9-3	58°29'10.0400"N	01°41'38.4600"E	2118	2052	1918	1751	1713	
15/9-4	58°24'00.2600"N	01°47'06.9300"E	2295	2146	1988	1923	1840	
15/9-14	58°17'23.1900"N	01°41'28.0600"E	2357	2237	2112	1929	1870	
15/9-15	58°18'07.4500"N	01°55'19.6700"E	2147	2116	1997	1869	1857	
15/12-1	58°10'32.6000"N	01°44'23.1000"E	2431	2224	2100	2007	1916	
16/1-1	58°59'18.0000"N	02°02'03.0000"E	2170	2014	1824	1705	1527	
16/1-2	58°56'09.1500"N	02°13'20.0630"E	1947	1820	1764	1707	1530	
16/2-1	58°53'35.2000"N	02°21'25.7000"E	1567		1551	1517	1454	
16/7-1	58°20'23.0000"N	02°18'50.0000"E	1639			1541	1492	
16/8-2	58°20'59.8100"N	02°24'59.5800"E	1499			1406	1307	
16/9-1	58°22'41.5000"N	02°48'17.0000"E	1293			1218	1124	

17/4-1	58°35'47.0000"N	03°16'15.0000"E	998			953	796	
17/10-1	58°01'54.0000"N	03°09'58.0000"E	1295		1149	1094	960	
17/11-1	58°12'36.0000"N	03°20'35.0000"E	940		891	847	775	
17/12-3X	58°11'33.0000"N	03°51'44.0000"E	742		646	614	580	
24/9-1	59°16'09.4800"N	01°47'31.1800"E	2007	1885	1701	1554	1402	1096
24/9-3	59°22'25.9500"N	01°46'26.7200"E	2034	1845	1704	1494	1239	1015
24/12-1	59°02'29.8000"N	01°52'57.9300"E	2166	1985	1742	1569	1421	
25/1-1	59°53'17.4000"N	02°04'42.7000"E	2042	1807	1591	1436	1155	
25/1-2	59°56'08.0000"N	02°04'54.6000"E	2075	1866	1658	1333	1105	
25/1-4	59°59'52.6100"N	02°15'54.8000"E	2168	1924	1760	1496	1330	
25/1-6	59°46'57.6800"N	02°05'42.2300"E	2126	2083	1833	1667	1314	
25/2-5	59°48'01.4000"N	02°28'18.3000"E	2116	1988	1796	1711	1546	
25/4-1	59°34'27.0000"N	02°13'23.0000"E	1902	1782	1602	1367	1242	
25/4-2	59°35'46.5100"N	02°18'51.4000"E	1906	1687	1589	1403	1248	
25/10-2	59°09'38.4000"N	02°11'38.1000"E	1913	1816	1673	1448	1401	
25/10-3	59°12'59.0000"N	02°19'42.0000"E	1703	1599	1471	1362	1303	
25/11-3	59°10'36.1900"N	02°26'19.6000"E	1672	1581	1477	1293	1252	
25/11-10	59°10'09.2140"N	02°20'59.9220"E	1669	1592	1532	1453	1363	
30/2-1	60°52'04.8000"N	02°38'47.5000"E	1892	1813		1565	1404	
30/3-2	60°47'49.2000"N	02°55'18.0900"E	1890	1782		1517	1261	
30/4-1	60°37'20.8700"N	02°09'34.6100"E	1888	1710	1602	1443	1368	
30/7-3	60°17'09.2400"N	02°14'54.4400"E	2079	2012	1908	1588	1277	
30/7-6	60°29'29.8200"N	02°03'26.1400"E	1931	1756	1677	1451	1253	
30/9-1	60°28'25.0900"N	02°52'25.0900"E	2079	1843	1769	1649	1584	
30/10-5	60°00'25.8800"N	02°04'07.1700"E	2074	1958	1745	1501	1251	
31/2-5	60°46'16.0000"N	03°25'53.0000"E	2007	1782		1252	1091	
31/2-6	60°54'13.5700"N	03°38'49.4300"E	1083			1000	672	
31/4-5	60°33'30.9200"N	03°03'25.1700"E	1747			1582	1431	
33/12-2	61°13'31.8000"N	01°51'25.9700"E	1644		1497	1362	1237	
34/4-1	61°32'49.2300"N	02°16'23.6600"E	1657	1604		1522	1372	
34/4-2	61°30'30.9300"N	02°04'17.0400"E	1612	1553		1469	1390	
34/4-3	61°36'32.9500"N	02°07'34.4200"E	1693	1632		1539	1417	
34/4-4	61°30'20.8500"N	02°14'09.5400"E	1610	1561		1511	1201	
34/10-1	61°10'46.8400"N	02°12'43.6700"E	1748		1460	1300	1200	
34/10-2	61°06'07.9200"N	02°13'39.9600"E	1768		1649	1450	1332	
34/10-3	61°12'49.4800"N	02°11'55.0300"E	1538		1438	1332	1219	
35/8-1	61°21'26.0000"N	03°21'46.0000"E	1649	1593		1364	1189	
35/8-2	61°16'15.4200"N	03°21'58.7100"E	1648	1554		1417	1255	
UK Sector Wells								
2/5-5	60°56'08.0000"N	00°50'07.0000"E	909		686	577	485	
3/1-1	60°56'43.4900"N	01°09'31.9400"E	1221		1102	1004	822	726
3/1-2	60°53'21.0800"N	01°09'17.7800"E	1248		1059	947	798	688
3/2-3	60°57'35.6000"N	01°13'48.4000"E	1257		1129	964	846	760
3/2-4	60°53'06.3000"N	01°17'33.3000"E	1277		1138	1000	872	771
3/3-4A	60°51'44.5000"N	01°31'00.0000"E	1378	1317	1256	1139	1043	875
3/3-5A	60°51'05.1030"N	01°24'44.8100"E	1358		1202	1064	907	826
3/3-8	60°52'37.0000"N	01°32'28.0000"E	1374	1346	1300	1221	1145	912
3/4-6	60°50'07.9700"N	01°44'56.9800"E	1682	1501	1408	1314		
3/7-3	60°40'20.1000"N	01°18'53.2000"E	1304		1164	987	887	714
3/8-2	60°47'09.8000"N	01°25'56.2000"E	1347		1217	1102	974	838
3/8A-7	60°43'49.7600"N	01°28'46.5200"E	1422		1312	1099	967	873
3/9A-1	60°48'27.8900"N	01°42'10.3500"E	1425		1228	1125	1020	
3/11A-6	60°31'55.9800"N	01°05'09.5500"E	1061	952	645	567	506	440

3/12-1	60°32'36.3000"N	01°19'51.1000"E	1361		1214	965	928	791
3/15-1	60°36'04.6000"N	01°49'53.0000"E	1872	1723	1460	1343	1185	1058
3/19-1	60°27'36.5000"N	01°45'12.3000"E	1838	1634	1518	1273	1123	953
3/21-2	60°17'19.9000"N	01°09'36.7000"E	927	854	679	549	497	427
3/22-1	60°16'27.1000"N	01°22'48.1000"E	1409		1260	939	879	729
3/23A-2	60°16'31.2000"N	01°29'35.7000"E	1592	1430	1220	1138	1083	931
3/25-1	60°16'06.9000"N	01°52'33.6000"E	1920	1734	1507	1320	1199	1133
3/28-2A	60°00'33.7700"N	01°25'27.8000"E	951	917	805	707	670	477
3/29-1	60°06'46.5000"N	01°44'21.9000"E	2016	1812	1600	1337	1239	1206
3/30-2A	60°00'04.7000"N	01°59'00.3800"E	2247	2073	1967	1667	1258	
9/3-1	59°56'43.5700"N	01°31'12.6800"E	1093	1011	895	700	671	543
9/4-1	59°53'45.2200"N	01°41'21.3600"E	1805	1703	1482	1357	1142	944
9/7-1	59°41'32.4000"N	01°14'46.9000"E	1027	856	710	645	600	442
9/8-1	59°43'32.1000"N	01°33'28.3000"E	1561	1367	1278	1164	1052	882
9/8-4	59°47'02.6000"N	01°32'10.9000"E	1334	1185	1119	1051	968	847
9/9B-2B	59°45'02.4200"N	01°38'57.2600"E	1573	1437	1317	1182	1102	927
9/9B-5	59°48'15.9000"N	01°42'48.6000"E	1860	1743	1503	1342	1135	982
9/13-1	59°33'00.0000"N	01°32'00.0000"E	1539	1427	1251	1191	1051	892
9/13-3A	59°37'21.9840"N	01°27'38.6550"E	1407	1256	1076	1036	967	850
9/13-5	59°30'04.7000"N	01°32'32.8000"E	1555	1445	1304	1211	1119	929
9/13a-27	59°31'56.1943"N	01°26'49.9998"E	1604	1370	1108	1077	1053	896
9/16-1	59°29'12.0000"N	01°04'32.6000"E	1044	885	644	620		513
9/17-1A	59°20'52.0000"N	01°18'41.2000"E	1384	1258	1019	929	891	739
9/23-1	59°14'55.8000"N	01°32'19.1000"E	1568	1459	1347	1177	1122	939
9/23-2	59°15'31.1000"N	01°28'57.9000"E	1666	1556	1444	1384	1121	923
9/23A-3	59°17'08.8000"N	01°33'54.6000"E	1534	1410	1352	1215	1135	911
9/24B-1A	59°12'03.4500"N	01°38'05.2000"E	1987	1747	1529	1340	1290	1065
9/27-1	59°08'34.3200"N	01°19'56.7600"E	1296	1139	900	776	715	639
9/28-1A	59°03'52.9000"N	01°30'34.2000"E	1805	1653	1497	1385	1255	993
13/30-1	58°05'44.1060"N	01°03'14.2840"W	238			204		
14/4-1	58°59'51.7610"N	00°23'44.9000"W	363			263		
14/10A-2	58°46'23.4100"N	00°05'50.6800"W	636	611	545	521	467	
14/14-1	58°32'48.8130"N	00°15'28.2920"W	690	626	551	478	416	
14/15-1	58°36'08.6000"N	00°05'43.4000"W	708	596	547	482	427	
14/15-2	58°30'39.8600"N	00°01'09.2000"W	773	690	633	583	485	
14/19-11	58°23'42.3100"N	00°22'51.8300"W	581		521	447	401	
14/19-4	58°26'16.7000"N	00°13'22.2000"W	672		584	511	458	
14/20-5	58°23'39.7500"N	00°07'23.0500"W	763		681	574	510	
14/25-1	58°10'11.4000"N	00°00'56.4000"W	1041			756	652	
14/26-1	58°01'54.1870"N	00°54'39.1710"W	351			256		
14/29-1	58°06'26.5300"N	00°15'16.9500"W	735		726	605	543	
14/29A-2	58°01'30.1000"N	00°21'58.5000"W	710			570	509	
14/30-1	58°07'52.5950"N	00°10'45.3970"W	807			674	571	
15/4-1	58°56'59.9000"N	00°42'57.4000"E	932	829	685	564	537	
15/6-1	58°40'33.4592"N	00°11'05.9445"E	800	693	550	503		
15/12-1	58°30'10.0000"N	00°18'30.0000"E	1008	955	637	564		
15/13-1	58°33'37.9000"N	00°25'06.9000"E	1018	958	598	571	560	
15/16-5	58°22'22.2380"N	00°05'54.5300"E	1025	970	790	674	600	
15/17-4	58°29'03.7000"N	00°17'21.1000"E	981	923	701	579	543	
15/17-5	58°27'13.8500"N	00°17'56.0000"E	1056	1018	710			
15/17-7	58°26'55.9000"N	00°13'35.0000"E	1023	946	805	739	704	
15/17-8A	58°22'06.9000"N	00°22'27.4000"E	1381	1282	955	701		673
15/18-2	58°25'00.0000"N	00°26'00.0000"E	1357	1217	984	872	817	776

15/19-1	58°24'54.7000"N	00°39'01.9000"E	1504	1345	1119	1072	1022	925
15/20-1	58°28'55.7600"N	00°57'59.5700"E	1770	1655	1402	1212	1174	1065
15/20-2	58°21'55.2500"N	00°55'56.5500"E	1888	1778	1530	1348	1224	1132
15/21-1	58°13'21.6000"N	00°05'07.2000"E	1052	1033	984	768	675	
15/21-2	58°16'19.0000"N	00°04'32.0000"E	1147	1091	924	740	700	
15/21-3	58°10'54.5880"N	00°05'58.8600"E	1163	1108	1038	770	691	652
15/22-2	58°12'24.9300"N	00°16'56.4800"E	1441	1410	1105	939	850	725
15/22-5	58°15'52.4000"N	00°13'48.3700"E	1495	1438	1326	1103	859	757
15/23-3	58°12'48.9740"N	00°25'30.4890"E	1609	1521	1187	999	896	785
15/23-4+4B	58°18'29.1200"N	00°25'56.0900"E	1607	1508	1170	936	875	772
15/24-1	58°18'49.2000"N	00°42'13.2000"E	1618	1587	1197	1086	973	885
15/26A-3	58°06'10.2200"N	00°05'48.1100"E	1300	1246	1151	793	690	
15/27-3	58°03'48.7000"N	00°12'15.4000"E	1453	1345	1211	1049	936	
15/28-1	58°03'12.6000"N	00°30'41.3000"E	1665	1561	1261	1237	1191	1128
15/28A-3	58°07'06.7520"N	00°30'58.0690"E	1724	1652	1294	1258	1211	1132
15/30-2	58°06'11.0000"N	00°50'36.5000"E	2049	1931	1800	1629	1528	1324
15/30-3	58°05'51.3000"N	00°59'45.2000"E	2194	2073	1901	1768	1555	1439
16/3A-1	58°52'53.3190"N	01°31'29.0540"E	2069	2004	1781	1606	1428	1196
16/8-1	58°44'53.7000"N	01°32'18.4000"E	2005	1873	1740	1627	1540	1384
16/11-1	58°32'02.2570"N	01°02'53.8700"E	1806	1629	1508	1381	1290	1122
16/12-1	58°37'56.1000"N	01°14'21.3000"E	2048	1956	1652	1503	1408	1275
16/17-1	58°23'02.4840"N	01°17'29.1420"E	2291	2200	2044	1918	1693	
16/17-2A	58°26'46.8000"N	01°16'27.4000"E	2326	2153	2044	1843	1621	
16/17-8a	58°29'39.4200"N	01°16'28.9560"E	2119	1951	1750	1610	1546	
16/18-1	58°21'37.1000"N	01°32'17.7400"E	2332	2217	2122	2029	1826	
16/21A-2	58°14'00.6790"N	01°08'02.2150"E	2015	1910	1782	1614	1559	
16/21A-3	58°13'45.7790"N	01°05'15.2600"E	1999	1931	1768	1591	1438	
16/22-1	58°15'57.4900"N	01°15'55.4300"E	2063	1994	1933	1815	1639	
16/22-2	58°13'05.7500"N	01°22'25.8700"E	2435	2339	2220	1918	1825	
16/23-2	58°15'46.8000"N	01°31'29.1000"E	2334	2242	1986	1939	1858	
16/26-1A	58°06'20.5000"N	01°08'35.2000"E	2175	2109	1953	1822	1677	
16/26-3	58°03'44.5500"N	01°10'06.7000"E	2287	2201	2046	1912	1811	
16/27A-2	58°02'54.1100"N	01°22'46.4300"E	2411	2354	2306	2188	2152	
16/28-1	58°02'52.8000"N	01°24'22.8000"E	2421	2383	2216	2102	2040	
16/28-3	58°08'23.9160"N	01°32'45.1150"E	2446	2344	2236	2064	1998	
16/29-2	58°07'58.4500"N	01°40'57.1900"E	2429	2328	2115	2039	1938	
20/1-2	57°54'49.5660"N	00°51'24.6090"W	350					
20/3-1	57°55'30.2000"N	00°29'57.2800"W	654			545	464	
20/3-4	57°51'03.1510"N	00°25'37.4590"W	721			620	520	
20/3-5	57°53'24.3100"N	00°34'03.2600"W	595			547	496	
20/10-1	57°47'38.9000"N	00°07'38.7000"W	964		889	828	774	
20/10-2	57°40'08.3480"N	00°08'56.0760"W	855		764	723	649	
20/19-1	57°21'57.8000"N	00°15'40.8000"W	623			495		
21/1-1	57°54'00.9000"N	00°00'04.0000"E	995		885	811	748	
21/1A-12	57°58'57.5990"N	00°09'18.4520"E	1308		1196	1076	1000	
21/2-1	57°55'14.4900"N	00°15'46.9300"E	1491	1428	1248	1166	1118	
21/3-2	57°57'39.4900"N	00°35'47.3500"E	1928	1831	1665	1620	1480	
21/6-1	57°49'39.6080"N	00°06'51.7250"E	1206		1125	1055	975	
21/6-2	57°48'09.5675"N	00°00'13.9811"E	999		908	874	843	
21/9-1	57°42'20.4000"N	00°46'05.5000"E	2068	2041	1987	1906	1827	
21/10-1	57°43'50.2000"N	00°58'29.5000"E	2035	2022	1963	1918	1847	
21/10-4	57°47'28.3000"N	00°50'50.6000"E	2141	2107	2093	1912	1803	
21/12-1	57°33'34.5000"N	00°18'12.0000"E	1735	1724	1680	1498	1402	

21/14-1	57°37'23.0000"N	00°39'35.5000"E	2073	2061	1988	1869	1843
21/15A-1	57°33'45.3090"N	00°53'02.9830"E	2282	2262	2202	2122	2055
21/15A-2	57°39'34.4800"N	00°53'36.2000"E	2259	2225	2153	2069	2012
21/20A-1	57°27'04.9620"N	00°59'21.9850"E	2466	2414	2348	2262	2188
21/20A-2	57°22'17.1800"N	00°48'54.0800"E	2413	2387	2331	2256	2145
21/20B-3	57°28'06.2800"N	00°48'39.8100"E	2310	2300	2210	2143	2065
21/21-1	57°12'37.6000"N	00°10'05.7000"E	1041		1009	954	914
21/28-1	57°06'49.0000"N	00°24'14.3000"E	1148		1059	1010	959
21/28A-4	57°07'53.3860"N	00°32'04.5130"E	1441		1370	1271	1169
22/1-1A	57°53'21.5080"N	01°07'28.2930"E	2352	2266	2163	2065	1965
22/5A-10	57°55'56.2400"N	01°48'44.3400"E	2578	2487	2360	2208	2119
22/5A-11	57°53'33.2500"N	01°49'43.7500"E	2630	2564	2428	2255	2150
22/5A-1A	57°59'19.4270"N	01°49'31.0000"E	2411	2351	2244	2120	2073
22/5A-6	57°51'36.7340"N	01°53'57.5680"E	2288	2255	2140	2069	2002
22/8-1	57°44'17.5400"N	01°28'50.1600"E	2485	2431	2318	2234	2163
22/9-1	57°42'27.5400"N	01°47'44.1000"E	2416	2359	2298	2219	2161
22/10-1	57°47'47.5840"N	01°57'08.8800"E	2252	2230	2143	2085	1992
22/10A-2	57°48'13.4050"N	01°48'45.6170"E	2425	2373	2268	2156	2063
22/10A-4	57°44'08.4700"N	01°50'26.5900"E	2388	2341	2284	2172	2051
22/11-1	57°39'55.0000"N	01°07'10.0000"E	2163	2131	2067	2021	1981
22/11-2	57°39'35.6540"N	01°03'04.7620"E	2188	2163	2114	2041	1977
22/12A-1	57°38'18.4700"N	01°21'17.8400"E	2368	2339	2284	2205	2129
22/14-1X	57°36'38.3560"N	01°41'56.7740"E	2481	2393	2319	2208	2097
22/16-1	57°27'38.5000"N	01°11'52.1000"E	2503	2473	2314	2256	2171
22/17-1	57°27'42.1000"N	01°20'42.2000"E	2418	2397	2311	2201	2100
22/17-T1	57°22'30.0190"N	01°23'00.0810"E	2948	2895	2791	2739	2623
22/18-2	57°27'22.4000"N	01°24'24.2000"E	2398	2383	2268	2149	2058
22/18-3	57°27'37.5990"N	01°33'09.8220"E	2532	2510	2385	2320	2252
22/18-4	57°22'39.0930"N	01°28'57.2250"E	2480	2431	2303	2202	2108
22/19-2	57°28'01.0370"N	01°44'31.2000"E	2565	2497	2409	2274	2227
22/26A-1	57°04'10.1600"N	01°02'24.6000"E	2364	2264			2176
23/11-1	57°34'40.4000"N	02°05'41.2000"E	2370	2303	2179	2072	2006
23/21-1	57°17'39.8000"N	02°09'46.0000"E	2486	2386	2329	2283	2234
23/26A-3	57°03'12.6860"N	02°03'46.9130"E	3083	3009	2949	2839	2747
23/27-1	57°08'34.1000"N	02°18'59.9000"E	2738	2685	2638	2571	2490
27/3-1	56°57'30.5000"N	00°32'20.2000"W	282			184	
27/10-1	56°42'29.6220"N	00°01'30.9640"W	468			370	
29/2-1	56°56'43.9000"N	01°19'39.5000"E	2665	2578	2500	2457	2425
29/5A-1	56°50'18.7000"N	01°48'52.5000"E	2804	2713	2670	2590	2558
29/6A-1	56°49'24.0000"N	01°09'22.0000"E	2504	2321	2140	1977	1890
29/7-2	56°41'20.4000"N	01°18'41.2000"E	2292	2116	1942	1826	1775
29/12-1	56°37'53.5200"N	01°23'55.1900"E	2123	1995	1779	1574	1536
30/8-1	56°42'09.4000"N	02°27'30.7300"E	2919	2834	2772	2710	2610
30/11B-1	56°33'11.3400"N	02°04'52.7200"E	2925	2874	2820	2747	2651
30/12B-2	56°31'48.6000"N	02°17'08.9000"E	2887	2830	2708	2641	2567
30/12B-3	56°30'56.9000"N	02°16'36.5200"E	2937	2821	2726	2648	2550
30/13-1X	56°34'01.3000"N	02°31'45.0000"E	2789	2711	2602	2541	2449
30/16-6	56°29'21.7680"N	02°09'09.7780"E	2736	2676	2579	2517	2467
30/17-1X	56°23'45.2340"N	02°12'29.4320"E	2640	2527	2475	2375	2301
30/17A-4	56°25'51.1200"N	02°12'11.9900"E	2656	2542	2463	2374	2305
30/19-1	56°26'47.9930"N	02°42'17.9040"E	2826	2632		2568	2516
30/27-1	56°09'46.0660"N	02°18'26.7460"E	1971	1743	1676	1592	1506
210/5-1	61°52'21.3600"N	00°49'56.1400"E	1459		1412	1350	1284

210/13-1	61°39'02.9580"N	00°28'26.2510"E	1312		1041	915		
210/15-1x	61°34'30.9000"N	00°56'13.5000"E	1407		1250	1194	1114	
210/24-1	61°13'33.0700"N	00°40'03.6400"E	889		658		556	
210/24-2	61°15'36.8200"N	00°43'55.5400"E	992		786		670	
210/25-2	61°14'29.8700"N	00°55'11.6030"E	1198		978	871	776	718
210/30-1	61°04'07.4124"N	00°54'05.5440"E	1238	1167	1085	817	755	645
211/7A-2	61°41'16.4350"N	01°16'38.5380"E	1361		1239	1108	971	
211/11-1	61°35'47.6500"N	01°09'53.2500"E	1383		1261	1162	1029	
211/12-6	61°39'07.6240"N	01°20'31.7080"E	1346		1189	1069	1008	
211/12-7	61°37'23.7310"N	01°14'45.3570"E	1370		1251	1072	1024	
211/12A-1	61°39'35.1530"N	01°21'57.8940"E	1363		1230	1132	1032	
211/19-1	61°21'25.5000"N	01°36'37.7000"E	1575		1400	1237	1142	1106
211/24-5	61°14'16.7000"N	01°37'59.4000"E	1613		1421	1268	1157	
211/27-7	61°05'10.6500"N	01°22'07.0000"E	1337		1217	1082	948	861
211/27-8	61°08'23.0400"N	01°15'53.2100"E	1311		1170	959	888	847

BIBLIOGRAPHY

Armentrout, J.M., Malecek, S.J., Fearn, L.B., Sheppard, C.E., Naylor, P.H., Miles, A.W., Desmarais, R.J., and Dunay, R.E., 1993, Log-motif analysis of Paleogene depositional systems tracts, Central and Northern North Sea: defined by sequence stratigraphic analysis, *in* Parker, J.R., ed., Petroleum Geology of Northwest Europe: Proceedings of the Fourth Conference: London, The Geological Society of London, p. 45-57.

Armentrout, J.M., 1991, Paleontologic constraints on depositional modeling: examples of integration of biostratigraphy and seismic stratigraphy, Pliocene-Pleistocene, Gulf of Mexico, in Weimer, P., and Link, M.H., eds., Seismic Facies and Sedimentary Processes of Submarine Fans and Turbidite Systems: New York, Springer-Verlag, p. 137-170.

Armstrong, L.A., Ten Have, A., and Johnson, H.D., 1987, The geology of the Gannet fields, central North Sea, U.K. sector, *in* Brooks, J., and Glennie, K.W., eds., Petroleum Geology of Northwest Europe: London, Graham and Trotman, p. 533-548.

Badley, M.E., Price, J.D., Rambech Dahl, C. and Agdestein, T., 1988. The structural evolution of the northern Viking Graben and its bearing upon extensional modes of basin formation: Journal of the Geological Society of London, v. 145, p. 455-472.

Baird, R.A., 1986, Maturation and source rock evaluation of Kimmeridgian Clay, Norwegian North Sea: American Association of Petroleum Geologists Bulletin, v. 70, p. 1-11.

Banner, J.A., Chatellier, J-Y., Feurer, J.R. and Neuhaus, D., 1992, Guillemot D: a successful appraisal through alternative interpretation, *in* Hardman, R.F.P., ed., Exploration Britain: Geological insights for the next decade: London, Geological Society of London, Special Publication No. 67, p. 129-149.

Barron, J., Larsen, B., and Baldauf, J.G., 1991, Evidence for Late Eocene to Early Oligocene Antarctic glaciation and observations on Late Neogene glacial history of Antarctica: Results from Leg 119, *in* Barron, J., and others, Proceedings of the Ocean Drilling Program, Scientific Results: v. 119, p. 869-891.

Barnard, P.C., and Cooper, B.S., 1981, Oil and source rocks of the North Sea area, *in* Illing, L.V, and Hobson, G.D., eds., Petroleum Geology of the Continental Shelf of North West Europe: London, Heyden and Son, p. 169-175.

Beach, A., 1987, A regional model for linked tectonics in north-west Europe, *in* Brooks, J., and Glennie, K.W., eds., Petroleum Geology of North West Europe: London, Graham and Trotman, p. 43-48.

Berggren, W. A., and Aubert, J., 1975, Paleocene benthonic foraminiferal biostratigraphy, paleobiogeography and paleoecology of Atlantic-Tethyan regions: Midway-type fauna: Paleogeography, Paleoclimatology, Paleoecology, v. 18, p. 73-192.

Berstad, S., and Dypvik, H., 1982, Sedimentological evolution and natural radioactivity of Tertiary sediments from the central North Sea: Journal of Petroleum Geology, v. 5, p. 77-88.

Blow, W.H., 1969, The late Middle Eocene to Recent planktonic foraminiferal biostratigraphy, *in* Bronnimann, P., and Renz, H.H., eds., Proceedings of the First Conference on Planktonic Microfossils: Leiden, E.J. Brill, p. 199-422.

Bøggild, O.B., 1918, Den vulkanske aske i Moleret samt en oversigt over Danmarks aeldre Tertiaebjergarter: Danmarks Geologiske Undersøgelse, raekke 2, v. 33.

Bond, G.C., and Kominz, M.A., 1984, Construction of tectonic subsidence curves for the early Paleozoic miogeocline, southern Canadian Rocky Mountains: Implications for subsidence mechanisms, age of breakup, and crustal thinning: Geological Society of America Bulletin, v. 95, p. 155-173.

Bray, J.R., and Curtis, J.T., 1957, An ordination of upland forest communities of southern Wisconsin: Ecological Monographs, v. 27, p. 325-349.

Brewster, J., and Jeangeot, G., 1987, The production geology of the Frigg Field, *in* Kleppe, J., and others, eds., North Sea Oil and Gas Reservoirs: London, Graham and Trotman for the Norwegian Institute of Technology, p. 75-88.

Buchardt, B., 1978, Oxygen isotope paleotemperatures from the Tertiary period in the North Sea area: Nature, v. 275, p. 121-123.

Bujak, J.P., and Mudge, D.C., *in press*, A high resolution North Sea Eocene dinocyst zonation.

Cartwright, J.A., 1994, Episodic basin-wide hydrofracturing of overpressured Early Cenozoic mudrock sequences in the North Sea Basin: Marine and Petroleum Geology, v.11, p. 587-607.

Christie-Blick, N., 1990, Sequence stratigraphy and sea-level changes in Cretaceous time, *in* Ginsburg, R.E., and Beaudoin, B., eds., Cretaceous Resources, Events, and Rhythms: North Atlantic Treaty Organization (NATO) ASI Series C, v. 304, p. 1-21.

Cloetingh, S., 1986, Intraplate stress: A new tectonic mechanism for fluctuations of relative sea level: Geology, v. 14, p. 617-620.

Cloetingh, S., Lambeck, K., and McQueen, H., 1987, Apparent sea-level fluctuations and a paleostress field for the North Sea region, *in* Brooks, J., and Glennie, K.W., eds., Petroleum Geology of North West Europe: London, Graham and Trotman, p. 49-57.

Cloetingh, S., 1988, Intraplate stresses: A tectonic cause for third-order cycles in apparent sea level? *in* Wilgus, C.K., and others, eds., Sea-Level Changes, An Integrated Approach: Tulsa, Oklahoma, Society of Economic Paleontologists and Mineralogists, Special Publication No. 42, p. 19-29.

Cloetingh, S., and Kooi, H., 1989, Tectonic subsidence and sea-level changes: A reappraisal, *in* Collinson, J.D., ed., Correlation in Hydrocarbon Exploration: London, Graham and Trotman, p. 3-11.

Coleman, J., 1990, Depositional systems and tectonic/eustatic history of the lower Oligocene Vicksburg episode of the northern Gulf Coast: Ph.D. dissertation, University of Texas at Austin, 538 p.

Condon, P.J., 1988, Seismic stratigraphy and distribution of Paleogene sediments west and east of Shetland: unpublished Ph.D. Dissertation, University of Edinburgh, 367 p.

Condon, P.J., Jolley, D.W., and Morton, A.C., 1992, Eocene succession on the East Shetland Platform: Marine and Petroleum Geology, v. 9, p. 633-647.

Conort, A., 1986, Habitat of Tertiary hydrocarbons, South Viking Graben, *in* Spencer, A.M., and others, eds., Habitat of Hydrocarbons on the Norwegian Continental Shelf: London, Graham and Trotman, p. 159-170.

Costa, L.I., and Manum, S.B., 1988, The description of the interregional zonation of the Paleogene (D1-D15) and the Miocene (D16-D20), *in* Vinken, R., ed., The Northwest European Tertiary Basin, Results of the International Geological Correlation Programme, Project No. 124, Geologisches Jahrbuch A, v. 100, p. 321-332.

Cushman, J.A., 1925, Some new foraminifera from the Velasco shale of Mexico, Contributions to the Cushman Foundation for Foraminiferal Research, v. 1, p. 18-23.

Cushman, J.A., 1926, The Foraminifera of the Velasco Shale of the Tampico Embayment, American Association of Petroleum Geologists Bulletin, v. 10, p. 581-612.

Deegan, C.E., and Scull, B.J., 1977, A proposed standard lithostratigraphic nomenclature for the central and northern North Sea: Reports of the Institute of Geological Sciences (Great Britain), v. 77, no. 25, 36 p.

De Clarens, P., Ducazeaux, J., Morice, M., and Bourges, P., 1992, Sequence stratigraphy method interpretation of the Tertiary of the Viking Graben (North Sea), abstract, Symposium on Mesozoic and Cenozoic Sequence Stratigraphy of European Basins, Dijon, France, May, 1992.

Dewey, J.F., and Windley, B.F., 1988, Palaeocene-Oligocene tectonics of NW Europe, *in* Morton, A.C., and Parson, L.M., eds., Early Tertiary Volcanism and the Opening of the NE Atlantic: London, Geological Society of London, Special Publication No. 39, p. 25-31.

Donato, J.A., and Tully, M.C., 1981, A regional interpretation of North Sea gravity data, *in* Illing, L.V. and Hobson, G.D., eds., Petroleum Geology of the Continental Shelf of North-West Europe: London, Heyden and Son, p. 65-75.

Elliott, W.C., Aronson, J.L., and Millard, H.T., Jr., 1992, Iridium content of basaltic tuffs and enclosing black shales of the Balder Formation, North Sea, Geochemica et Cosmochemica, v. 56, p. 2955-2961.

Enjolras, J.M., Gouadain, J., Mutti, E., and Pizon, J., 1986, New turbiditic model for the Lower Tertiary sands in the south Viking Graben, *in* Spencer, A.M., and others, eds., Habitat of Hydrocarbons on the Norwegian Continental Shelf: London, Graham and Trotman, p. 171-178.

Eynon, G., 1981, Basin development and sedimentation in the Middle Jurassic of the Northern North Sea, *in* Illing, L.V. and Hobson, G.D., eds., Petroleum Geology of the Continental Shelf of North-West Europe: London, Heyden and Son, p. 196-204.

Fisher, W.L., 1969, Facies characterization of Gulf Coast basin delta systems, with some Holocene analogues: Gulf Coast Association of Geological Societies Transactions, v. 19, p. 239-261.

Fowler, C., 1975, The geology of the Montrose Field, *in* Woodland, A.W., ed., Petroleum and the Continental Shelf of North West Europe: New York, John Wiley, p. 467-476.

Frazier, D.E., 1974, Depositional episodes: their relationship to the Quaternary stratigraphic framework in the north-western portion of the Gulf basin: University of Texas at Austin, Bureau of Economic Geology, Circular 74-1, 28 p.

Frisch, W., 1981, Plate motions in the Alpine region and their correlation to the opening of the Atlantic ocean: Geologische Rundschau, v. 70, p. 402-411.

Galloway, W.E., 1968, Depositional systems of the lower Wilcox Group, north-central Gulf Coast basin: Gulf Coast Association of Geological Societies Transactions, v. 18, p. 275-289.

Galloway, W.E., and Hobday, D.K., 1983, Terrigenous clastic depositional systems: New York, Springer-Verlag, 423 p.

Galloway, W.E., 1989a, Genetic stratigraphic sequences in basin analysis I: architecture and genesis of flooding-surface bounded depositional units: American Association of Petroleum Geologists Bulletin, v. 73, p. 125-142.

Galloway, W.E., 1989b, Genetic stratigraphic sequences in basin analysis II: application to Northwest Gulf of Mexico Basin: American Association of Petroleum Geologists Bulletin, v. 73, p. 123-154.

Galloway, W.E., Garber, J.L., Liu, X., and Sloan, B.J., 1993, Sequence stratigraphic and depositional framework of the Cenozoic fill, Central and Northern North Sea Basin, *in* Parker, J.R., ed., Petroleum Geology of Northwest Europe: Proceedings of the Fourth Conference: London, The Geological Society of London, p. 33-43.

Garber, J., in preparation, Oligocene and Miocene sequence stratigraphy of the North Sea Basin: M.A. thesis, University of Texas at Austin.

Glennie, K.W., Brooks, J., and Brooks, J.R.V., 1987, Hydrocarbon exploration and geological history of North West Europe, *in* Brooks, J., and Glennie, K.W., eds., Petroleum Geology of North West Europe: London, Graham and Trotman, p. 1-10.

Goldhammer, R.K., Dunn, P.A., and Hardie, L.A., 1987, High frequency glacio-eustatic sealevel oscillations with Milankovitch characteristics recorded in Middle Triassic platform carbonates in Italy: American Journal of Science, v. 287, p. 853-892.

Gradstein, F.M., Kaminski, M.A., Berggren, W.A., Kristiansen, I.L, and D'Ioro, M.A., 1994, Cenozoic biostratigraphy of the North Sea and Labrador Shelf: Micropaleontology, v. 40, supplement, 152 p.

Gradstein, F. M., and Berggren, W. A., 1981, Flysch-type agglutinated foraminifera and the Maestrichtian to Paleogene history of the Labrador and North Seas: Marine Micropaleontology, v. 6, p. 211-268.

Gradstein, F.M., Kaminski, M.A., and Berggren, W.A., 1988, Cenozoic foraminiferal biostratigraphy, Cental North Sea, *in* Rögl, F., and Gradstein, F.M., eds., Second Workshop on Agglutinated Foraminifera, Vienna, 1986, Proceedings: Abhandlungen der Geologischen Bundesanstalt, v. 41, p. 97-108.

Gradstein, F.M., Kristiansen, I.L., Loemo, L., and Kaminski, M.A., 1992, Cenozoic foraminiferal and dinoflagellate cyst stratigraphy of the central North Sea: Micropaleontology, v. 38, p. 101-137.

Grzybowski, J., 1896, Otwornice czerwonych itow z wadowic: Rozpr. Akad. Um. Krakowie, Wydz. Mar.-Przyr., Ser. 2, v. 30, p. 261-308.

Guidish, T.M., Kendall, G., Lerche, I., Toth, D.J., and Yarzab, R.F., 1985, Basin evaluation using burial history calculations: An overview: American Association of Petroleum Geologists Bulletin, v. 69, p. 92-105.

Hallam, A., and Sellwood, B.W., 1976, Middle Mesozoic sedimentation in relation to tectonics in the British area: Journal of Geology, v. 84, p.302-321.

Hallam, A., 1988, A re-evaluation of Jurassic eustasy in the light of new data and the revised Exxon curve, *in* Wilgus, C.K., Hastings, B.S., Kendall, C.G.St.C., Posamentier, H.W., Ross, C.A., and Van Wagoner, J.C., eds., Sea-Level Changes - An Integrated Approach: Tulsa, Oklahoma, Society of Economic Paleontologists and Mineralogists, Special Publication No. 42, p. 261-274.

Hancock, J.M., 1984, Cretaceous, *in* Glennie, K.W., ed., Introduction to Petroleum Geology of the North Sea: Oxford, Blackwell Scientific Publications, p. 161-178.

Hanslien, S., 1987, Balder, *in* Spencer, A.M., and others, eds., Geology of the Norwegian Oil and Gas Fields: London, Graham and Trotman for the Norwegian Petroleum Society, p. 193-201.

Haq, B.U., Hardenbol, J., and Vail, P.R., 1987, Chronology of fluctuating sea levels since the Triassic: Science, v. 235, p. 1156-1166.

Haq, B.U., Hardenbol, J., and Vail, P.R., 1988, Mesozoic and Cenozoic chronostratigraphy and cycles of sea-level change, *in* Wilgus, C.K., Hastings, B.S., Kendall, C.G.St.C., Posamentier, H.W., Ross, C.A., and Van Wagoner, J.C., eds., Sea-Level Changes - An Integrated Approach: Tulsa, Oklahoma, Society of Economic Paleontologists and Mineralogists, Special Publication No. 42, p. 71-108.

Hardenbol, J., and Berggren, W.A., 1978, A new Paleogene numerical time scale, *in* Cohee, G.V., Glaessner, M.F., and Hedberg, H.D., eds., Contributions to the Geologic Time Scale, papers given at the Geological Time Scale Symposium 106.6: 25th International Geological Congress, Sydney, Australia August 1976, Tulsa, Oklahoma, American Association of Petroleum Geologists, Studies in Geology, v. 6, p. 213-234.

Harding, A.W., Humphrey, T.J., Latham, A., Lunsford, M.K., and Strider, M.H., 1990, Controls on Eocene submarine fan deposition in the Witch Ground Graben, *in* Hardman, R.F.P., and Brooks, J., eds., Tectonic Events Responsible for Britain's Oil and Gas Reserves: London, The Geological Society of London, Special Publication No. 55, p. 353-367.

Hardman, R.F.P., and Brooks, J., eds., 1990, Tectonic Events Responsible for Britain's Oil and Gas Reserves: London, The Geological Society of London, Special Publication No. 55, 404 p.

Harland, W.B., Armstrong, R.L., Cox, A.V., Craig, L.E., Smith, A.G., and Smith, D.G., 1990, A geological time scale 1989: Cambridge, Cambridge University Press, 263 p.

Harris, J.P., and Fowler, R.M., 1987, Enhanced prospectivity of the Mid-Late Jurassic sediments of the South Viking Graben, northern North Sea, *in* Brooks, J., and Glennie, K.W., eds., Petroleum Geology of North West Europe: London, Graham and Trotman, p. 879-898.

Hay, W.W., and Mohler, H.P., 1967, Calcareous nannoplankton from early Tertiary rocks at Pont Labau, France and Paleocene-early Ecoene correlations: Journal of Paleontology, v. 41, p. 1121-1132.

Hayes, D.E., and Pitman, W.C., III, 1970, Magetic lineations in the North Pacific, *in* Hays, J.D., ed., Geological Investigations of the North Pacific: Boulder, Colorado, Geological Society of America, Memoir No. 126, p. 291-314.

Heritier, F.E., Lossel, P., and Whathne, E., 1979, Frigg Field - large submarine fan trap in lower Eocene rocks of North Sea Viking Graben: American Association of Petroleum Geologists Bulletin, v. 63, p. 1999-2020.

Hitchen, K., and Ritchie, J.D., 1987, Geological review of the West Shetland area, *in* Brooks, J., and Glennie, K.W., eds., Petroleum Geology of North West Europe: London, Graham and Trotman, p. 737-749.

Houthuys, R., and Gullentops, F., 1988, The Vlierzele sands (Eocene, Belgium): A tidal ridge system, in de Boer, P.L., and others, eds., Tide-Influenced Sedimentary Environments and Facies: D. Reidel Publishing Company, p. 139-152.

Ingle, J.C., 1980, Cenozoic paleobathymetry and depositional history of selected sequences with the southern California continental borderland: Washington, D.C., Cushman Foundation, Special Publication No. 19, Memorial to Orville Bandy, p. 163-195.

Ioakim, C., 1979, Étude comparative des dinoflagellés du Tertiaire inférieur de la Mer du Labrador et de la Mer du Nord: Thése de troisieme cycle, Université Pierre et Marie Curie, Paris, 204 p.

Jacqué, M., and Thouvenin, J., 1975, Lower Tertiary tuffs and volcanic activity in the North Sea, *in* Woodland, A.W., ed., Petroleum and the Continental Shelf of North West Europe: New York, John Wiley, p. 455-465.

Jenssen, A.I., Bergslien, D., Rye-Larsen, M., and Lindholm, R.M., 1993, *in* Parker, J.R., ed., Petroleum Geology of Northwest Europe, Proceedings of the Fourth Conference: London, The Geological Society of London, p. 135-143.

Jervey, M.T., 1988, Quantitative geological modeling of siliciclastic rock sequences and their seismic expression, *in* Wilgus, C.K., and others, eds., Sea-Level Changes, An Integrated Approach: Tulsa, Oklahoma, Society of Economic Paleontologists and Mineralogists, Special Publication No. 42, p. 47-69.

Jones, G. D., 1988, A paleoecological model of late Paleocene "flysch-type" agglutinated foraminifera using the paleoslope transect approach, Viking Graben, North Sea: Abhandlungen der Geologischen Bundesanstalt, v. 41, p. 143-153.

Jones, R.W., and Milton, N.J., 1994, Sequence development during uplift: Palaeogene stratigraphy and relative sea-level history of the Outer Moray Firth, UK North Sea: Marine and Petroleum Geology, v. 11, p. 157-165.

Joy, A.M., 1992, Estimation of Cenozoic water depths in the Western Central Graben, UK North Sea, by subsidence modeling, *in* Hardman, R.F.P., ed., Exploration Britain: Geological insights for the next decade: London, Geological Society of London, Special Publication No. 67, p. 107-125.

Kellough, G.R., 1959, Biostratigraphic and paleoecologic study of Midway Foraminifera along Tehvacana Creek, Limestone County, Texas: Transactions of the Gulf Coast Association of Geologic Societies, v. 9, p. 146-160.

Kellough, G.R., 1965, Paleoecology of the Foraminiferida of the Wills Point Formation (Midway Group) in northeast Texas: Transactions of the Gulf Coast Association of Geological Societies, v. 15, p. 73-153.

Kendall, C.G.St.C., and Lerche, I., 1988, The rise and fall of eustasy, *in* Wilgus, C.K., Hastings, B.S., Kendall, C.G.St.C., Posamentier, H.W., Ross, C.A., and Van Wagoner, J.C., eds., Sea-Level Changes - An Integrated Approach: Tulsa, Oklahoma, Society of Economic Paleontologists and Mineralogists, Special Publication No. 42, p. 3-18.

King, C., 1981, The stratigraphy of the London Clay and associated deposits: Backhuys, Rotterdam, Tertiary Research, Special Paper No. 6, 158 p.

King, C., 1983, Cainozoic micropaleontological biostratigraphy of the North Sea: London, Institute of Geological Sciences (Great Britain), Report 82/7, 40 p.

King, C., 1989, Cenozoic of the North Sea, *in* Jenkins, D.G., and Murray, J.W., eds., Stratigraphical Atlas of Fossil Foraminifera, Second edition: Chichester, England, Ellis Horwood Ltd., p. 418-489.

Knox, R.W.O'B., Morton, A.C., and Harland, R., 1981, Stratigraphical relationships of Palaeocene sands in the UK sector of the central North Sea, *in* Illing, L.V, and Hobson, G.D., eds., Petroleum Geology of the Continental Shelf of North West Europe: London, Heyden and Son, p. 267-281.

Knox, R.W.O'B., and Morton, A.C., 1988, The record of early Tertiary N. Atlantic volcanism in sediments of the North Sea Basin, *in* Morton, A.C., and Parsons, L.M., eds., Early Tertiary Volcanism and the Opening of the NE Atlantic: London, Geological Society of London, Special Publication No. 39, p. 407-419.

Knox, R.W.O'B., and Holloway, S., 1992, Paleogene of the Central and Northern North Sea, *in* Knox, R.W.O'B., and Cordey, W.G., eds., Lithostratigraphic Nomenclature of the UK North Sea: Nottingham, UK, British Geological Survey.

Koerschner, W.F. III, and Read, J.F., 1989, Field and modeling studies of Cambrian carbonate cycles, Virginia Appalachians: Journal of Sedimentary Petrology, v. 59, p. 654-687.

Kooi, H., Cloetingh, S., and Remmelts, G., 1989, Intraplate stresses and the stratigraphic evolution of the North Sea Central Graben: Geologie en Mijnbouw, v. 68, p. 49-72.

Kooi, H., Hettema, M., and Cloetingh, S., 1991, Lithospheric dynamics and the rapid Pliocene-Quaternary subsidence phase in the southern North Sea basin: Tectonophysics, v. 192, p. 245-259.

Kominz, M., 1984, Ocean ridge volumes and sea level changes: An error analysis: Tulsa, Oklahoma, American Association of Petroleum Geologists, Memoir No. 36, p. 10-127.

Le Pichon, X., Bergerat, F., and Roulet, M-J., 1988, Plate kinematics and tectonics leading to the Alpine belt formation: a new analysis: Boulder, Colorado, Geological Society of America, Special Paper No. 218, p. 111-131.

Letouzey, J., 1986, Cenozoic paleo-stress pattern in the Alpine Foreland and structural interpretation in a platform basin: Tectonophysics, v. 132, p. 215-231.

Liu, X., in preparation, Quantitative analysis of genetic sequence development in the Tertiary North Sea, Ph.D. dissertation, University of Texas at Austin.

Liu, X., and Galloway, W.E., 1993, Sediment accumulation rate: Problems and new approach, in Armentrout, J.M., Bloch, R., Olson, H., and Perkins, B.F., eds., Rates of Geologic Processes: Gulf Coast Section Society of Exploration Paleontologists and Mineralogists, 14th Annual Research Conference Proceedings, p. 101-107.

Loutit, T.S., Hardenbol, J., Vail, P.R., and Baum, G., 1988, Condensed sections: The key to age determinations and correlation of continental margin sequences, *in* Wilgus, C.K., and others, eds., Sea-Level Changes, An Integrated Approach: Tulsa, Oklahoma, Society of Economic Paleontologists and Mineralogists, Special Publication No. 42, p. 183-213.

Malm, O.A., Bruun Christensen, O., Furnes, H., Løvlie, R., and Ruselåtten, H., 1984, The Lower Tertiary Balder Formation: an organogenic and tuffaceous deposit in the North Sea region, *in* Spencer, A.M., and others, eds., Petroleum Geology of the North European Margin: London, Graham and Trotman, p. 149-170.

Martini, E., 1971, Standard Tertiary and Quaternary calcareous nannoplankton zonation, Farinacci, A., ed., Second Planktonic Conference Proceedings: Rome, Tecnoscienza, p. 739-785.

Matthews, R.K., and Poore, R.Z., 1980, Tertiary $\delta^{18}O$ record and glacio-eustatic sea-level fluctuations: Geology, v. 8, p. 501-504.

Mattingly, G.A., and Bretthauer, H.H., 1992, The Alba Field: A middle Eocene deep water channel system in the UK North Sea, *in* Halbouty, M.T., ed., Giant Oil and Gas Fields of the Decade 1978-1988: Tulsa, Oklahoma, American Association of Petroleum Geologists, p. 297-305.

McGovney, J.E., and Radovich, B.J., 1985, Seismic stratigraphy and facies of the Frigg Fan complex, *in* Berg, O.R., and Woolverton, D.G., eds., Seismic Stratigraphy II: An Integrated Approach to Hydrocarbon Exploration: Tulsa, Oklahoma, American Association of Petroleum Geologists, Memoir No. 39, p. 139-154.

Miall, A.D., 1986, Eustatic sea level changes interpreted from seismic stratigraphy: A critique of the methodology with particular reference to the North Sea Jurassic record: American Association of Petroleum Geologists Bulletin, v. 70, p. 131-137.

Miller, K.G., Fairbanks, R.G., and Mountain, G.S., 1987, Tertiary oxygen isotope synthesis, sea-level history, and continental margin erosion: Paleoceanography, v. 2, p. 119-127.

Miller, S.K., 1989, Genetic stratigraphic sequence analysis of the upper Wilcox, Gulf Basin: M.A. Thesis, University of Texas at Austin, 128 p.

Milton, N.J., Bertram, G.T., and Vann, I.R., 1990, Early Palaeogene tectonics and sedimentation in the Central North Sea, *in* Hardman, R.F.P., and Brooks, J., eds., Tectonic Events Responsible for Britain's Oil and Gas Reserves: London, Geological Society Special Publication No. 55, p. 339-351.

Mitchum, R.M., Jr., Vail, P.R., and Thompson, S., III, 1977, Seismic stratigraphy and global changes of sea level, part 2: the depositional sequence as a basic unit for stratigraphic analysis, *in* Payton, C.E., ed., Seismic stratigraphy - applications to hydrocarbon exploration: Tulsa, Oklahoma, American Association of Petroleum Geologists, Memoir No. 26, p. 53-97.

Mitchum, R.M., Jr., and Van Wagoner, J.C., 1990, High-frequency sequences and eustatic cycles in the Gulf of Mexico Basin, *in* Armentrout, J.M., and Perkins, B.F., eds., Gulf Coast Section Society of Economic Paleontologists and Mineralogists Foundation Eleventh Annual Research Conference, p. 257-267.

Morgan, R.K., 1990, Cenozoic subsidence and uplift in the North Sea region: implications for mechanisms of basin formation, *in* Hardman, R.F.P., and Brooks, J., Tectonic Events Responsible for Britain's Oil and Gas Reserves: Boulder, Colorado, Geological Society Special Publication No. 55, p. 369.

Morton, A.C., 1979, The provenance and distribution of the Paleocene sands of the Central North Sea: Journal of Petroleum Geology, v. 2, p. 11-21.

Morton, A.C., 1981, Lower Tertiary sand development in Viking Graben, North Sea: American Association of Petroleum Geologists Bulletin, v. 66, p. 1542-1559.

Morton, A.C., and Knox, R.W.O'B., 1990, Geochemistry of late Palaeocene and early Eocene tephras from the North Sea Basin: Journal of the Geological Society of London, v. 147, p. 425-437.

Mudge, D.C., and Bliss, G.M., 1983, Stratigraphy and sedimentation of the Palaeocene sands in the north North Sea, *in* Brooks, J., ed., Petroleum Geochemistry and Exploration of Europe: London, Geological Society of London, Special Publication No. 12, p. 95-111.

Mudge, D.C., and Bujak, J.P., 1994, Eocene stratigraphy of the North Sea basin: Marine and Petroleum Geology, v. 11, p. 166-181.

Mudge, D.C., and Copestake, P., 1992, Revised Lower Paleogene lithostratigraphy for the Outer Moray Firth, North Sea: Marine and Petroleum Geology, v 9, p. 53-69.

Mure, E., 1987, Frigg, *in* Spencer, A.M., and others, eds., Geology of the Norwegian Oil and Gas Fields: London, Graham and Trotman, p. 203-213.

Murray, J.W., 1992, Palaeogene and Neogene, *in* Cope, J.C.W., Ingham, J.K., and Rawson, P.F., Atlas of Palaeogeography and Lithofacies: London, Geological Society of London, p. 141-147.

Nadin, P.A., Kusznir, N.J., and Toth, J., in review, Dynamic uplift associated with the development of the Iceland plume: constraints from North Sea stratigraphy: submitted to Earth and Planetary Science Letters.

Neal, J.E., 1992, Paleogene sequence stratigraphy of central North Sea subsurface and select outcrops of northwest Europe, abstract: Symposium on Mesozoic and Cenozoic Sequence Stratigraphy of European Basins, Dijon, France, May, 1992.

Newman, M.St.J., Reeder, M.L., Woodruff, A.H.W., and Hatton, I.R., 1993, The geology of the Gryphon Oil Field, *in* Parker, J.R., ed., Petroleum Geology of Northwest Europe: Proceedings of the Fourth Conference: London, The Geological Society of London, p. 123-133.

Newton, S.K., and Flanagan, K.P., 1993, The Alba Field: evolution of the depositional model, *in* Parker, J.R., ed., Petroleum Geology of Northwest Europe: Proceedings of the Fourth Conference: London, The Geological Society of London, p. 161-171.

Nielsen, O.B., Sørensen, S., Thiede, J., and Skarbø, O., 1986, Cenozoic differential subsidence of the North Sea: American Association of Petroleum Geologists Bulletin, v. 70, p. 276-298.

Nilsen, T.H., and Kerr, D.R., 1978, Paleoclimatic and paleogeographic implications of a lower Tertiary laterite (latosol) on the Iceland-Faeroe Ridge, North Atlantic region: Geological Magazine, v. 115, p. 153-236.

Nyong, E.E., and Olsson, R.K., 1984, A paleoslope model of Campanian to Lower Maastrichtian foraminifera in the North America basin and adjacent continental margin: Marine Micropaleontology, v. 8, p. 437-477.

Park, R.A., 1974, A multivariate analytical strategy for classifying paleoenvironments, Mathematical Geology, v. 6, p. 333-352.

Parker, J.R., 1975, Lower Tertiary sand development in central North Sea, *in* Woodland, A.W., ed., Petroleum and the Continental Shelf of North -West Europe: New York, John Wiley, p. 447-453.

Parker, J.R., ed., 1993, Petroleum Geology of Northwest Europe: Proceedings of the Fourth Conference: London, The Geological Society of London, two volumes, 1542 p.

Partington, M.A., Mitchener, B.C., Milton, N.J., and Fraser, A.J., 1993, Genetic sequence stratigraphy for the North Sea Late Jurassic and Early Cretaceous: distribution and prediction of Kimmeridgian-Late Ryazanian reservoirs in the North Sea and adjacent areas, *in* Parker, J.R., ed., Petroleum Geology of Northwest Europe: Proceedings of the Fourth Conference: London, Geological Society of London, p. 347-370.

Plint, A.G., 1988, Sharp-based shoreface sequences and "offshore bars" in the Cardium Formation of Alberta: their relationship to relative changes in sea level, *in* Wilgus, C.K., and others, eds., Sea-Level Changes, An Integrated Approach: Tulsa, Oklahoma, Society of Economic Paleontologists and Mineralogists, Special Publication No. 42, p. 357-370.

Plummer, H.J., 1927, Foraminifera of the Midway Formation in Texas: Bulletin of the University of Texas, No. 2644, p. 3-206.

Pitman, W.C., III, and Talwani, M., 1972, Seafloor spreading in the North Atlantic: Geological Society of America Bulletin, v. 83, p. 619-646.

Pitman, W.C., 1978, Relationship between eustasy and stratigraphic sequences of passive margins: Geological Society of America Bulletin, v. 89, p. 1389-1403.

Powell, A.J., 1988, A modified dinoflagellate cyst biozonation for latest Paleocene and earliest Eocene sediments from the central North Sea: Reviews of Paleobotany and Palynology, v. 56, p. 322-344.

Prentice, M.L., and Matthews, R.K., 1990, Tertiary ice sheet dynamics: the snow gun hypothesis: Journal of Geophysical Research, v. 96, p. 6811-6827.

Rea, D.K., Zachos, J.C., Owen, R.M., and Gingerich, P.D., 1990, Global change at the Paleocene-Eocene boundary: climatic and evolutionary consequences of tectonic events: Palaeogeography, Palaeoclimatology, Palaeoecology, v. 79, p. 117-128.

Reinsborough, B.C., 1993, Sequence stratigraphy and depositional systems of the Paleocene Andrew Formation in the central North Sea : the evolution of a slope-to-basin system, unpublished M.A. thesis, University of Texas at Austin, 121 p.

Reynolds, J.D., Steckler, M.S., Coakley, B.J., 1991, The role of the sedimentary load in sequence stratigraphy: The influence of flexural isostasy and compaction: Journal of Geophysical Research, v. 96, p. 6931-6949.

Reynolds, T., 1994, Quantitative analysis of submarine fans in the Tertiary of the North Sea Basin: Marine and Petroleum Geology, v. 11, p. 202-207.

Richards, P.C., 1990, The early to mid-Jurassic evolution of the North Sea, *in* Hardman, R.F.P., and Brooks, J., eds., Tectonic Events Responsible for Britain's Oil and Gas Reserves: London, Geological Society of London, Special Publication No. 55, p. 191-205.

Ridd, M.F., 1983, Aspects of the Tertiary geology of the Faeroe-Shetland Channel, *in* Bott, M.H.P., Saxov, S., Talwani, M., and Thiede, J., eds., Structure and Development of the Greenland-Scotland Ridge: New York, Plenum Press, p. 91-108.

Robertson, G., 1993, Beryl Field: geological evolution and reservoir behaviour, *in* Parker, J.R., ed., Petroleum Geology of Northwest Europe: Proceedings of the Fourth Conference: London, Geological Society of London, p. 1491-1502.

Rochow, K.A., 1981, Seismic stratigraphy of North Sea 'Palaeocene' deposits, *in* Illing, L.V, and Hobson, G.D., eds., Petroleum Geology of the Continental Shelf of North West Europe: London, Heyden and Son, p. 255-265.

Rona, P.A., and Richardson, E.S., 1978, Early Cenozoic global plate reorganization: Earth and Planetary Science Letters, v. 40, p. 1-11.

Ronnevik, H., Bergsager, E.I., Moe, A., Øvrebø, O., Navrestad, T., and Stangenes, J., 1975, The geology of the Norwegian continental shelf, *in* Woodland, A.W., ed., Petroleum and the Continental Shelf of North West Europe: New York, John Wiley, p. 117-129.

Rundberg, Y., and Smalley, P.C., 1989, High-resolution dating of Cenozoic sediments from Northern North Sea using $^{87}Sr/^{86}Sr$ stratigraphy: American Association of Petroleum Geologists Bulletin, v. 73, p.298-308.

Sarg, J.F., and Skjold, L.J., 1982, Stratigraphic traps in Paleocene sands in the Balder area, North Sea, *in* Halbouty, M.T., ed., The Deliberate Search for the Subtle Trap: Tulsa, Oklahoma, American Association of Petroleum Geologists, Memoir No. 32, p. 197-206.

Schafer, C.T., Cole, F.E., and Carter, L., 1983, Paraecology of bathyal zone arenaceous foraminifera genera and species associations off northeast Newfoundland, *in* Verdenius, J. G., van Hinte, J. E., and Fortuin, A. R., eds., Proceedings of the First Workshop on Arenaceous Foraminifera: Trondeim, Norway, Institutt for kontinentalsokkelundersokelser (IKU), p. 133-145.

Schaffer, B.L., 1990, The nature and significance of condensed sections in Gulf Coast late Neogene sequence stratigraphy: Gulf Coast Association of Geological Societies Transactions, v. XL, p. 186-195.

Schröder, C.J., 1986, Deep-water arenaceous foraminifera in the northwest Atlantic Ocean: Canadian Technical Report of Hydrography and Ocean Sciences No. 71, 191 p.

Schwan, W., 1980, Geodynamic peaks in Alpinotype orogenies and changes in ocean-floor spreading during Late Jurassic-Late Tertiary time: American Association of Petroleum Geologists Bulletin, v. 64, p. 359-373.

Schwan, W., 1985, The worldwide active Middle/Late Eocene geodynamic episode with peaks at ±45 and ±37 M.Y. B.P., and implications and problems of orogeny and sea-floor spreading: Tectonophysics, v. 115, p. 197-234.

Sclater, J.G., and Christie, P.A.F., 1980, Continental stretching: An explanation of the post-mid-Cretaceous subsidence of the Central North Sea Basin: Journal of Geophysical Research, v. 85, p. 3711-3739.

Sears, R.A., Harbury, A.R., Protoy, A.J.G., and Stewart, D.J., 1993, Structural styles from the Central Graben in the UK and Norway, *in* Parker, J.R., ed., Petroleum Geology of Northwest Europe: Proceedings of the Fourth Conference: London, Geological Society of London, p. 1231-1244.

Selley, R.C., 1976, Subsurface environmental analysis of North Sea sediments: American Association of Petroleum Geologists Bulletin, v. 60, p. 184-195.

Selley, R.C., 1979, Dipmeter and log motifs in the North Sea submarine-fan sands: American Association of Petroleum Geologists Bulletin, v. 63, p. 905-917.

Shackleton, N.J., and Kennett, J.P., 1975, Paleotemperature history of the Cenozoic and the initiation of Antarctic glaciation: oxygen and carbon isotope analyses in DSDP Sites 277, 279, and 281, *in* Kennett, J.P., and others, Initial Reports of the Deep Sea Drilling Program: v. 29, p. 743-755.

Sleep, N.H., 1976, Sequences of the cratonic interior of North America: Tectonophysics, v. 36, p. 45-56.

Sloss, L.L., 1991, The tectonic factor in sea level change: A countervailing view: Journal of Geophysical Research, v. 96, p. 6609-6617.

Spencer, A.M., and others, eds., 1987, Geology of the Norwegian oil and gas fields: London, Graham and Trotman for the Norwegian Petroleum Society, 493 p.

Staesche, K., and Hiltermann, H., 1940, Mikrofaunen aus dem Tertiär Nordwestdeutschlands: Abhandlungen Reichsanst. Bodenforsch., N.F., v. 201, p. 6-26.

Srivastava, S.P., and Tapscott, C.R., 1986, Plate kinematics of the North Atlantic, in vogt, P.R., and Tucholke, B.E., eds., The Geology of North America, Volume M, The Western North Atlantic Region: Boulder, Colorado, Geological Society of America, p. 379-397.

Steckler, M.S., and Watts, A.B., 1978, Subsidence of the Atlantic-type continental margin off New York: Earth and Planetary Science Planetary Letters, v. 41, p. 1-13.

Stewart, I.J., 1987, A revised stratigraphic interpretation of the Early Palaeogene of the Central North Sea, *in* Brooks, J., and Glennie, K.W., eds., Petroleum Geology of Northwest Europe: London, Graham and Trotman Ltd., p. 557-576.

Stille, H., 1924, Grundfragen der vergleichenden Tektonik: Berlin, Borntraeger.

Timbrell, G., 1993, Sandstone architecture of the Balder Formation depositional system, UK Quadrant 9 and adjacent area, *in* Parker, J.R., ed., Petroleum Geology of Northwest Europe: Proceedings of the Fourth Conference: London, Geological Society of London, p. 107-121.

Thomas, A.N., Walmsley, P.J., and Jenkins, D.A.L., 1974, Forties Field, North Sea: American Association of Petroleum Geologists Bulletin, v. 58, p. 396-406.

Thorne, J.A., and Watts, A. B., 1989, Quantitative analysis of North Sea subsidence: American Association of Petroleum Geologists Bulletin, v. 73, p. 88-116.

Tjalsma, R. C., and Lohmann, G. P., 1983, Paleocene-Eocene bathyal and abyssal benthic foraminifera from the Atlantic Ocean: Micropaleontology, Special Publication No. 4, 90 p.

Tyson, R.V., and Funnell, B.M., 1987, European Cretaceous shorelines, stage by stage: Palaeogeography, Paleoclimatology, Palaeoecology, v. 59, p. 69-91.

Underhill, J.R, and Partington, M.A., 1993, Jurassic thermal doming and deflation in the North Sea: Implications of the sequence stratigraphic evidence, *in* Parker, J.R., ed., Petroleum Geology of Northwest Europe: Proceedings of the Fourth Conference: London, Geological Society of London, p. 337-346.

Vail, P.R., and Hardenbol, J., 1981, Sea level changes during the Tertiary: Oceanus, v. 22, p. 71-79.

Vail, P.R., Hardenbol, J., and Todd, R.G., 1984, Jurassic unconformities, chronostratigraphy, and sea level changes from seismic stratigraphy and biostratigraphy: American Association of Petroleum Geologists Bulletin, Memoir 36, p.129-144.

Vail, P.R., and Jacquin, T., eds., 1992, Symposium on Mesozoic and Cenozoic Sequence Stratigraphy of European Basins, abstract volume: Dijon, France, May, 1992.

Vail, P.R., Mitchum, R.M., Jr., Todd, R.G., Widmier, J.M., Thompson, S., III, Sangree, J.B., Bubb, J.N., and Hatlelid, W.G., 1977, Seismic stratigraphy and global changes of sea level, *in* Payton, C.E, ed., Seismic Stratigraphy - applications to hydrocarbon exploration: Tulsa, Oklahoma, American Association of Petroleum Geologists, Memoir No. 26, p. 49-212.

Van Hinte, J.E., 1978, Geohistory analysis - application of micropaleontology in exploration geology: American Association of Petroleum Geologists Bulletin, v. 62, p. 201-222.

Van Wagoner, J.C., Posamentier, H.W., Mitchum, R.M., Vail, P.R., Sarg, J.F., Loutit, T.S., and Hardenbol, J., 1988, An overview of the fundamentals of sequence stratigraphy and key definitions, *in* Wilgus, C.K., Hastings, B.S., Kendall, C.G.St.C., Posamentier, H.W., Ross, C.A., and Van Wagoner, J.C., eds., Sea-Level Changes - An Integrated Approach: Tulsa, Oklahoma, Society of Economic Paleontologists and Mineralogists, Special Publication No. 42, p. 39-69.

White, R.S., 1988, A hot-spot model for early Tertiary volcanism in the N Atlantic, *in* Morton, A.C., and Parson, L.M., Early Tertiary Volcanism and the Opening of the NE Atlantic: London, Geological Society of London, Special Publication No. 39, p. 3-13.

Wood, R.J., 1981, The subsidence history of Conoco well 15/30-1, central North Sea: Earth and Planetary Science Letters, v. 54, p. 306-312.

Wood, R., and Barton, P., 1983, Crustal thinning and subsidence in the North Sea: Nature, v. 302, p. 134-136.

Wornardt, W.W., Jr., 1989, Calcareous nannofossils and condensed sections in sequence stratigraphy (abstract): International Nannoplankton Association Conference, Florence, Italy, p. 3.

Wornardt, W.W., Jr., 1992, Abundance and diversity histograms - The key to interpreting systems tracts, condensed sections and sequence boundaries (abstract): Symposium on Mesozoic and Cenozoic Sequence Stratigraphy of European Basins, Dijon, France, May, 1992.

Xue, L., 1994, Genetic stratigraphic sequences and depositional systems of the lower and middle Wilcox strata, Texas Gulf Coast Basin, Ph.D. dissertation, University of Texas at Austin, 201 p.

Xue, L., and Galloway, W.E., 1993, Genetic sequence stratigraphic framework, depositional style, and hydrocarbon occurrence of the Upper Cretaceous QYN Formations in the Songliao lacustrine basin, northeastern China: American Association of Petroleum Geologists Bulletin, v. 77, p. 1792-1808.

Ziegler, P.A., 1978, North-western Europe: tectonics and basin development: Geologie en Mijnbouw, v. 57, p. 589-626.

Ziegler, P.A., 1982, Geological atlas of Western and Central Europe: New York, Elsevier Scientific Publishing Company, 2 volumes.

Ziegler, P.A., 1988, Evolution of the Arctic-North Atlantic and the Western Tethys: Tulsa, Oklahoma, American Association of Petroleum Geologists, Memoir No. 43, 198 p.

Ziegler, P.A., 1990, Tectonic and paleogeographic development of the North Sea rift system, *in* Blundell, D.J., and Gibbs, A.D., eds., Tectonic Evolution of the North Sea Rifts: Oxford, Oxford University Press, p. 1-36.

Ziegler, P.A., 1992, North Sea rift system: Tectonophysics, v. 208, p. 55-75.

Ziegler, P.A., and van Hoorn, B., 1989, Evolution of North Sea rift system, *in* Tankard, A.J., and Balkwill, H.R., eds., Extensional Tectonics and Stratigraphy of the North Atlantic Margins: Tulsa, Oklahoma, American Association of Petroleum Geologists, Memoir No. 46, p. 471-500.